MINERALS MANAGEMENT SERVICE

POST MORTEM PLATFORM FAILURE EVALUATION STUDY

FINAL REPORT

PMB ENGINEERING INC.
SAN FRANCISCO, CALIFORNIA

AUGUST, 1994

Table of Contents

Section		Page
	Executive Summary	**ES-1**
1	**Introduction**	**1-1**
1.1	Background	1-1
1.2	Acknowledgements	1-1
1.3	Contract Information	1-2
2	**Onshore Platform Inspection**	**2-1**
2.1	Platform Configuration	2-1
2.2	Platform Salvage Configuration	2-1
2.3	X Joint Inspections	2-2
2.4	K Joint Inspections	2-3
2.5	KT Joint Inspections	2-3
2.6	Leg Inspections	2-4
2.7	Transverse Diagonal Brace Inspections	2-5
2.8	Fatigue and Corrosion Inspections	2-5
2.9	Other Inspections	2-5
2.10	Joints Selected for Further Testing	2-6
3	**Computer Analysis**	**3-1**
3.1	Introduction	3-1
3.2	Description of Model	3-1
3.3	Environmental Loads	3-4
3.4	Member and Joint Modeling	3-5
3.5	Analysis Results	3-8
3.6	Conclusions	3-13

Table of Contents

Section		Page
4	**Conclusions and Recommendations**	**4-1**
	4.1 Platform Inspection	4-1
	4.2 Platform Analysis	4-1
5	**References**	**5-1**
	Appendix A Joints Selected for Further Testing	
	Appendix B Joint Capacity Methodology	

LIST OF FIGURES

Figure 2-1 Platform ST 177 B - General Configuration

Figure 2-2 Plan View of Platform Sections

Figure 3-1 CAP Computer Model

Figure 3-2 Comparison of Plastic and Brittle Joint Modes

Figure 3-3 Comparison of Analyses Results

Figure 3-4 Basic Model - Initial Member Failure

Figure 3-5 Basic Model - Intermediate Load Step

Figure 3-6 Basic Model - Analysis Results

Figure 3-7 Soil Improved 50% - Analysis Results

Figure 3-8 Soil Improved 100% - Intermediate Load Step

Figure 3-9 Soil Improved 100% - Analysis Results

Figure 3-10 Fixed Base - Initial Member Failure

Figure 3-11 Fixed Base - Intermediate Load Step

Figure 3-12 Fixed Base - Final Load Step

Figure 3-13 Fixed Base - Analysis Results

Figure 3-14 Brittle K Joints - Initial Failure

Figure 3-15 Brittle K Joints - Intermediate Load Step

Figure 3-16 Brittle Joints - Final Load Step

Figure 3-17 Brittle Joints - Analysis Results

LIST OF PHOTOS

Photo 2-1	ST 151 K - Similar Configuration to ST 177 B
Photo 2-2	Broadside View of Platform Sections
Photo 2-3	End-On View of Platform Sections
Photo 2-4	Closeup view of Section BN (Bottom North)
Photo 2-5	Closeup View of Section TN (Top North)
Photo 2-6	Closeup View of Section BS (Bottom South)
Photo 2-7	Damaged X Joint Row 2
Photo 2-8	Closeup of X Joint Crack
Photo 2-9	Closeup of X joint Bulge
Photo 2-10	B AUX X Joint Crack
Photo 2-11	Closeup of B AUX X Joint
Photo 2-12	K Joint Row 2
Photo 2-13	K Joint Row 1
Photo 2-14	K Joint on BS (Compression Side)
Photo 2-15	Interior K joint BN Row 2
Photo 2-16	Closeup of Interior K Joint Row 2
Photo 2-17	Closeup of Crack on Interior K Joint Row 2
Photo 2-18	Cleaned Joint at B1 - Tension Brace
Photo 2-19	Cleaned Joint at B1 - Compression Brace

Photo 2-20 View of Leg A2 (BN)

Photo 2-21 View of Leg A1 (BN)

Photo 2-22 View of Leg A2 (TN)

Photo 2-23 View of Leg C1

Photo 2-24 View of Leg C2

Photo 2-25 Cleaned Compression Joint at Mudline

Photo 2-26 Cleaned Tension Joint at Mudline

Photo 2-27 Cleaned Complex Joint at Mudline Leg B2

Photo 2-28 Cleaned Complex Joint at Mudline Leg A1

Photo 2-29 Support for Original Platform Anode

Photo 2-30 Retrofit Anode

Photo 2-31 Leg Section Showing Grout

Photo 2-32 Conductor Section

EXECUTIVE SUMMARY

Background

In 1992, Hurricane Andrew passed through a large number of platforms in the Gulf of Mexico. While most platforms were unaffected, several were severely damaged or toppled.

Working under contract for the MMS, PMB subsequently performed an onshore, "post-mortem" inspection of one of the damaged platforms that was in the process of being salvaged. PMB also performed a nonlinear analysis of the platform to determine if the observed damage could be predicted analytically. Results of the onshore inspection and results of the analytical evaluation are documented in this report.

The platform was of eight leg configuration, located in 140 ft water depth in the South Timbalier region, and was installed in 1965. Framing consisted of diagonal racing in the longitudinal direction and K bracing in the transverse direction.

Onshore Inspection

The platform was severely damaged but did not topple in Andrew, and was inspected onshore after the platform had been cut into several large pieces for salvage (see Section 2, Photos 2-2 and 2-3). The platform had suffered significant joint damage including cracked X joints, complete sever of several K joints, and damaged KT joints. There were no joint cans at any of the damaged joints. There was also a noticeable curvature in the platform legs.

The X joints contained a 2+ ft crack at the centerline of the tension member, which was also the through member of the compression-tension pair. The tension member was also crushed by the compression members, creating an oval cross-section with the crack located along the narrow apex of the oval (Photos 2-10 and 2-11).

All of the K joints on the platform were damaged by complete sever of the chord (Photo 2-12). It appeared that the chord severed due to excessive beam shear. The failure plane was located along a line parallel to the compression member of the K. The failure can be attributed to the chord and K brace members having the same diameter and thickness, with the chord unable to carry the shear load along the approximate 2 inch gap between the two K braces.

The interior KT joints (nearby the highly wave loaded conductors) showed some bulging and cracks, but were generally still intact and capable of carrying load (Photo 2-16). It appears that the vertical member of the KT, which eliminated the gap, provides the additional strength to carry loads along the chord.

The platform legs in the lower elevations where the K bracing had completely failed had a slight curvature in the direction of the Andrew waves (Photos 2-20 and 2-21). This curvature was possible since the complete loss of the K joints allowed for the formation of large deformations in the legs.

Several of the platform joints near the mudline where sandblasted clean to allow for close visual inspection of the joints for cracks caused by high stresses during Andrew or by long term fatigue. All of the cleaned joints (which included both tension and compression braces) showed no signs of cracks or other damage.

Structural Analysis

A three dimensional, nonlinear computer model of the deck, jacket and foundation was used to evaluate the platform using PMB's computer code CAP (Capacity Analysis Program). Nonlinear elements were used for the braces, legs, piles and soils. Andrew metocean conditions were based upon a hindcast by Oceanweather.

There were two key aspects of the platform studied. The first was joint capacity and joint force-deformation relationships, based upon the severed joint damage observed in the inspection. The second was foundation performance, since previous study of this platform in during the Andrew Joint Industry Project (JIP), indicated that joint damage should have occurred, yet none was observed.

Capacity of the joints was determined based upon a literature survey of available joint test results and parametric equations. A combination of joint capacity work by Billington, Lalani and Tebbet (1982) and Ma and Tebbet (1988), was used to determine the capacity of a majority of joints. These equations are believed to be a more realistic estimate of joint capacity than the API RP 2A equations used in the Andrew Joint Industry Project (JIP), since the API equations represent a lower bound of joint strength, whereas the equations used by this study use a median joint strength.

Several methods were used to model joint force-deformation. The first was an elastic-plastic relationship, similar to that of the Andrew JIP. This predicted that the platform would have survived Andrew. This type of modeling does not allow for sufficient load shedding that occurs when a joint completely fails as observed in the inspection.

A second and more realistic method of modeling joints using an elastic-brittle relationship showed a much better comparison, with the model predicting that the platform would have been severely damaged in Andrew, with the damage similar to that observed.

The foundation was first modeled as-is using API RP 2A procedures to define pile-soil nonlinear

spring characteristics (p-y, t-z and q-z). This model showed that the platform would fail in the foundation with no failures of any of the jacket members. The soil shear strength was then increased to force failures into the jacket as observed following Andrew. This was used as a simplified method to account for possible conservatism in the API pile-soil formulations. The result was that analytically predicted platform member failures best match those observed when the soil shear strength is increased by 100%. While this is by no means a conclusive study, since only one platform under one loading condition was evaluated, it does indicate possible conservatism in the API pile-soil formulations.

Conclusions and Recommendations

Platform Inspection

The ST 177B structures sustained serious damage to joints at the intersection of X, K and KT braces. The failures appear to be attributable to the lack of joint cans and the problem of chord and brace diameters of the same size. This is a problem that probably exists in a number of platform of this vintage and needs to be accounted for when evaluating the platform for fitness of purpose.

Note that there were no joint failures at the legs (which were grouted), helping to confirm the industry perception of increased joint strength due to the composite action of the leg, grout and pile.

The platform legs showed a slight curvature in the direction of the Andrew waves. This "damage" is attributable to large deformation of the legs once the K joints had sheared. This frame action resistance by the legs ultimately allowed the platform to remain standing after Andrew even though almost all of the joints had been damaged.

Overall, there were no other signs of damage of any kind to the platform, such as fatigue cracking, dented members or corrosion. Joints sand blasted clean during the inspection were in remarkably good condition for a 28 year old platform. It appeared that the platform operator's maintenance program provided an adequate job for this particular structure.

Several intact and damaged joint specimens were cut from the platform and placed in storage in one of Chevron's yards in the New Orleans area. It recommended that these joints be used for further testing of material properties as well as ultimate strength. These joints are unique since they provide the specific type of steel materials and fabrication techniques (rolling, welding, etc.) typical of the 1960's vintage of platforms.

One possibility is to propose the effort in the form of a Joint Industry Project (JIP) funded by industry and regulators such as the MMS and HSE. The testing could be performed at a

university or other testing facility that can handle large specimens. The work would be similar to that previously performed at Texas A&M for damaged platform braces under a JIP managed by PMB (PMB, 1990).

Platform Analysis

The initial "Base Case" computer model predicted that the platform would have collapsed during Andrew. The failure mode predicted by the analysis was in the foundation, with little or no damage to the jacket. However, the post Andrew platform inspection indicated that the failure mode was instead in the jacket, with serious damage to almost all of the joints in the jacket. There was no indication of foundation damage or failure.

The computer models were therefore adjusted in terms of the foundation and jacket joint modeling in order to try to adjust the analytical evaluation until it more closely matched the observed results.

The foundation adjustments indicate that an increase in soil shear strength on the order of 50 to 100 percent provides sufficient foundation resistance to allow joint failures in the jacket prior to failure of the platform. A similar pattern of analytically predicted foundation failures, yet none that were observed in the filed, was seen in the Andrew JIP.

The jacket joint strength adjustments indicate that elastic-brittle joint modeling of the K joints, which mimics the complete shear of the joint as seen in the platform inspection, provides a good match to the observed platform performance and damage that occurred in Andrew. The brittle joint model also included the adjusted foundation with increased soil shear strength. The model predicted that almost all of the jacket joints would have failed in Andrew but the platform would have survived due to bending resistance of the grouted leg-pile. There would also have been some initial yielding of the legs. This is essential the same type of damage as indicated by the platform inspection.

For this particular study, the computer model was modified until it predicted that the platform would perform as indicated by the onshore inspection. The analytical "recipe" that worked well for this case (i.e. increased foundation strength and brittle joints) needs to be tested using other platforms that were damaged or survived large storms. A parallel study being performed by PMB for the MMS (PMB, 1994d) that is evaluating three more platforms from Andrew, indicates that the "recipe" that worked well for this platform does not perform as well for two of the three platforms, where the recipe indicates that the platform should have collapsed, or at least seriously damaged, yet the platforms survived undamaged.

Based upon the above, it is obvious that further study is required before a well established recipe for evaluating platforms under extreme environmental conditions can be developed. The recipe

first identified in the Andrew JIP and then further refined in this study appears promising, but several adjustments are still required. Foundation strength is currently being further studied by PMB in a study funded by the MMS and API (PMB, 1994a). Joint strength and modeling will be one of the key issues investigated in the proposed Andrew Phase II JIP, where the joint specialist firm of MSL Engineering will be assisting PMB on the further evaluation of platform performance in Andrew. Both of these projects will enable development and testing of a much improved recipe.

SECTION 1 INTRODUCTION

1.1 BACKGROUND

During August 1992 Hurricane Andrew passed through the Gulf of Mexico and severely damaged a number of offshore platforms. The Minerals Management Service (MMS) subsequently contracted PMB to perform a "Post Mortem Platform Failure Evaluation Study" on one of the more severely damaged or toppled structures. There were two main tasks for the study:

1. Platform Inspection and Evaluation. Two eight leg, 140 ft water depth, platforms that were severely damaged but did not topple in Andrew were inspected onshore after the platforms had been cut into several large pieces for salvage. The platforms had suffered significant joint damage including cracked X joints, complete sever of several K joints and damaged KT joints. The platforms provided a unique opportunity to study these types of member failures. The results of the inspection were subsequently used as a comparison against nonlinear analysis of one of the platforms to determine if the damage could be predicted. An iterative process was used to modify the computer model until the analytical results matched the observed.

2. Offshore Platform Evaluation System (OPES). In 1991, PMB developed a prototype of a computer based system called OPES that links inspection results with structural analysis results via a central database system. OPES provides a powerful tool that provides quick access to the key information regarding a platform's current state such as extent of damage (if any), platform capacity based upon structural analysis, primary load carrying members, etc. The work was performed for the MMS. OPES was subsequently further developed via a technical grant from PMB's parent company Bechtel. For this project, a prototype of OPES was loaded with inspection information gathered during a parallel study for the MMS (A&E Contract, PMB 1994d) that involved platform inspections and analysis of several platforms affected by Andrew.

This reports presents the approach, results and conclusions associated with the first effort associated with the platform inspection and evaluation. A separate report describes OPES, including a prototype version of the program.

1.2 ACKNOWLEDGEMENTS

The MMS and PMB appreciate the assistance Chevron in providing the opportunity to inspect several Chevron platforms for use in the project. Particular thanks go to Mr. Dirceu Botelho, Mr. Ron Perego and Mr. Paul Versowsky of Chevron who were instrumental in providing access to the ST 177 B and ST 177 B AUX platforms, in addition to drawings and other

pertinent information necessary for both the inspection and analysis work.

1.3 CONTRACT INFORMATION

This work was performed for the MMS, as part of BAA No. MMS-93-01, Contract No. 1435-0001-30742. The work was performed during the period from September 1993 to August 1994.

SECTION 2 ONSHORE PLATFORM INSPECTION

2.1 PLATFORM CONFIGURATION

The ST 177 B platform general configuration and key characteristics are shown in Figure 2-1. The ST 177 B AUX platform is essentially the same. Appendix A provides additional information on the ST 177 B platform including member sizes. Photo 2-1 shows an above water view of the ST 151 K platform which is very similar to the ST 177 B and ST 177 B AUX configuration.

As previously noted, both platforms were seriously damaged in Andrew with significant joint failures as determined by underwater inspections. It was also noted by Chevron personnel who visited the platform immediately following Andrew that the platforms vibrated due to the passage of typical everyday waves.

Chevron decide to "scrap" the platforms and sold them to a salvage company which cut the platforms into large sections for transport to shore where they were eventually cut into small pieces for scrap. The deck was first removed by cutting it in half vertically, resulting in two smaller deck sections similar to a "four pile" deck. The conductors were next removed (after the wells had been plugged) by explosives located below the mudline, with the conductors lifted free and put on a salvage barge along with the deck sections for transport to shore.

The jacket, which is the primary interest of this study, was cut into four pieces which were also brought to shore aboard a cargo barge. The piles where first cut below the mudline by cutting a window in the pile/leg just below the top-of-jacket, and lowering explosives down the center of the pile until the proper depth is reached below the mudline (15-20 ft). This allows the lower jacket sections to be later be lifted free from the mud with the piles remaining in-place (with the pile cut at the proper elevation below the mud per MMS requirements).

The jacket was cut into the sections by divers using underwater cutting tools or explosives to cut the jacket into four pieces. The jacket was cut down the middle between Rows B and C and then cut horizontally at approximately the (-)60 ft elevation. The jacket pieces were placed on a barge (typically 2-3 pieces per barge load) and transported to shore to be further cut into scrap.

2.2 PLATFORM SALVAGE CONFIGURATION

Photos 2-2 and 2-3 show broadside and end-on views of three jacket sections from ST 177 B resting on one of the transport barges. This is the set of jacket components that served as a basis for most of the inspections. As described later, some components of the ST 177 B AUX platform in the process of being scrapped nearby where also investigated.

Figure 2-2 shows the plan view of the ST 177 B sections. The Bottom North (BN) section is to the left, the Top North (TN) section is in the middle, and the Bottom South (BS) section is to the right. Thus BN on the right was connected to BS (think of it as rotating BS 180 clockwise degrees in Photo 2-2 and then connecting it to BN) and TN was on top of BN (think of this by simply placing TN without any rotation on top of BN in Photo 2-2).

A closer look at Photo 2-2 reveals clearly damaged K joints on the BN (left side) and BS (right side). Closer inspection showed even more damage to the X and K joints on the TN (center) and other K and KT joints of the bottom section. Several of the mudline joints on the bottom sections were sandblasted clean and inspected for possible fatigue damage.

Photo 2-4 shows a closeup of BN, Photo 2-5 shows a closeup of TN and Photo 2-6 shows a closeup of BS. The following sections describe the findings of the inspections.

2.3 X JOINT INSPECTIONS

The X joints were located in the upperbays of the platform just below the water line of TN (Photo 2-5). Photo 2-7 shows a closeup of the BN X joint in the transverse frame Row 2. The through brace (and coincidentally the tension brace) extends from the bottom right side to the upper left side. The most severe Andrew waves moved basically from right to left of the photo. A crack is clearly seen at the intersection of the braces along the tension brace.

Photo 2-8 shows a further closeup of the crack which is approximately 1 inch in width at the widest point and about 30 inches in length. Photo 2-9 shows another closeup of the joint including an obvious bulge on the tension member. These photos indicate that the two ends of the compression brace at the joint basically "squeezed" the tension member until it deformed into an oval cross-section and began to bulge and eventually crack.

Similar cracks were seen on the remaining portion of the X braces of the ST 177 B AUX structure as shown in Photo 2-10. A closeup of one of these joints, as shown in Photo 2-11, also reveals a similar bulging on the tension member.

Note that the X joint on the outside Row 1 was not damaged in terms of a crack or bulge. This is likely due to the higher loads on the interior transverse rows due to the presence of the conductors which were located between Rows 2 and 3.

It is also interesting to note that these failures may have a different mode if it had been the through member that was in compression. With the through member in tension, it allowed the compression braces to slowly squeeze the tension member during high loading. If the through member was in compression, there would be no member to squeeze, and perhaps the member would have instead failed by buckling out of plane (although the tension brace would have

helped prevent this).

2.4 K JOINT INSPECTIONS

K joints were located in the middle two elevations. The uppermost K (closest to the waterline) is located on the lower section of TN (Photo 2-5). A closeup of the K joint on ROW 2 is shown in Photo 2-12. Andrew waves moved basically from right to left in the photo. The failure occurred due to complete shear through the chord. The shear plane is in a plane directly along the bottom of the compression brace. Note that the right hand side of the K brace has dropped downward approximately 1 foot. This is due to the portal action of the legs as discussed din Section 2-6.

The chord and braces are of the same diameter and thickness for the K joints, with the upper K being 16 inch diameter by 0.406 inches thick and the lower K being 18 inch diameter by 0.438 inch thick.

The ST 177 B joints were designed with approximately a 2 inch gap between the braces and no joint can. This allows high shear stresses in the chord, which eventually failed. As discussed later, the KT joints (which had no gap due to the presence of the vertical T member) did not exhibit this failure mode.

Photo 2-13 shows the K on Row 1 which also had the same type of failure. Again the shear failure in the chord is along a plane on the bottom of the compression brace. Note that for the K braces, both the interior and exterior transverse row joints were damaged (unlike the X joints which were only damaged on the interior rows closest to the conductors).

Photo 2-14 shows a closeup of the compression member side of the K joint on BS (top K in Photo 2-6). Note that the compression member is on the right hand side of the BS section since it is rotated 180 degrees compared to the previously discussed TN section. In this case the compression member punched into the chord prior to chord failure. This photo provides clear evidence of the inability of the chord to transfer load between the compression and tension brace pair at the K joint when there is no joint can present. Similar to the TN section, both the interior and exterior K joints failed.

The upper K joints of BN (Photo 2-4) showed the same type of failures, with both the interior and the exterior joints completely severed at the chord.

2.5 KT JOINT INSPECTIONS

Proceeding down the platform to the mudline are the lower KT joints which differ from the K joints due to the presence of the vertical T member, resulting in an overlapped joint. Photo 2-15

shows a closeup of the interior KT joint on Row 2 on BN (Photo 2-4). At first the joint appeared to be undamaged, however closer inspection revealed a slight bulge on the chord above the compression member as can be seen to the right of the joint in Photo 2-15.

Photo 2-16 shows a closer view of the joint with the bulge more visible. A vertical crack can be seen starting at about the middle of the vertical member approximately 1 ft below the chord and proceeding up to the weld at the chord. Photo 2-17 shows an even closer view of the crack, also revealing a hole in the vertical member at the intersection of the chord, vertical member and tension member. A slight crack along the compression brace weld with the chord can also be seen. This damage indicates that the joint was highly loaded and perhaps on the verge of complete failure, similar to the K joints. However, the presence of the vertical member provides for a stronger joint, and in particular, a stronger chord cross-section in the joint region.

Note that for the KT joints, the chord was 20 inch diameter (0.438 inch thick), the diagonal braces were 18 inch diameter (0.438 inch thick) and the vertical T member was 14 inch diameter (0.375 inch thick). This too helped prevent failure of the chord as seen for the K braces.

Similar damage was found at the interior Row 3 KT joint on BS (Photo 2-5). However, on both BN and BS the exterior KT joints were intact with no signs of damage. Again this can be attributed to the presence of the conductors in the inner regions and the resulting higher loads imparted to the interior jacket rows.

The two brace diagonals along Row B on BN were sandblasted clean at the joints closest to the mudline to check for cracks that could have been caused by high loading (or fatigue as described later). The joint at B1 for the tension brace is shown in Photo 2-18 and the joint at B2 for the compression brace is shown in Photo 2-19. Both joints were in good condition with no signs of cracking or bulging due to overload. Note that the leg-pile is grouted.

2.6 LEG INSPECTIONS

At first glance, the legs appeared to be in good condition. There were no signs of cracks, bulging or other problems. However, after viewing the platform sections for some time, it became apparent that all of the legs on each section contained a slight curvature.

Close inspection of Photo 2-4 shows curvature of the BN legs (left section of photo) away from the direction of the Andrew waves as anticipated (which came from the right for this section). For this section, the K joints had completely failed, leaving only the portal action for the legs to resist Andrew loads. The bending appears to be generally equally distributed along the length of the member, although in some of the legs there appeared to be a slightly larger bend at the horizontal framing locations. Photo 2-20 shows a view up the B2 leg showing a convex curvature away from the Andrew waves. Photo 2-21 shows a view up the B1 leg showing a

concave curvature away from the Andrew waves.

Photo 2-2 shows leg bending on TN where the legs curve to the right. Note that this curvature is against the direction of the Andrew waves (for this section, the waves where coming from the right). Photo 2-22 shows a view up the B2 leg showing a slight convex curvature into the Andrew waves. Photo 2-23 shows a view up the B1 leg showing a slight concave curvature into the Andrew waves. This "reverse" curvature (compared to the direction of the Andrew waves) is probably due to the action of the X braces which remained basically intact, keeping the upper bay square. The result is a reverse in curvature of the legs in this region. This reverse curvature is also caused in part by the battered legs.

The other bottom section BS (right of Photo 2-2) shows similar leg bending as the other bottom section BN. Note that in Photo 2-2, BS is rotated 180 degrees counterclockwise from BN, so Andrew waves approached from the left, as indicated by the pile bending. Photo 2-24 shows a view up the D1 leg showing concave bending and Photo 2-25 shows a view up the D2 leg showing concave bending, with both legs bent away from the Andrew waves.

2-7 TRANSVERSE DIAGONAL BRACE INSPECTIONS

The longitudinal diagonal bracing extending between each major horizontal frame showed no signs of damage. These braces can be seen in Photos 2-2 through 2-5 and are the diagonal braces that are in the plane that is perpendicular to the paper.

Computer analysis of this platform for the Andrew JIP (PMB, 1993) indicated that several of these braces would be highly loaded in Andrew, particularly those near the mudline. Therefor several joints of these members were sand blasted clean allowing a close visual inspection of the welds. The joints were those located near the mudline since they were most accessible. Photo 2-26 shows the BN B2 leg at the mudline which was cleaned near the joints as seen in the photo. Photo 2-27 shows a closeup of another the mudline joint which was in tension during Andrew. There are no signs of any damage, with the welds appearing to be in remarkably good shape for 28 year old structure.

2.8 FATIGUE AND CORROSION INSPECTIONS

Several mudline joints on BN were also cleaned and checked visually for any fatigue cracking or corrosion pitting. Photo 2-28 shows a complex joint on Leg B2 and Photo 2-29 shows a complex joint on Leg A1. The joints and welds were again in excellent condition.

Corrosion on the jacket appeared to be minimal. There were no signs of loss of material or pitting, although for the upper jacket sections there was marine growth covering almost all of the jacket steel, and it was difficult to ascertain for sure that there was not any corrosion.

The original anodes had been completely depleted. These original anodes were held on by small angles extending between the horizontal members and the legs as shown in Photo 2-30. Retrofit anodes had been placed on the platform (Photo 2-31) and appeared to have been performing an adequate job, although several appeared to be ready for replacement in the near future.

2.9 OTHER INSPECTIONS

The ST 117 B AUX platform was almost fully scrapped by time of the inspection, however, several of the platform's remaining pieces showed some interesting points.

Photo 2-32 shows a piece of one of the platform's 33 inch diameter leg sections with a piece of the leg removed to expose the grout. A piece of the cut leg section can be seen in the lower right hand corner of the photo. The 30 inch diameter pile can be seen at the end of the member. The grout is only about 1 to 1 1/2 inches thick, but the grout job appears to have been good with full coverage as can be seen in the photo. There was a fair amount of cracking in the grout, but this may have been caused by the demolition process.

Photo 2-33 shows one of the conductors with the drill strings clearly visible. Note the offset of the drill strings. Note also the large amount of grout which makes the conductors very stiff but also very heavy. Although the mass is not a problem for these structures, it would be an issue for similar platforms offshore California and is taken into account in seismic analysis.

2.10 JOINTS SELECTED FOR FURTHER TESTING

Several joints and material samples were identified during the onshore inspection to be saved for possible use at a later date in a testing program. This included damaged as well as intact joints. The joints were trucked to a Chevron yard in the new Orleans area and put in storage at a Chevron yard. Appendix A contains photos of the specimens selected for further testing.

The intent of such a program would be to test the samples in order to determine material strength and characteristics of the steel material typically used for this vintage of platforms. The damaged samples could be further inspected by material experts to help define the method of failure and why failure occurred. The intact specimens could be tested to failure in order to determine strength characteristic of these joints.

Such testing would require a large facility capable of handling and testing the large test specimens. The testing program would be similar to the Damaged Brace JIP performed by PMB and Texas A&M in 1990.

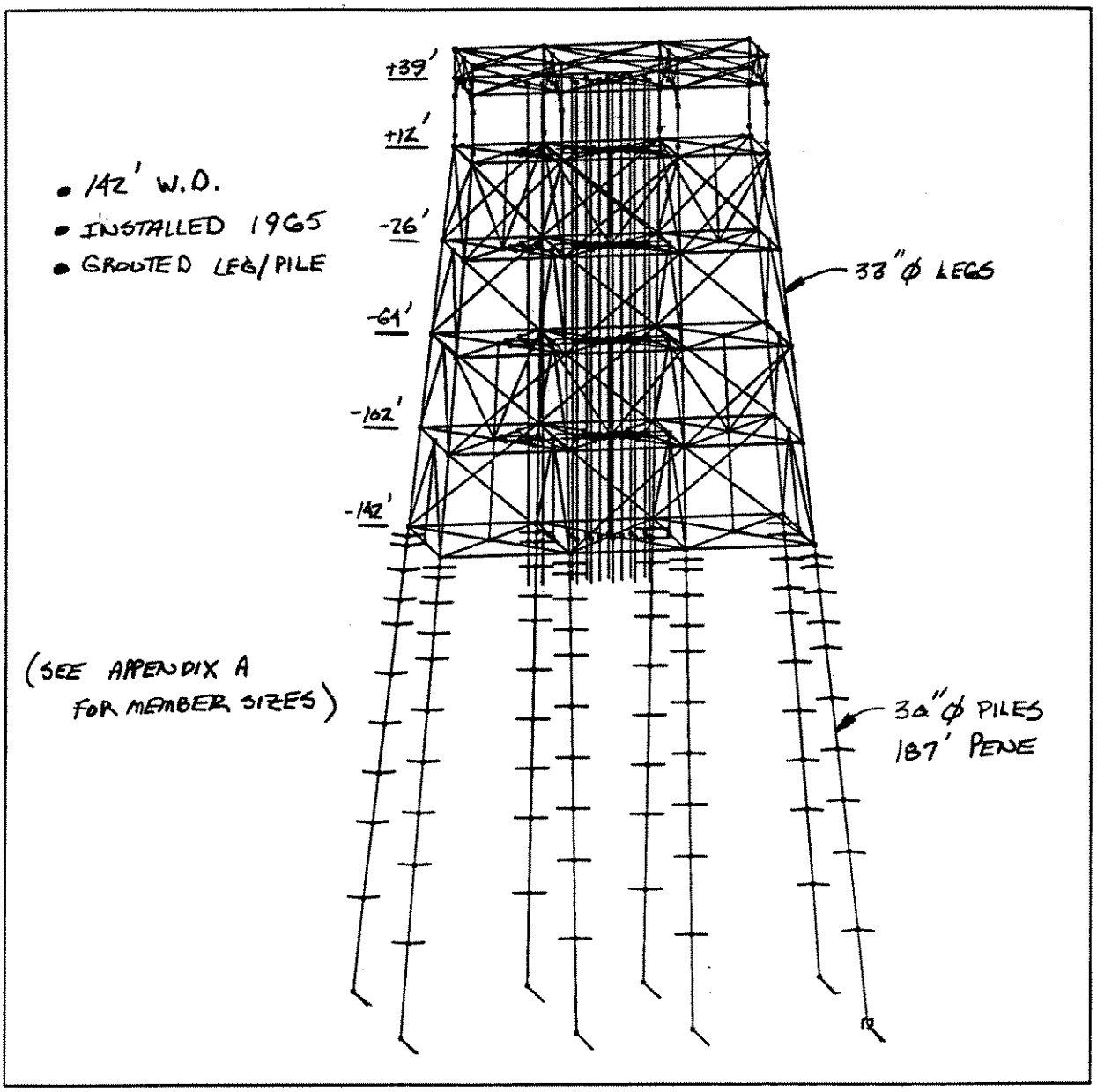

Figure 2-1 Platform ST 177 B - General Configuration

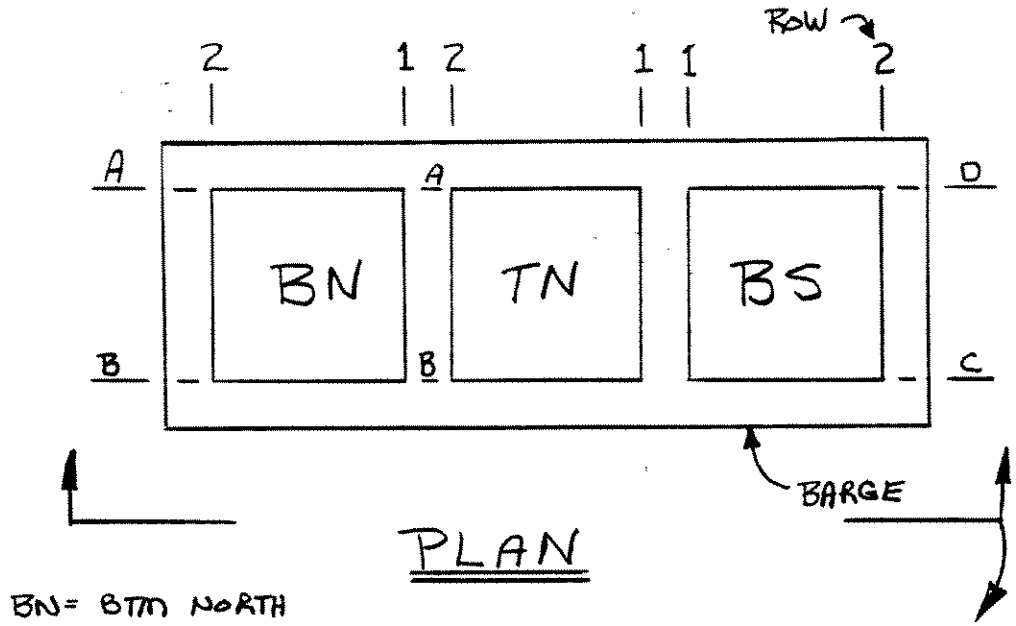

PLAN

BN = BTM NORTH
TN = TOP NORTH
BS = BTM SOUTH

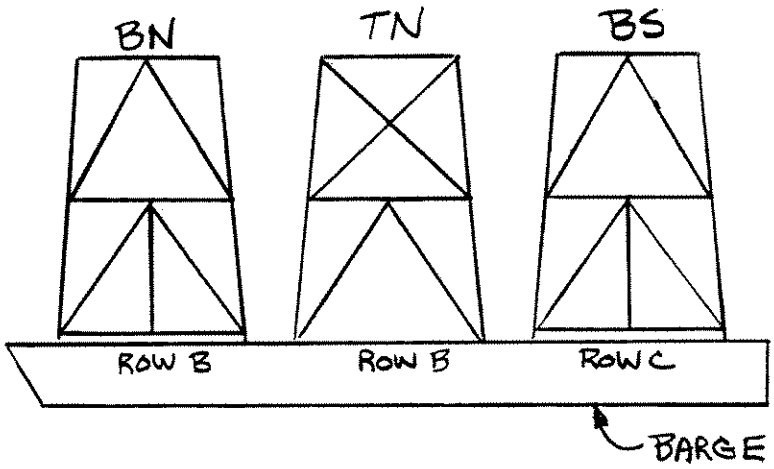

ELEVATION

Figure 2-2 View of Platform Sections

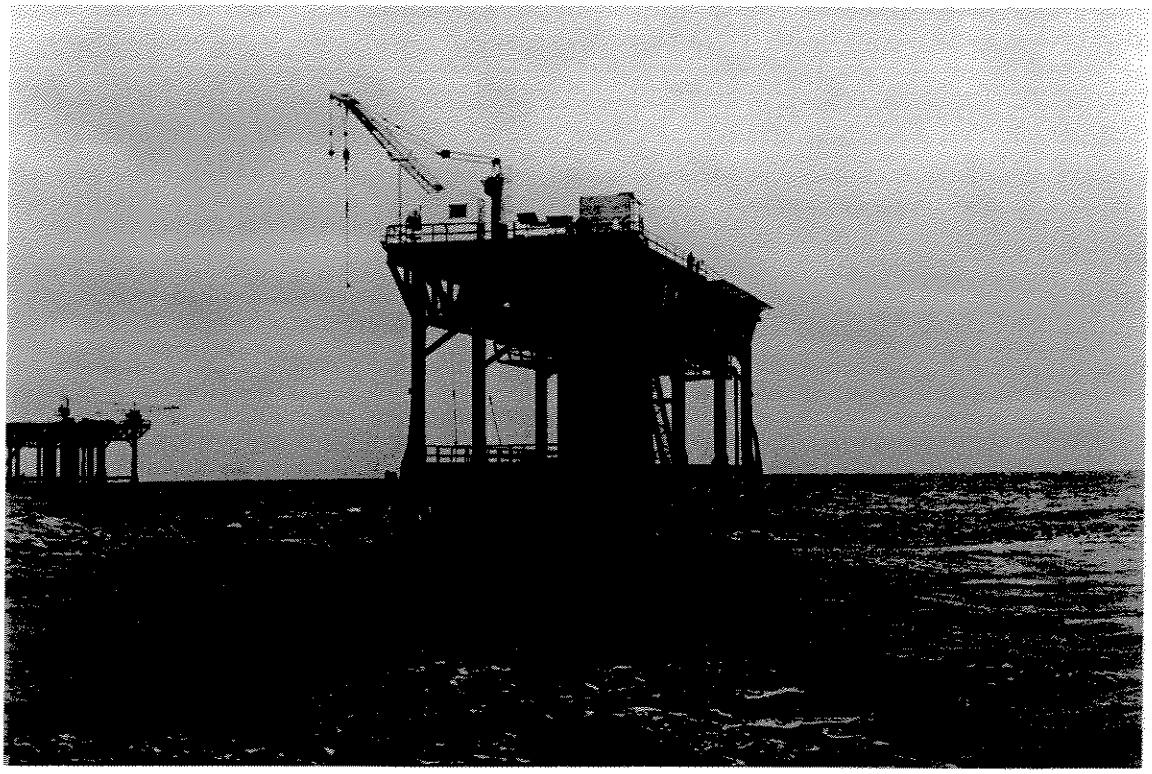

Photo 2-1 ST 151 K - Similar Configuration to ST 177 B

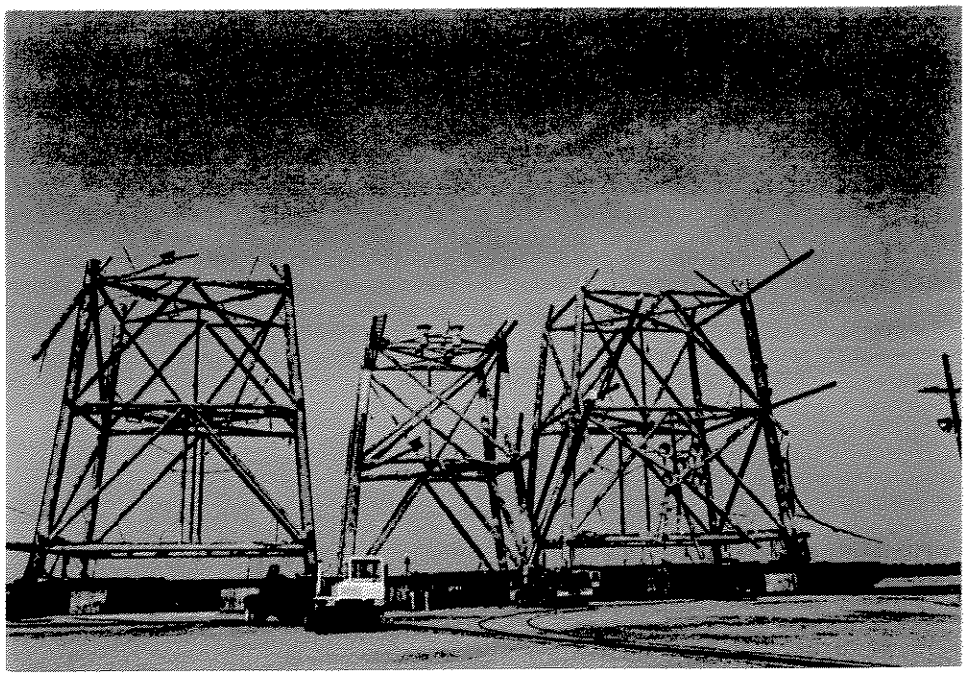

Photo 2-2 Broadside View of Platform Sections

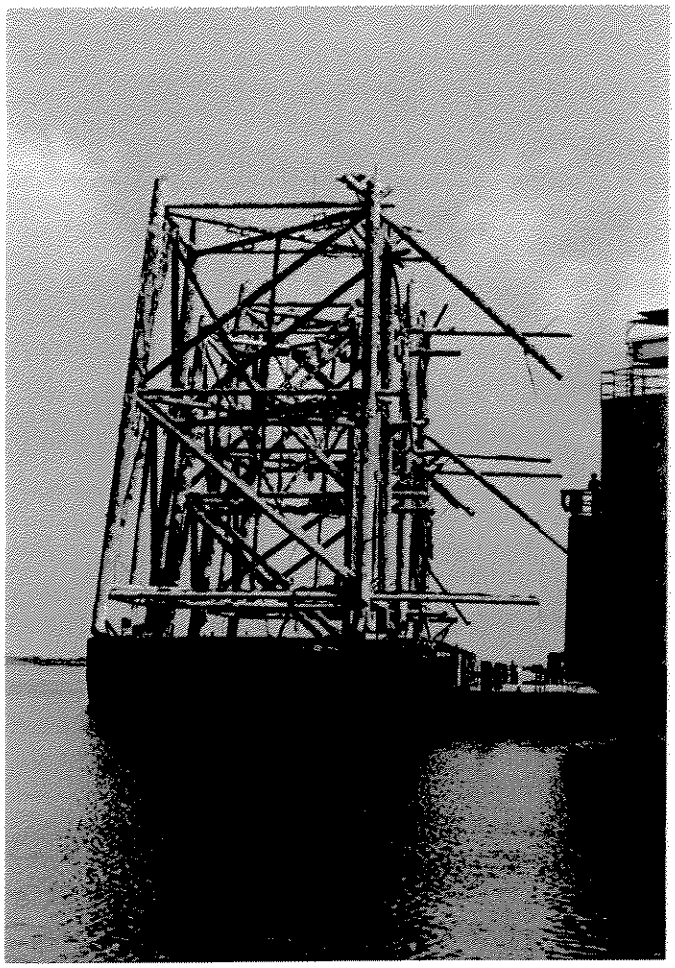

Photo 2-3 End-On View of Platform Sections

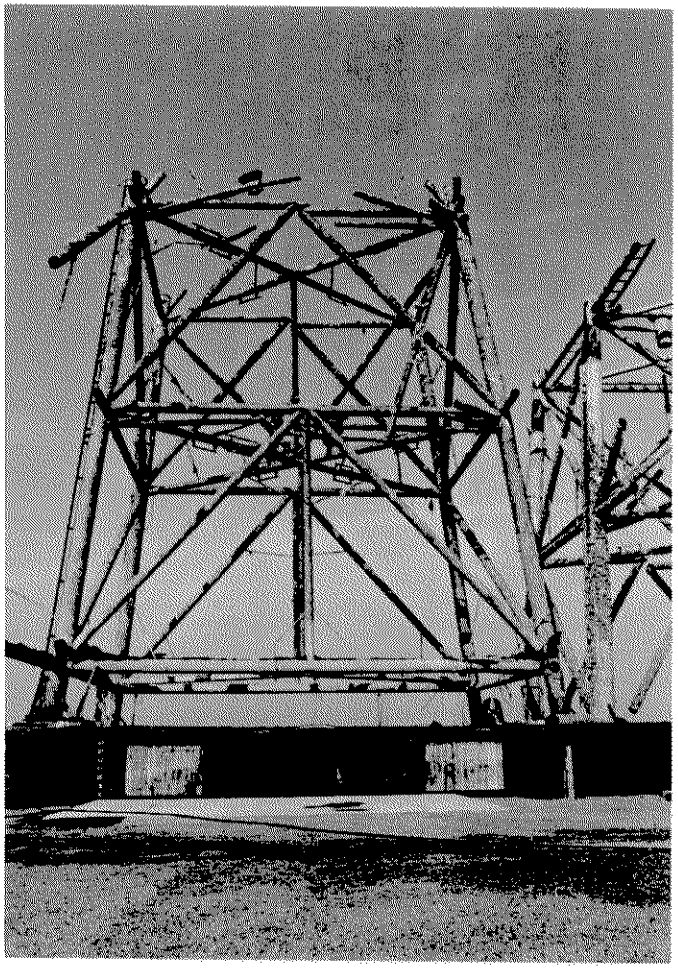

Photo 2-4 Closeup view of Section BN (Bottom North)

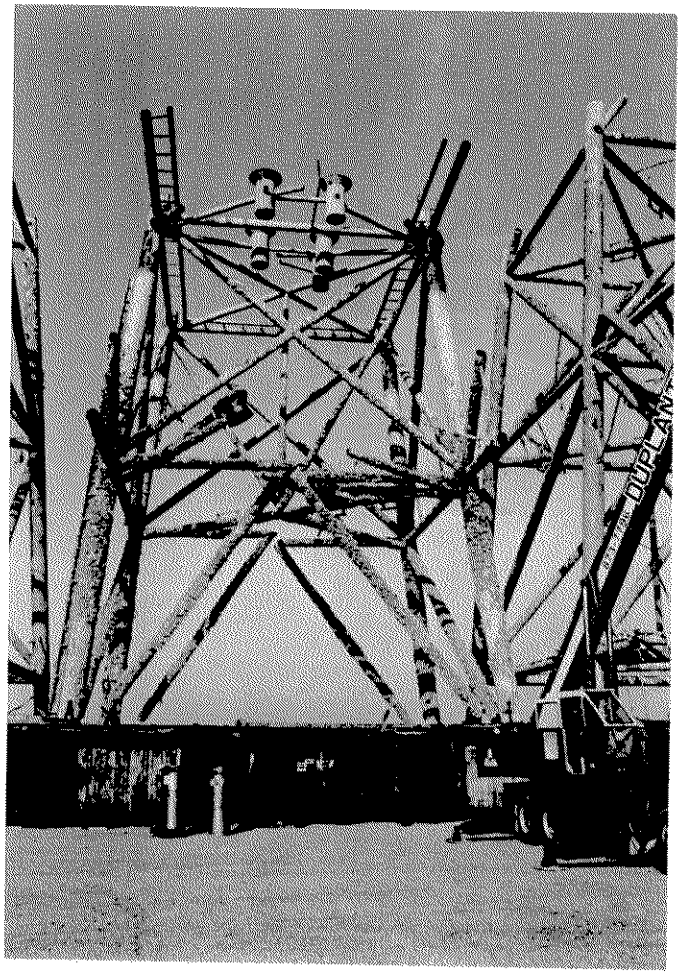

Photo 2-5 Closeup View of Section TN (Top North)

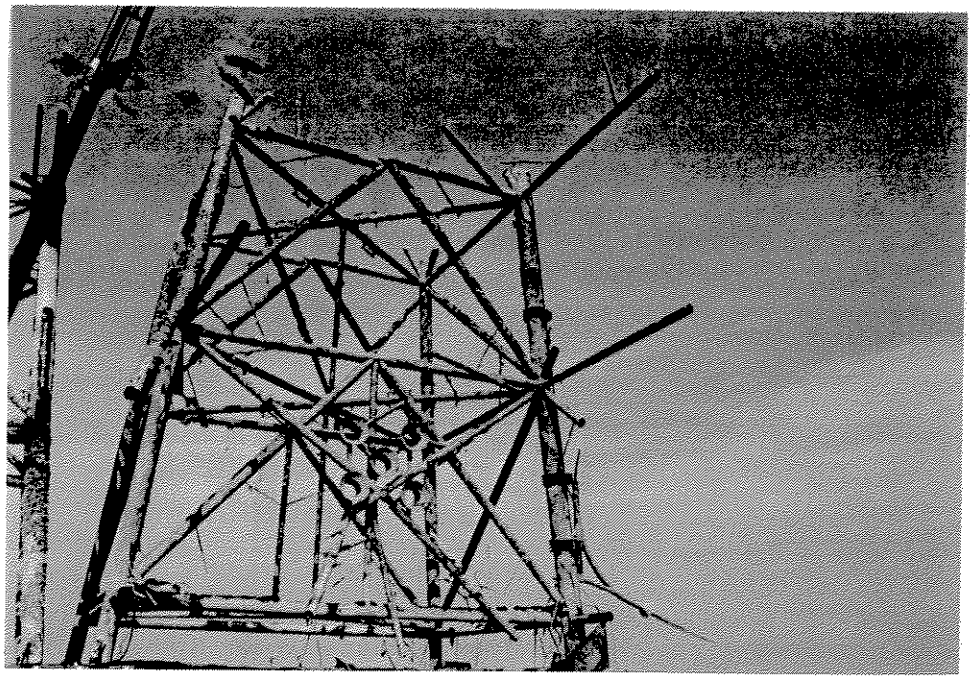

Photo 2-6 Closeup View of Section BS (Bottom South)

Photo 2-7 Damaged X Joint Row 2

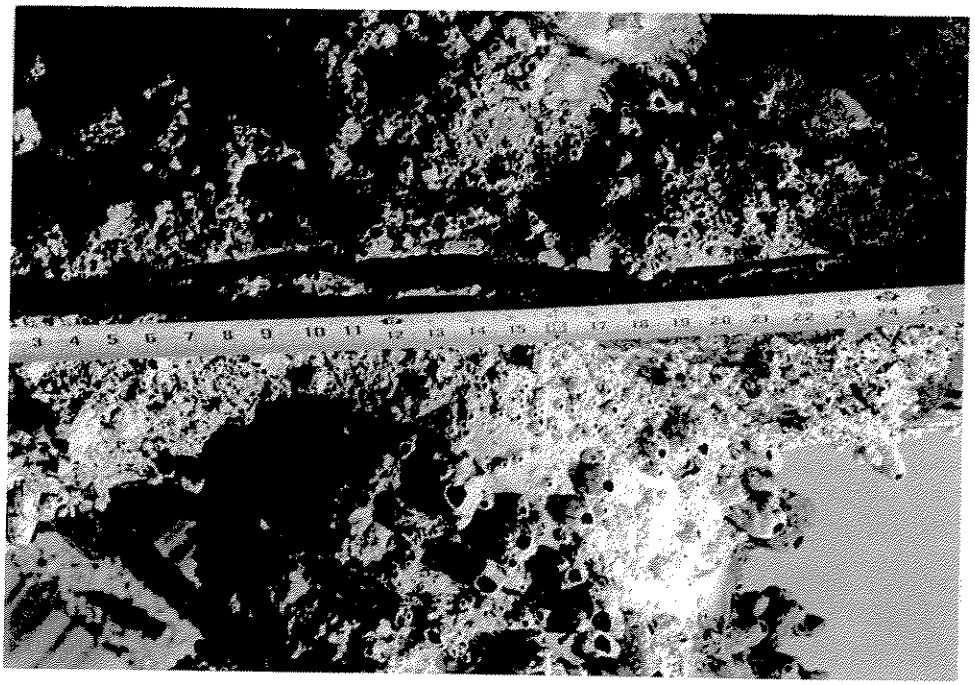

Photo 2-8 Closeup of X Joint Crack

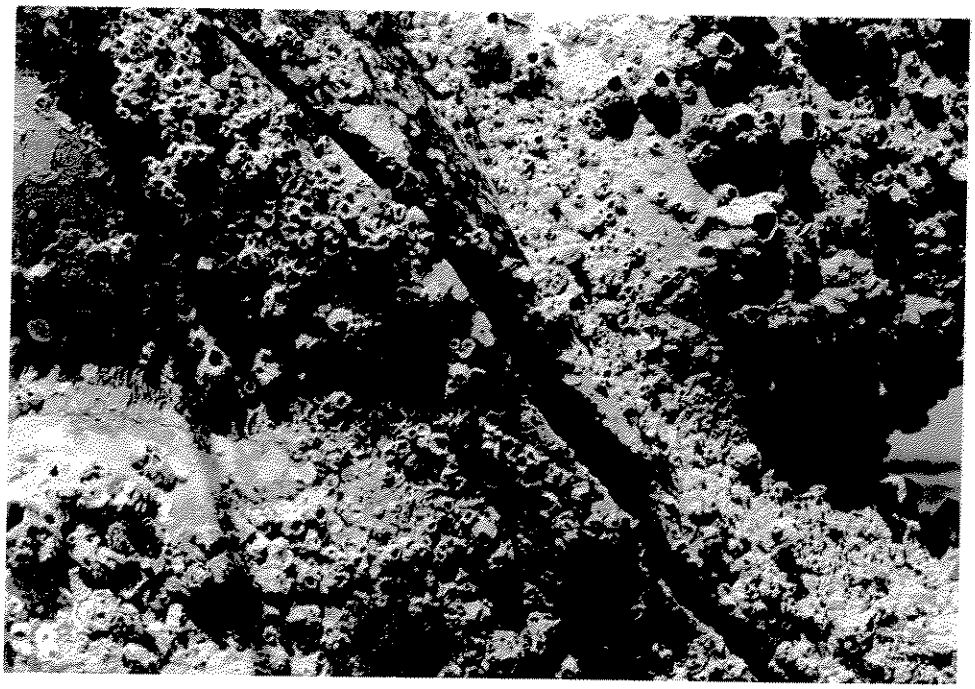

Photo 2-9 Closeup of X joint Bulge

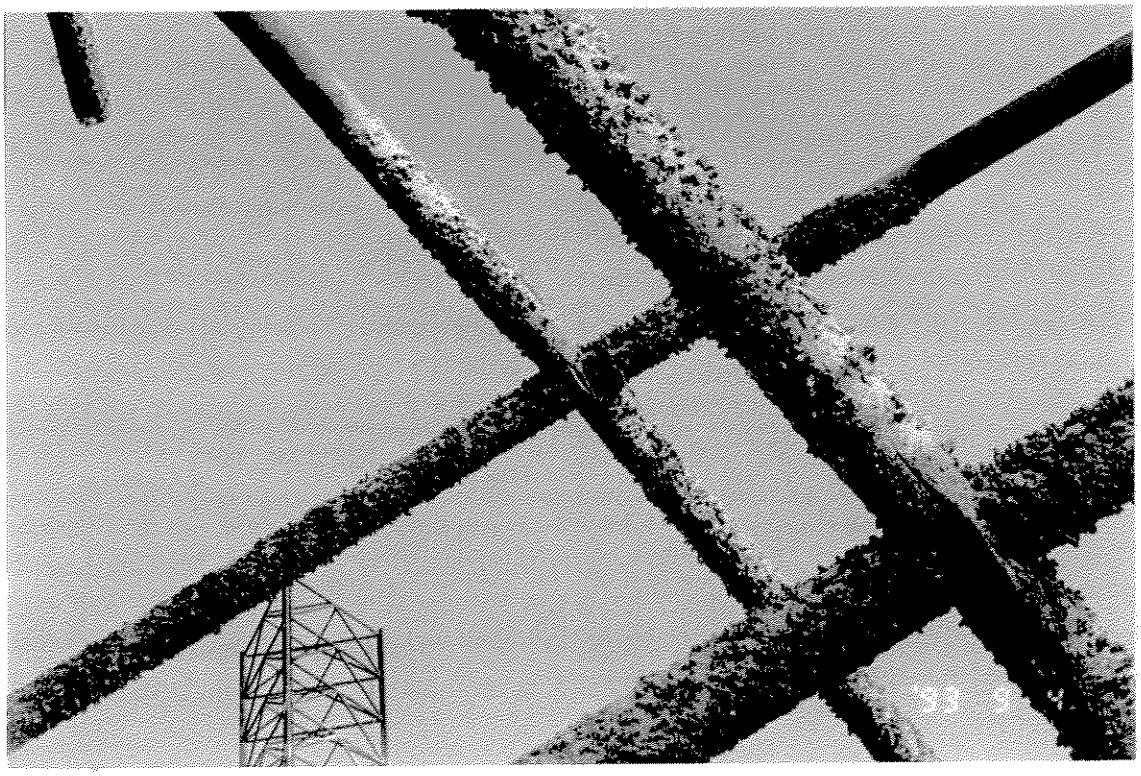

Photo 2-10 B AUX X Joint Crack

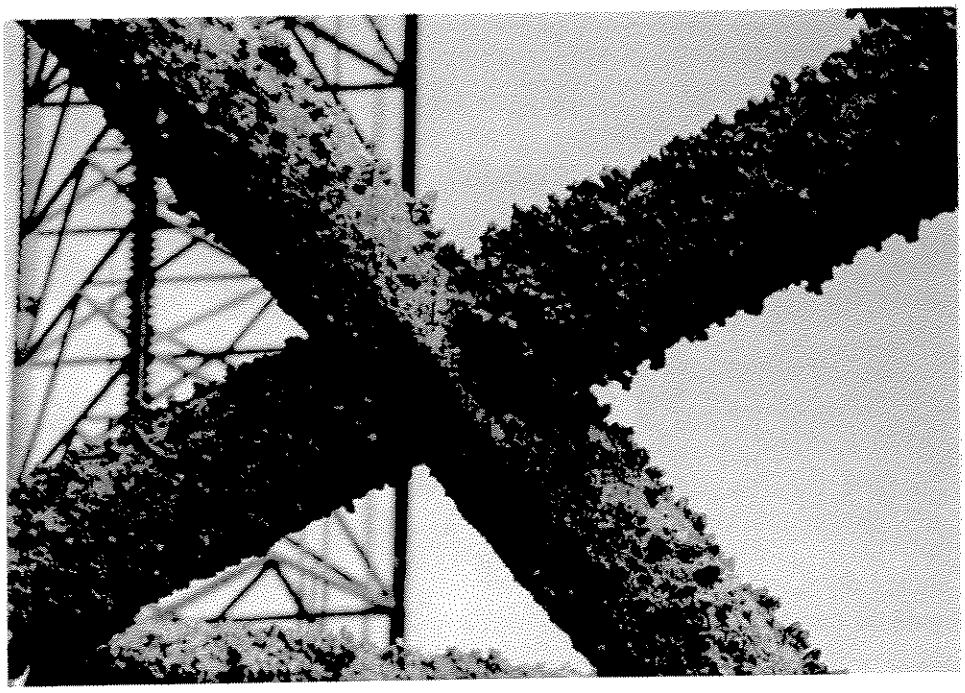

Photo 2-11 Closeup of B AUX X Joint

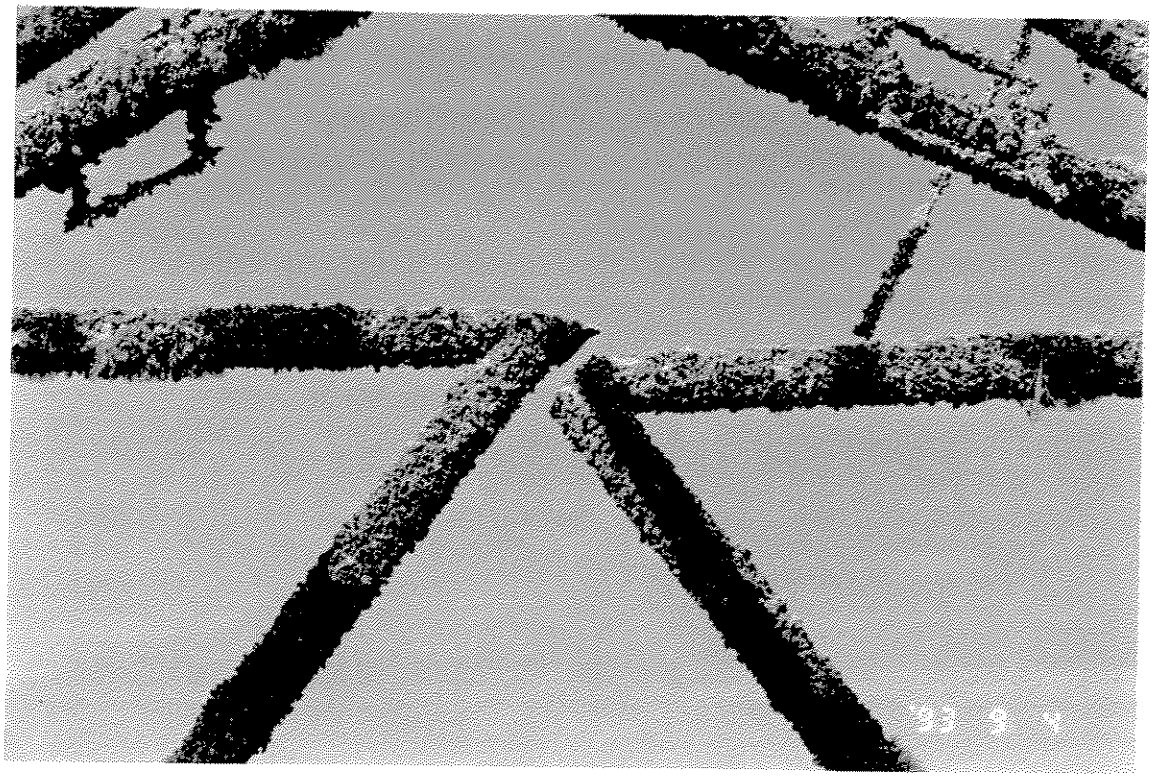

Photo 2-12 K Joint Row A (TN)

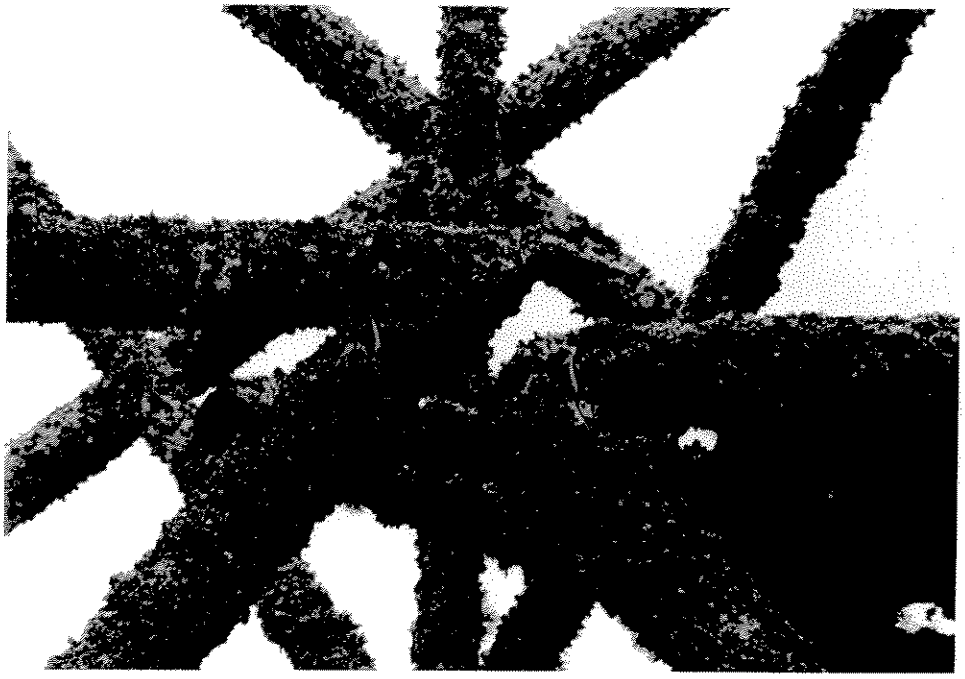

Photo 2-13 K Joint Row B (TN)

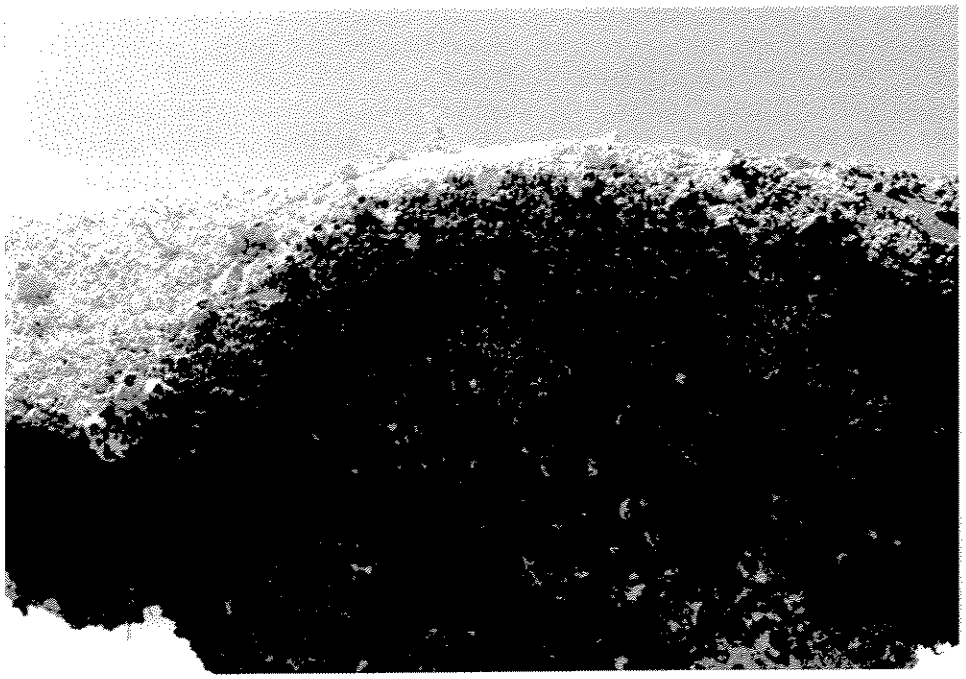

Photo 2-14 K Joint on BS (Compression Side)

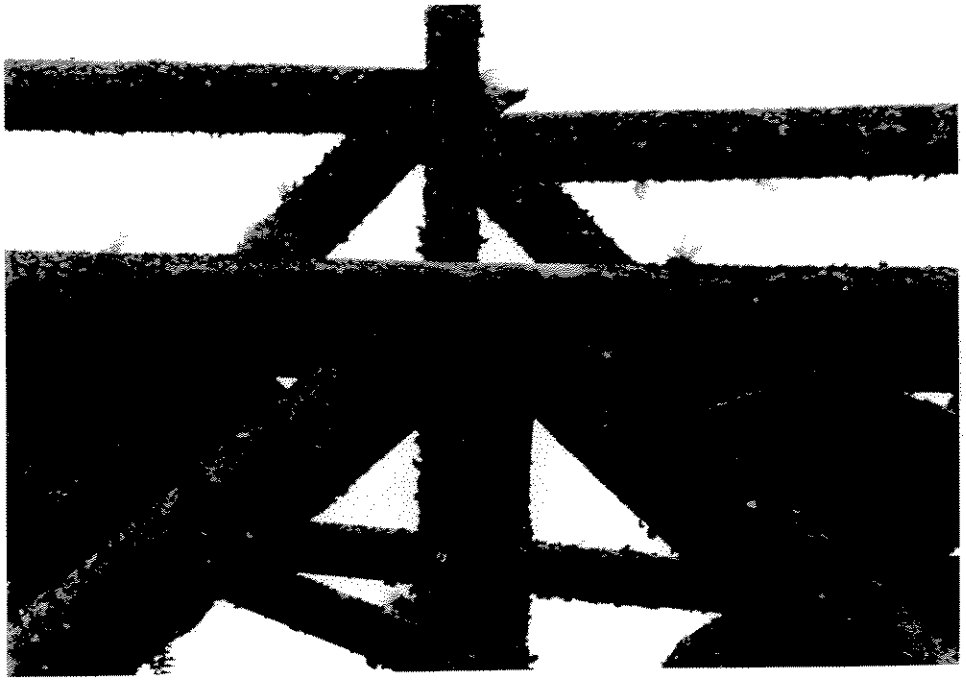

Photo 2-15 Interior KT Joint Row B (BN)

Photo 2-16 Closeup of Interior KT Joint Row B (BN)

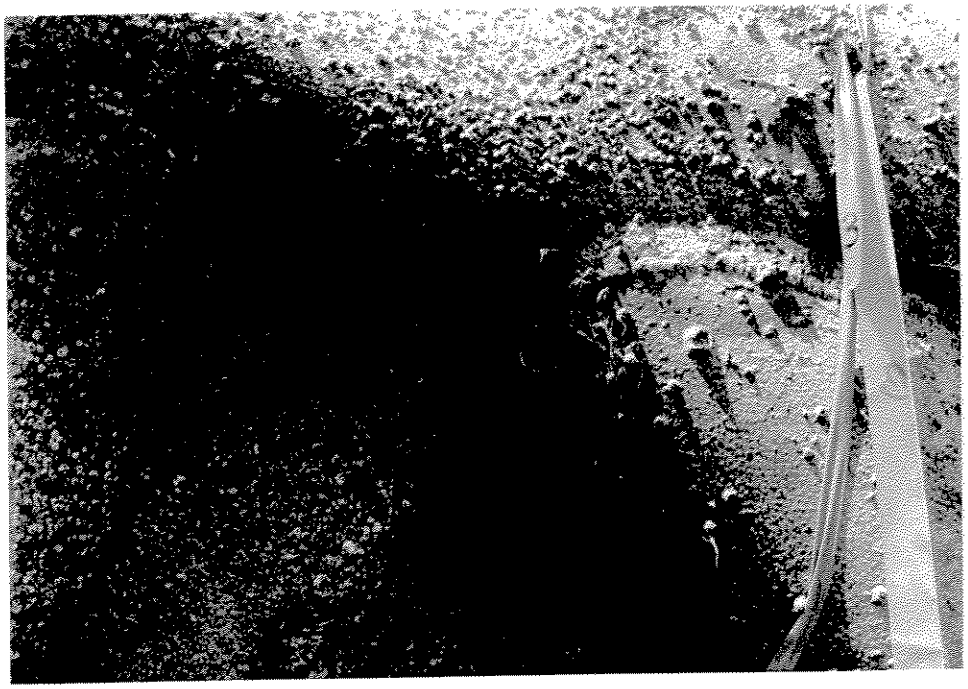

Photo 2-17 Closeup of Crack on Interior KT Joint Row B (BN)

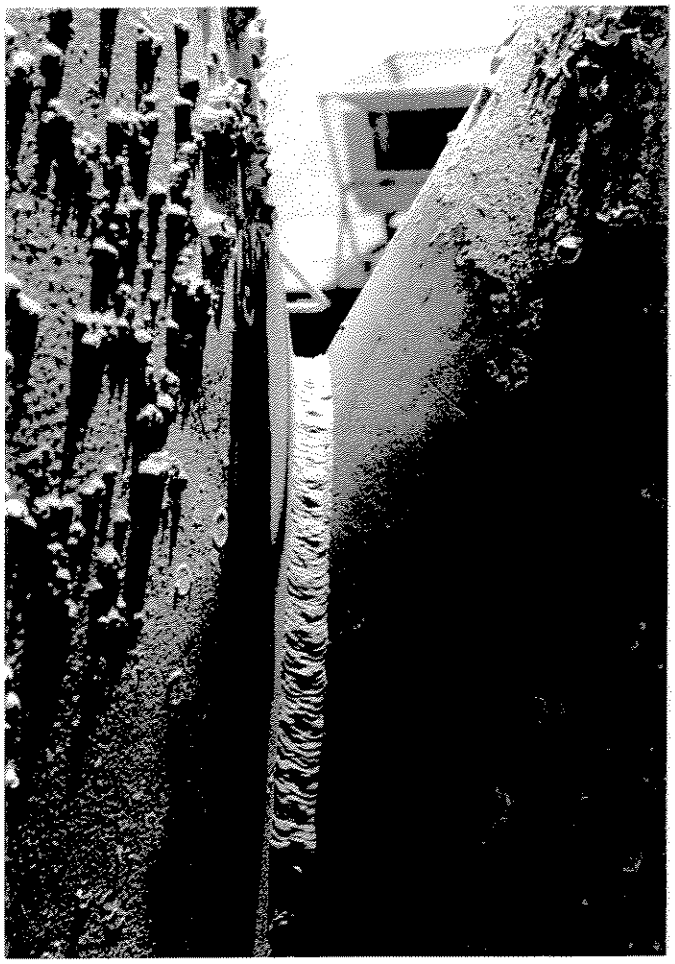

Photo 2-18 Cleaned Joint at B1 - Tension Brace

Photo 2-19 Cleaned Joint at B2 - Compression Brace

Photo 2-20 View of Leg B2 (BN)

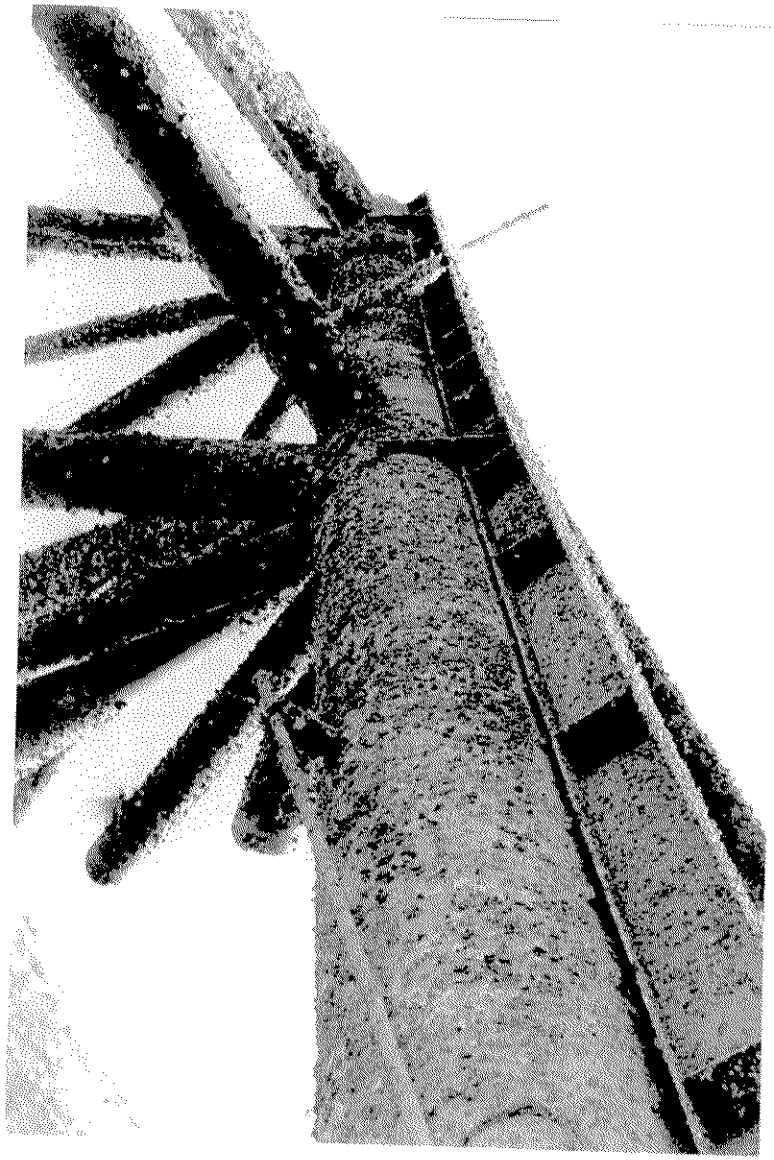

Photo 2-21 View of Leg B1 (BN)

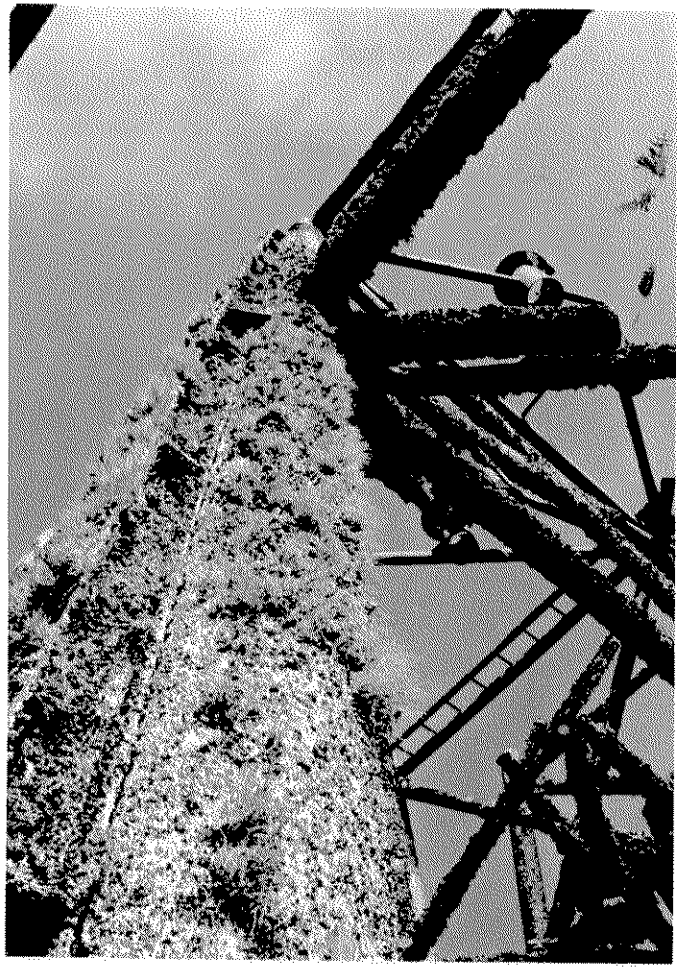

Photo 2-22 View of Leg B2 (TN)

Photo 2-23 View of Leg B1 (TN)

Photo 2-24 View of Leg D1 (BS)

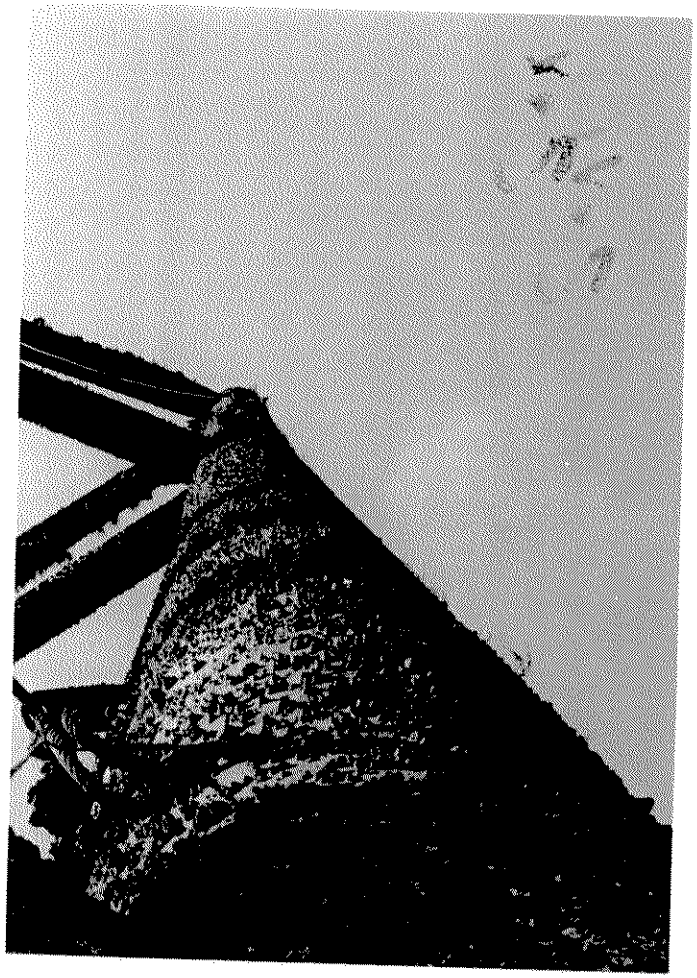

Photo 2-25 View of Leg D2 (BS)

Photo 2-26 Cleaned Compression Joint at Mudline

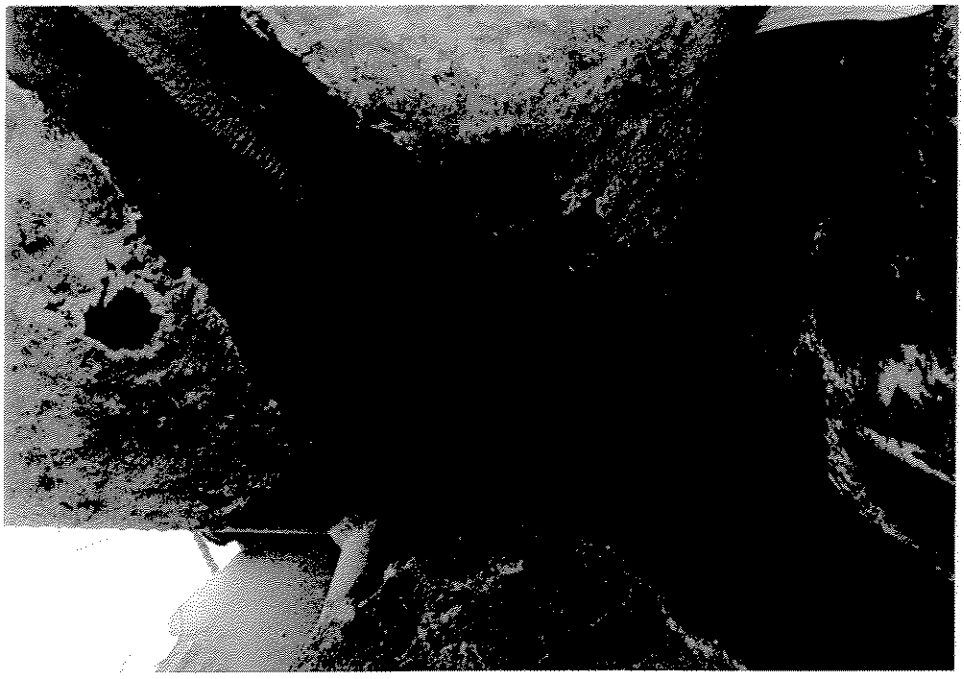

Photo 2-27 Cleaned Tension Joint at Mudline

Photo 2-28 Cleaned Complex Joint at Mudline Leg B2

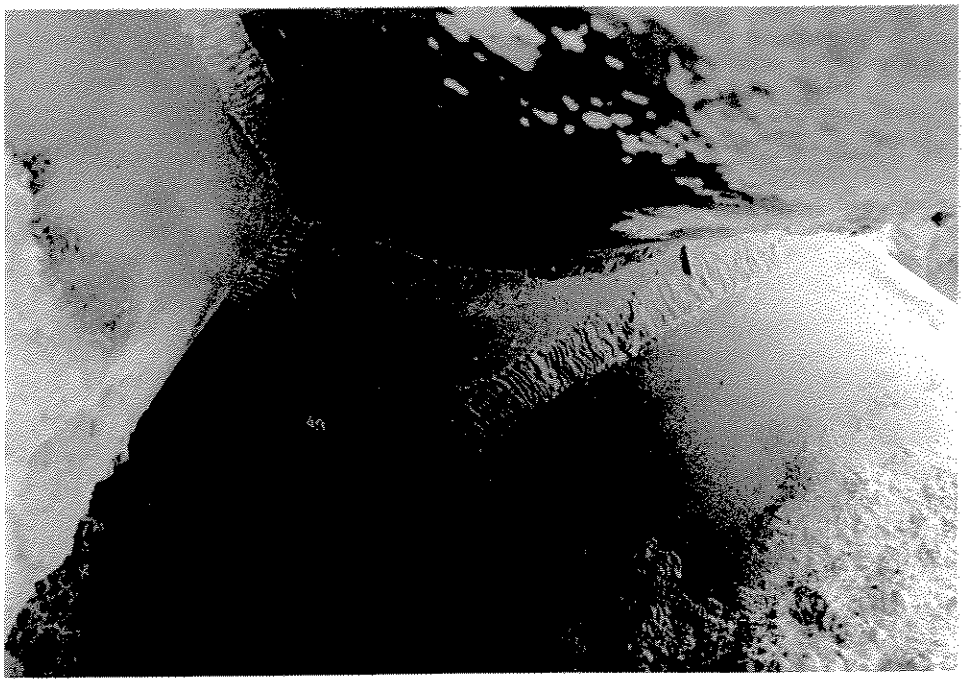

Photo 2-29 Cleaned Complex Joint at Mudline Leg A1

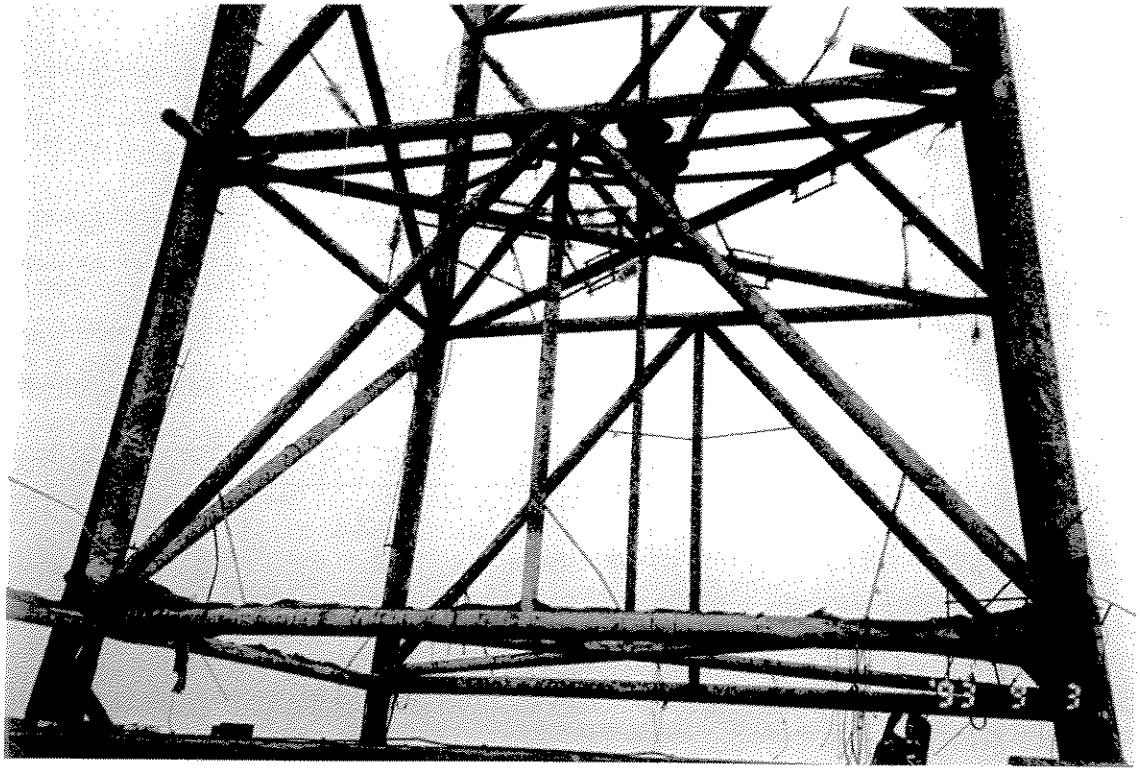

Photo 2-30 Support for Original Platform Anode

Photo 2-31 Retrofit Anode

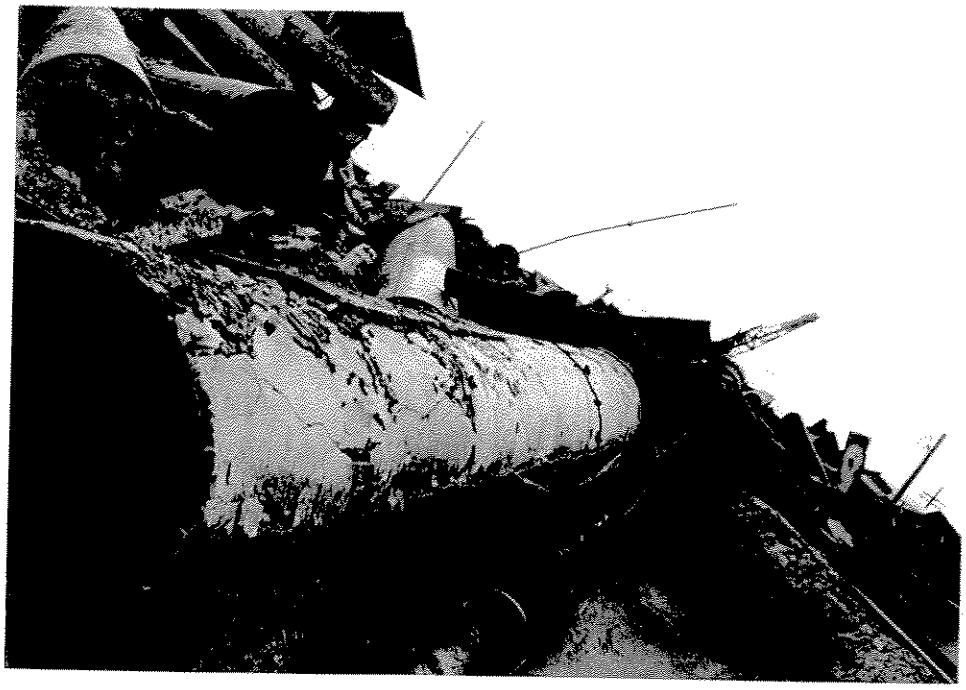

Photo 2-32 Leg Section Showing Grout

Photo 2-33 Conductor Section

SECTION 3 COMPUTER ANALYSIS

3.1 INTRODUCTION

A CAP (Capacity Analysis Program) model was created of the ST-177B structure, based on the model provided by Chevron and updated by PMB for the Andrew JIP (PMB, 1993). Pushover analyses were performed using environmental loads generated based on the most severe hour of Hurricane Andrew. A set of analyses of increasing sophistication were performed and their results compared in order to determine the effect of analysis assumptions.

The following analyses were performed:

- Basic Model

  Full nominal soil strength, elasto-plastic joint failure.

- 50% Increase in Soil Strength

  Same as the basic model, except that the soil strength is increased by 50%. This is intended to investigate possible conservatism in the API RP 2A soil strength recipe.

- 100% Increase Soil Strength

  Same as the basic model, except that the soil strength is doubled. These soil properties are used for all subsequent analyses.

- Soil Nodes Fixed

  All nodes below the mudline fixed to determine the platform capacity based upon the jacket only.

- Brittle K-Joints

  Same as the 100% Increase Soil Strength model except that the K-joints are modeled to fail in a brittle fashion.

3.2 DESCRIPTION OF MODEL

A plot of the model is shown in Figure 3-1.

3.2.1 Substructure

The substructure was modeled explicitly, with the following exceptions and comments:

- Joint cans were neglected.
- Risers and caissons were neglected.

All material was assumed to be A36 steel, with a mean yield strength of 42 ksi.

3.2.2 Superstructure

The deck legs above the top of jacket were modeled explicitly, including the deck legs through the deck section. The remaining deck framing was replaced with stiff vertical and horizontal X bracing to minimize the size of the computer model.

The deck weight was 500 kips.

3.2.3 Conductors

The fourteen conductors were modeled explicitly. Equivalent linear beams were substituted for conductors below the mudline, based upon previous work in the Andrew JIP.

3.2.4 Piles and Soil

The piles are 30 inches in diameter and have a penetration of 180 feet. Soil properties used for the analysis were based upon a soil boring at the ST 151 K site. These are the same soil properties as used in the Andrew JIP.

The nonlinear lateral p-y, vertical t-z and tip q-z pile-soil properties were based upon the API RP 2A recipe, and were automatically generated by CAP.

3.2.5 Element Types

The following element types were used for the various portions of the basic model:

- Legs, Piles and Plan Horizontals: nonlinear beam-column elements, with plastic failure

behavior appropriate for A36 steel (i.e., the stiffness softens for a while before fully plastic behavior is reached)

- Longitudinal frame diagonal braces: brace capacity controls in this loading direction therefore the model used buckling Marshall struts which shed load following initial yield.

- Transverse frame K and X braces: joint capacities control in this loading direction therefore the model used nonlinear truss elements with capacities adjusted to reflect calculated joint capacity. In the earlier models, elasto-plastic truss elements were used which sustain a constant load following initial yield. In the later analysis, elastic-brittle truss elements were used which shed all load immediately following initial yield.

- All members expected to behave linearly (deck, plan bracing): linear beam elements

3.3 ENVIRONMENTAL LOADS

The environmental loads were based on the Oceanweather Hurricane Andrew Hindcast (Oceanweather, 1992) for the worst hour of the storm. The specific criteria is as follows:

- Maximum wave height = 60 ft
- Associated peak spectral period = 14 sec
- Associated current velocity = 3.46 ft/sec
- Maximum wind speed = 158 ft/s
- Environmental direction = 267 deg off true north, or 302 deg off project north

The following assumptions were made, based on API RP2A, 20th edition:

- Storm tide and surge = 2 ft
- Current blockage factor = 0.85 (for diagonal direction)
- Current profile is constant
- Wave spreading factor = 0.88
- Conductor shielding factor = 0.60

- Marine growth profile per on-shore visual inspection. Assume constant 1.5 inches on radius down to elevation -102 ft, then tapering down to no marine growth at the mudline

- Drag coefficient = 1.05 (0.65 for smooth members), inertia coefficient = 1.2 (1.6 for smooth members)

The wave reaches approximately five feet into the subcellar deck. Using API Preliminary Deck Force Guidelines (API, 1994) the calculated wave-in-deck load is 676 kips. This load is assumed to be divided equally at the cellar deck level among the eight legs.

Wind load on the deck was calculated using API RP2A 20th recommendations. The total wind force was 15 kips.

The combined wave and current load generated by CAP based on the above assumptions was 3875 kips, with the majority caused by the wave.

The resulting total environmental load used in the pushover analysis is 4566 kips. In the pushover analysis results, the "load ratio" is the actual pushover load divided by this load.

3.4 MEMBER AND JOINT CAPACITY CALCULATION AND MODELING

3.4.1 Member Failure Mode Determination

Joint capacities for the X- and K(and KT)-joints were calculated as discussed below. The broadside frame diagonals are not affected by joint capacity as the legs are fully grouted.

For the transverse frame X and K braces, the yielding and buckling capacities for the members were calculated, and it was found that joint capacity controls for these elements. Thus, these braces were modeled using nonlinear truss elements with adjusted yield capacity.

For the broadside frame diagonals, the yielding and buckling capacities were calculated, and it was found that buckling controls. Thus, these braces were modeled using buckling Marshall strut elements, which automatically model the braces' buckling behavior.

4.4.2 Joint Capacities

Joint capacities were calculated for the X and K joints in the transverse frames. The API RP 2A joint capacity equations were not used because they represent a lower bound, not mean, capacity, and even with that difference accounted for, they are overly conservative according to later laboratory test results (the API equations are based on tests performed before 1980). Thus, a more recently-derived set of joint capacity equations were used. A summary of the

approach is described below. More specific details are provided in Appendix B.

The X- and K-joint capacities were calculated using the formulas presented in a pair of papers, OTC 4189 (Billington, Lalani and Tebbett, 1982) and BOSS '88 (Ma and Tebbett), with API's Q_f term added to account for the effects of chord stress (as these papers do not study the effects of chord stress). Based on the drawings, it was determined that the brace members were the compression portion of the X, and the chord members were the tension portion of the X; thus the axial compression, not tension, formula is applicable. The out-of-plane bending formula was also used, as discussed below. Because the braces are modeled as truss elements, their in-plane bending moment is not modeled; however, this moment component is expected to be small and not significantly affect the behavior of the brace or structure.

The joint capacities were modeled by adjusting the yield stress of the brace elements so that they fail at the appropriate load level. This effective yield stress was adjusted to account for the effects of chord stress and lateral hydrodynamic forces according to the following methodology:

(1) Estimate the stress level in the chord in order to calculate a preliminary Q_f factor for use in the joint capacity equations. Calculate the axial capacity and out-of-plane bending capacity.

(2) Estimate the maximum water particle velocity (maximum wave-induced plus current with blockage) at the brace's average water depth.

(3) Given the element length, estimate the brace-end moments due to the drag force on the element. Assume partially fixed ends (i.e. the moment is 1/10 of the distributed load time the length squared). Assume a drag coefficient of 1.05 (for rough members with marine growth). For X braces, take the full length of each brace, not the half-length, because the crossing brace does not provide much restraint against out-of-plane bending.

(4) Use the API RP 2A (20th) axial/bending interaction equation. For simplicity, assume the moment calculated in the previous step is out-of-plane (which is close enough to correct). Find the axial force at combined axial/bending failure with this moment, based on the axial and out-of-plane bending capacities calculated in the first step. Take this to be the effective axial capacity for the element.

(5) After the analysis, determine the actual stresses in the chord at the end of the load step when the adjacent brace fails. Each of the three chord stresses (axial, in-plane bending, out-of-plane bending) should be calculated as the average of the stresses in the two adjacent chord elements, accounting for sign. If the combined (SRSS) stress is not close to the one originally estimated in the first step, go back to the first step with these improved chord stresses and repeat.

For the base case analysis, it was found that the chord stresses converged in one iteration (in addition to the original time through). A second iteration was performed to verify convergence. For the next several analysis cases, the chord stresses at failure were checked, and they were found to be close to the ones found in the base case. Thus, for the remainder of the analyses, the same joint capacities were used.

3.4.3 Brittle Joint Failure

The Andrew JIP modeled joint failure in an elastic perfectly plastic mode which allows the joint to continue to carry load following initial yield (which occurs at a load level determined by the above joint capacity equations). This assumption was based upon earlier modeling of joint failures at legs where the member would tend to punch into the leg in a ductile mode and not to separate from the leg. Figure 3-2 shows a typical force deformation curve for an elastic-plastic failure mode. The elastic-plastic approach to modeling joints has also been used in other platform assessment studies (Imm, 1994).

However, based on the inspection results, the K-braces in this structure fail in a brittle fashion, i.e. the joint fails completely and cannot carry any load. Thus, in order to improve the platform models, the K-braces were replaced in the later analysis with brittle truss elements, which fail completely and cease to carry load after they reach their effective yield stress. Figure 3-2 also shows a typical force deformation curve for an elastic-brittle failure mode.

3.4.4 Brittle Joint Modeling

The K-joint failures observed in ST-130A and similar structures actually involve the entire joint, not just the braces; when the joint failure occurs, the chord shears completely through between the tension and compression braces. For the analysis cases which model this brittle failure of the entire K-joint, another iterative solution was used, in which one of the two adjacent chord elements was replaced with a yielding beam-column element, which would experience a complete brittle failure soon after yielding, which effectively destroys the load path through the joint.

First, an analysis was performed in which each chord beam-column element was given an arbitrarily high yield stress to preclude it from failing. The actual axial force and bending moments at the ends of each beam-column chord, at the end of the load step when the adjacent brace fails, were obtained. Based on these forces, an effective chord yield stress was calculated which would cause the chord to yield by the end of the load step in which the brace fails. The analysis was then rerun with this yield stress in the chord. The result is that the chord member fails at approximately the same load level as the brace member, resulting in a complete loss of the load carrying capability through the joint as observed in the inspection.

3.5 ANALYSIS RESULTS

3.5.1 General Results

A summary plot of the pushover load ratio as a function of deck Y-direction lateral displacement for all major analyses is shown in Figure 3-3. As described below, the model containing the 100% soil increase and the brittle joints appears to most accurately match the observed platform performance in Andrew.

Analysis results presented in the following sections include inelastic event plots. These plots indicate which model elements have experienced non linearity - yielding or other failure. For beam column elements, a small dark "blot" at one end of the element indicates that first yield has been reached at that end. Further softening events, which approximate fully plastic behavior, are indicated by larger-diameter "blots". (In analysis cases with brittle failure of beam-column elements, these elements fail very soon after first yield. After brittle failure, the relevant member ends are marked with larger sized "blots".)

Analysis results also include plots of pushover load ratio versus lateral deck displacement. Displaced shape plots show the deformed shape of the platform following significant member failures. For all of the displaced shape plots, the displacements have been exaggerated 20 times.

3.5.2 Basic Model

The capacity of the basic model is 0.87 times the Hurricane Andrew environmental pushover load. The displaced shape at first yield is shown in Figure 3-4. The first yield is the joint of the X brace near the top of jacket (brace with dashed line). Yielded and failed elements with the corresponding displaced shapes for an intermediate step is shown in Figure 3-5, indicating failure of several X braces and initial lateral failure of one of the piles. The final results indicated that there was substantial yielding in all of the piles with lateral pile failure defining the platform failure mode.

The pushover load plot is shown in Figure 3-6, with major events indicated. The general behavior is a gradually, fairly smooth, decreasing stiffness, with no abrupt changes in behavior until the pile failure. The first elements to fail are the compression X-braces at a load level of 0.67 times the total environmental load. The piles begin to yield at a load ratio of 0.83. None of the K-braces fail in this analysis.

As described in Section 2, the onshore inspection of the platform revealed severe damage to almost all of the K braces, yet the computer analysis indicated no joint failures other than the upper row of X braces. The foundation appears to be controlling the platform failure

mechanism. It was therefore decided to arbitrarily increase the foundation strength by first 50% and then 100% to see if the failure mode could be "forced" into the jacket as was observed following Andrew. The next sections describe these analysis.

3.5.3 Soils Improved 50%

The capacity of the model with soils improved 50% is 1.01 times the Hurricane Andrew environmental pushover load, or about 16% greater than the basic model's capacity. The element failure sequence was very similar to that of the basic model (no soil strength increase) with lateral failure of the piles again being the platform failure mechanism. However, late in the analysis there were some failures of the several K braces just below the elevation with the X brace failures.

The pushover load plot is shown in Figure 3-7, with major events indicated. All of the compression X-bracing between the fourth and fifth level bays fail, as do the interior compression diagonals between the third and fourth level bays. The X-braces begin to fail at a load level of 0.69 times the total environmental load. The piles begin to yield at a load ratio of 0.87 and the compression diagonals (K-braces) begin to fail at a load ratio of 0.97. The failure of the compression diagonals at a load ratio of 0.97 implies that the strengthening of the soil succeeded in moving failures into the jacket as observed in Andrew.

3.5.4 Soils Improved 100%

The capacity of the model with soils improved 100% is 1.15 times the Hurricane Andrew environmental pushover load or about 32% greater than the basic model's capacity. The displaced shape intermediate load step where there is some initial pile yielding and where several braces have failed is shown in Figure 3-8. The platform failure mechanism was again lateral failure of the piles.

Although the global failure mechanism was in the foundation, there were a considerable number of failures in the jacket. All of the compression X-braces fail, as do all compression K-braces in the third level (from the mudline). Three of four compression diagonals failed in the first level, as did one interior diagonal in the second level.

The pushover load plot is shown in Figure 3-9, with major events indicated. The general behavior is that of a gradually, smoothly decreasing stiffness, with no abrupt changes in behavior. The X-braces start to fail at a load ratio of 0.69 times the total environmental load. The piles start to fail at 0.83 times the total environmental load. The K-braces start to fail at 1.01 times the environmental load and the legs start to fail at 1.11 times the environmental load. With the exception of the legs, all of the other elements that fail are failing or yielding at consistent load levels with the previous analyses.

3.5.5 Soil Nodes Fixed

The intent of this analysis was to determine the member failure sequence in the jacket when the foundation is eliminated from the model to see if the failures correspond to the observed failures.

The capacity of the model with all soil nodes fixed is 1.55 times the Hurricane Andrew environmental pushover load, or about 78% greater than the basic model's capacity. The displaced shape and first yield are shown in Figure 3-10. The X braces near the top of jacket are the first to yield as seen in the previous analyses with the strengthened foundation.

Figure 3-11 shows the displaced shape at an intermediate load step with all of the X joints failed, K joints failed a the third level (from the mud) and KT joints failed at the lowest level. Figure 3-12 shows the last load step before failure with all of the transverse joints having failed. There is also some initial yielding in the legs near the mudline which ultimately leads to the platform global failure mechanism.

The pushover load plot is shown in Figure 5-13, with major events indicated. The response of the jacket without the foundation soil springs is almost linear even after the compression X-braces have failed and continues until the first level KT-braces begin to yield. After the first level K-braces begin to fail there is a pronounced "kink" in the force-displacement curve as the jacket stiffness significantly decreases. The stiffness continues to decrease as additional K-braces in the upper levels continue to fail and the horizontals also begin to yield. The leg extensions just below the mudline begin to yield after the first level KT-braces yield. The X-braces fail at a ratio of 0.69 times the total environmental load. The KT-braces fail at a ratio of 1.01 times the total environmental load. The level of load at which the X- and K-braces fail is consistent with the previous models with the soil strength increased. The piles just below the mudline begin to yield at a load ratio of 1.17 times the total environmental load and the horizontals begin to yield at 1.39 times the total environmental load.

3.5.6 Brittle K-Joints

The previous analyses demonstrate that a majority of the transverse joints will fail first in the platform provided there is sufficient strength in the foundation. This matches with the observed platform failures. However, the previous models have used an elasto-plastic joint model for XS and K joints which allows for continued load at a joint following failure. For the K joints, this differs from the observed joint failures where the joints were found to be completely severed across the chord. This analysis uses the brittle joint approach as described in Section 3.4. The soil strength was increased to 100% above the basic model.

The capacity of the model with brittle K-joints, joint capacities reiterated (using the previous model's results), and soils improved 100% (in relation to the base model) is 1.19 times the

Hurricane Andrew environmental pushover load or about 37% greater than the basic model's capacity. The displaced shape and first yield are shown in Figure 3-14. The first member failures are again the X braces near the top of jacket. Note that the X braces are still modeled as elasto-plastic elements to match the observed performance of these joints which did not completely sever like the K joints.

Figure 3-15 shows the displaced shape at an intermediate load step. All of the upper X braces have now yielded. The first elevation KT joints and the second elevation K joints have failed in a brittle mode, forcing the load back into the legs for redistribution to other members. There is also some initial yielding due to bending at the two corner legs downstream from the wave direction. Recall that in the platform inspection there was a noticeable curvature to the platform legs in the same direction as indicated by the analysis. There is no indication of yielding in the piles.

Figure 3-16 shows the displaced shape just prior to failure which was controlled by bending failure in the platform legs. The last row of K joints have now failed. There is continued yielding of the corner legs, with yielding indicated along the entire leg length in the K and K region. The leg is still linear in the X brace region.

The pushover load plot is shown in Figure 3-17, with major events indicated. The general behavior is that of a system that suddenly loses a large portion of stiffness when the platform begins to "unzip" as first the X braces then K braces begin to fail. Since the K braces fail in a brittle mode, load is shed to the legs for redistribution in the platform system.

Following failure of the braces, the platform again picks up strength as the legs resist the applied load via frame action. The platform resistance increases to greater than about 1.2 times the Andrew load when system failure occurs as a result of multiple leg failures.

The fact that the multiple brace failures occur at 0.85 times the environmental load implies that this model would have predicted the brace failures observed in Andrew. Additionally, since the platform does not experience global failure at the Andrew load (the legs are still providing resistance) global failure at the computed ultimate capacity, the model's behavior could be correlated to the real case of the platform still standing after Hurricane Andrew, albeit in its damaged-beyond-repair condition.

As compared to the previous models, this model appears to most accurately predict the observed platform behavior in Andrew.

6.0 CONCLUSIONS

The actual failure of the structure involved the shearing of most K-joints and the crushing of the tension members in the X-braces. The structure did not collapse during the storm but lost enough of its load-bearing capacity that it was considered to have failed. There was little or no observable pile failure behavior.

Soil strength is one of the controlling factors in pushover analyses. It seems that an increase of 50% to 100% in the reported soil shear strength will more correctly model field conditions, since models with the increased soil strength demonstrated a better comparison to the observed platform damage.

Another factor is joint modeling. The earlier models used elastic-plastic joint models, with the analytical results not matching that well with observed results. The later analysis results using brittle joints more closely matched the observed platform performance.

When both the soil strength increase and the brittle failure of the K-joints are included in the model, the structure experiences joint failures at a load level below the full Andrew loading, but continues to stand even after the full level of Andrew loading is applied. There is some plastic behavior in the legs of the structure at load levels below the full Andrew loading but no failure mechanism is established at that point.

This corresponds to the actual behavior of the structure, where the K-braces had sheared and the jacket's load bearing capacity was reduced to the bending strength of its legs. The legs had begun to yield but had not completely failed at the Andrew loading, which would correspond with the observed "lean" in the jacket after the storm. Thus, the analytical model that combined the increased strength foundation with the brittle joints, appears to provide a reasonable "recipe" for evaluation of the ST 177 B platform during Andrew.

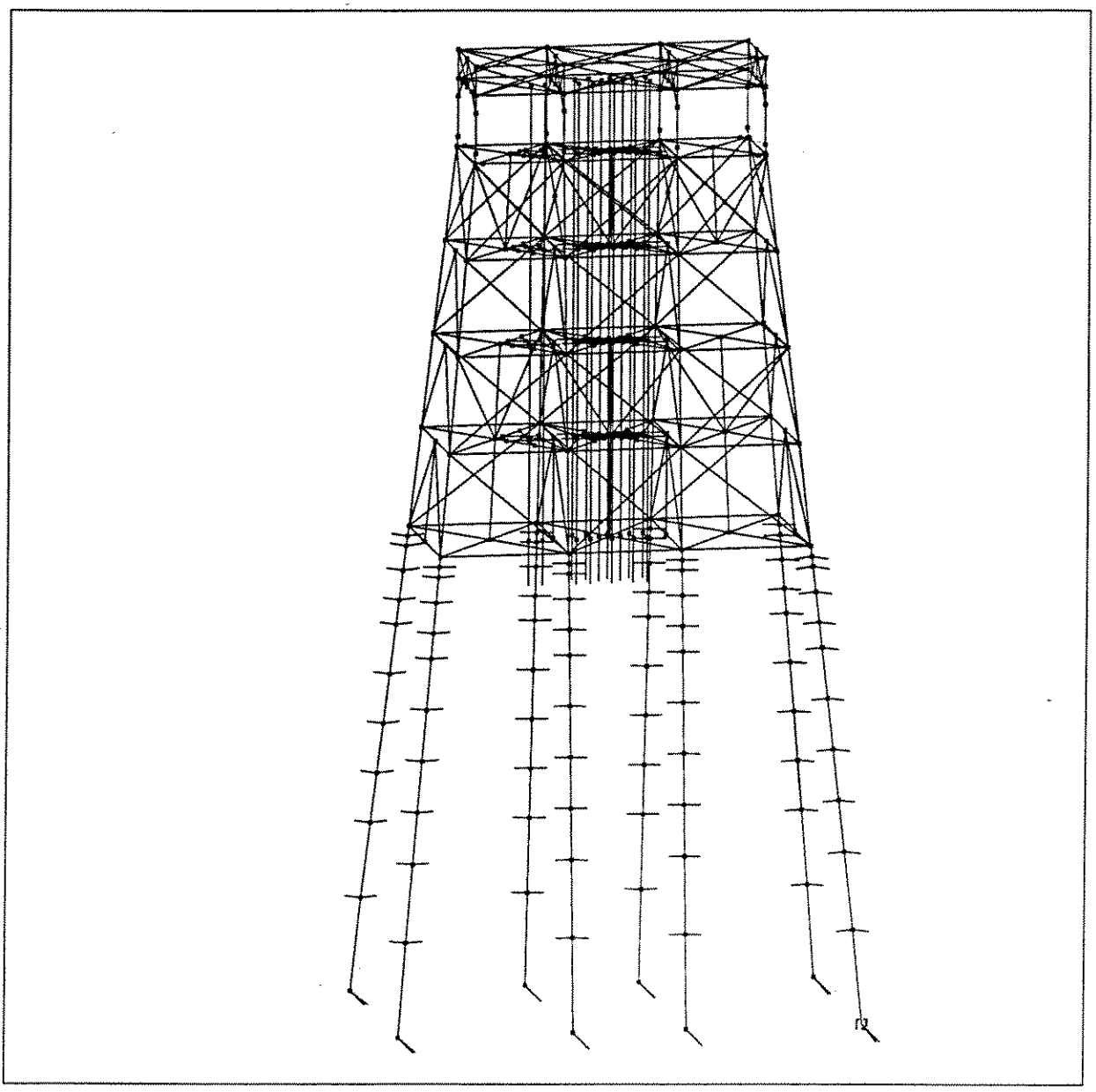

Figure 3-1 CAP Computer Model

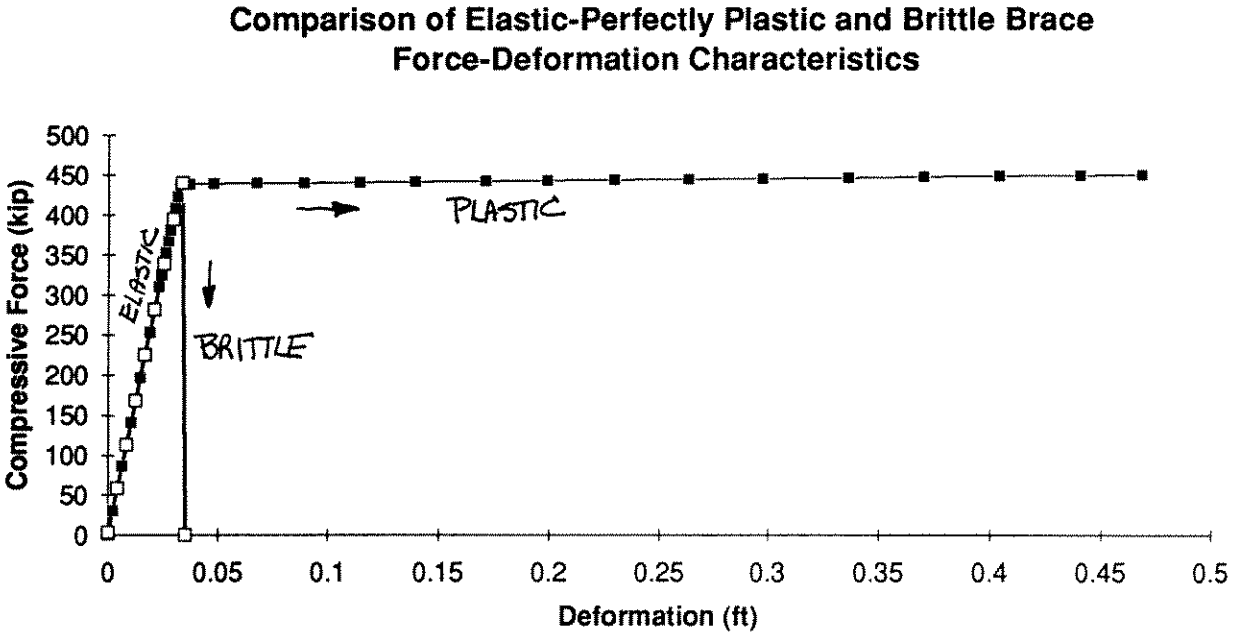

Figure 3-2 Comparison of Plastic and Brittle Joint Modes

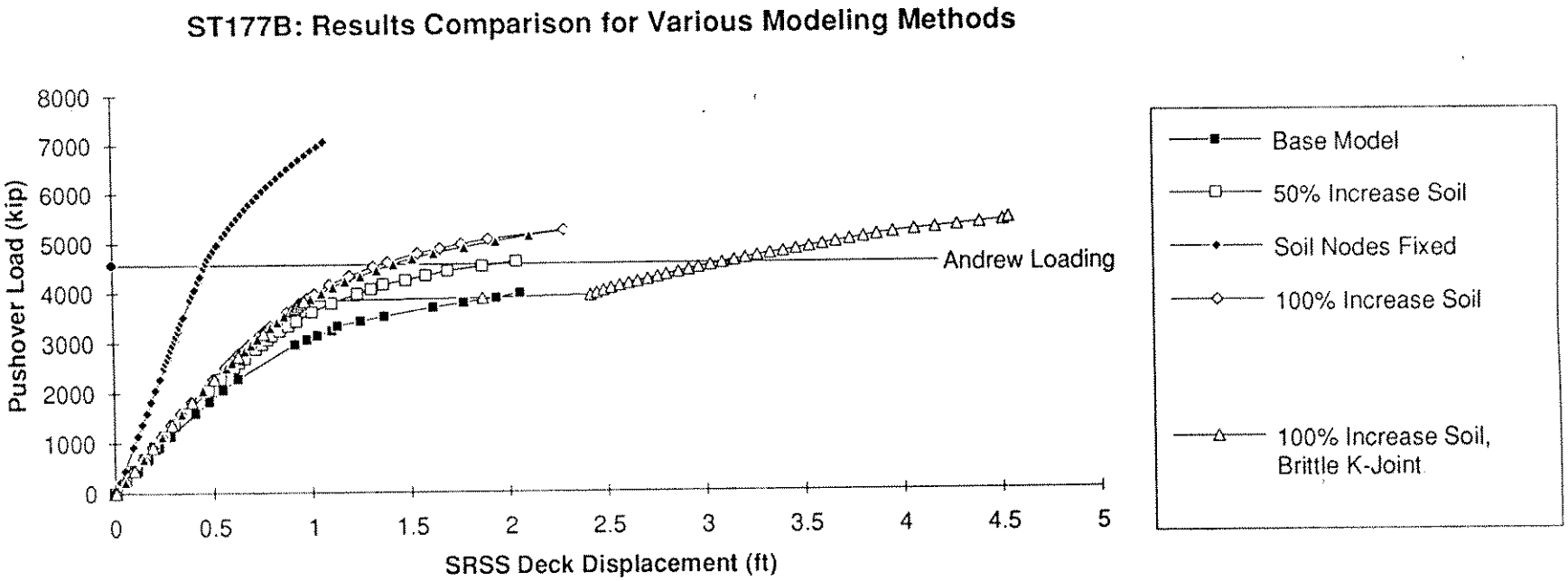

Figure 3-3 Comparison of Analyses Results

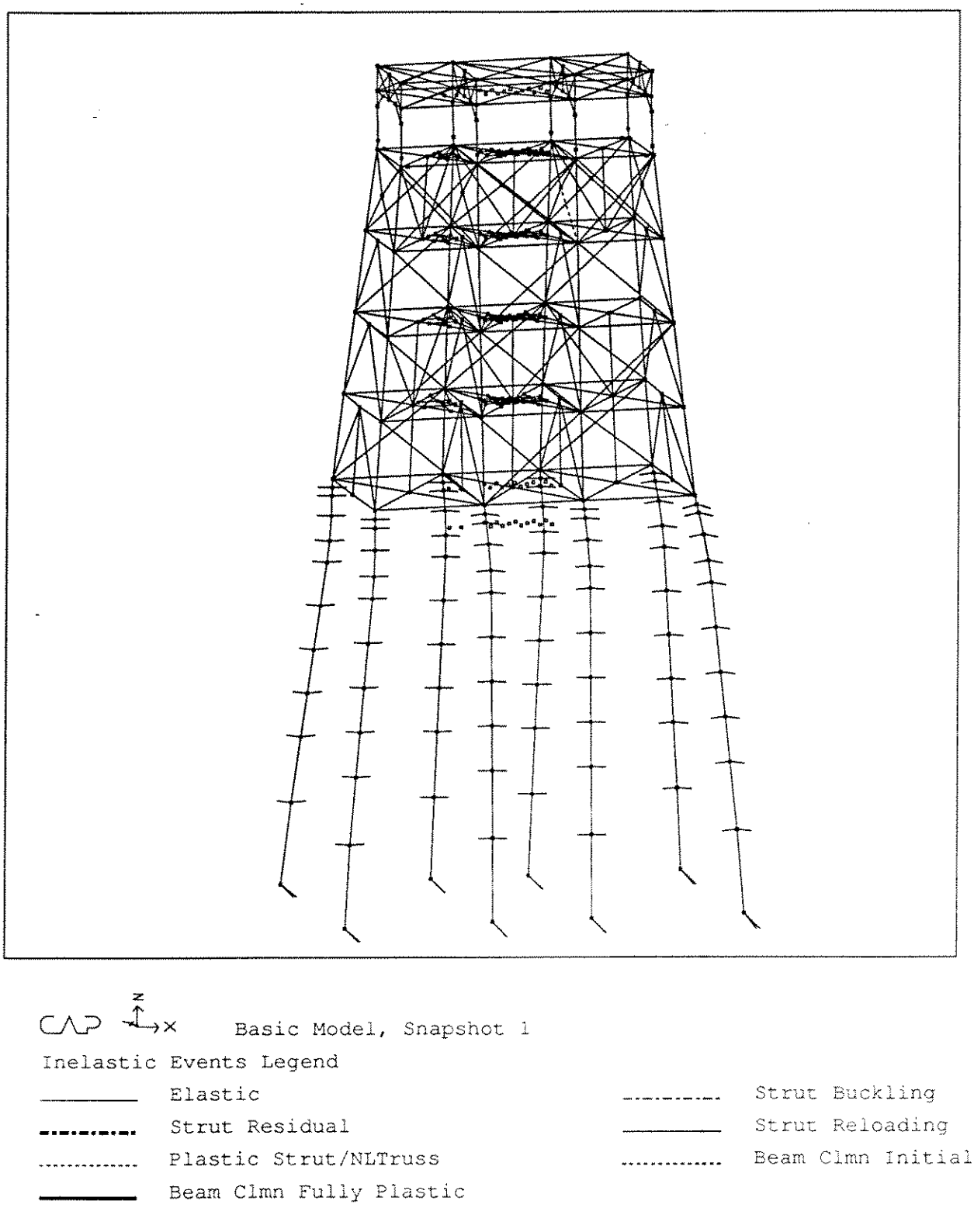

Figure 3-4 Basic Model - Initial Member Failure

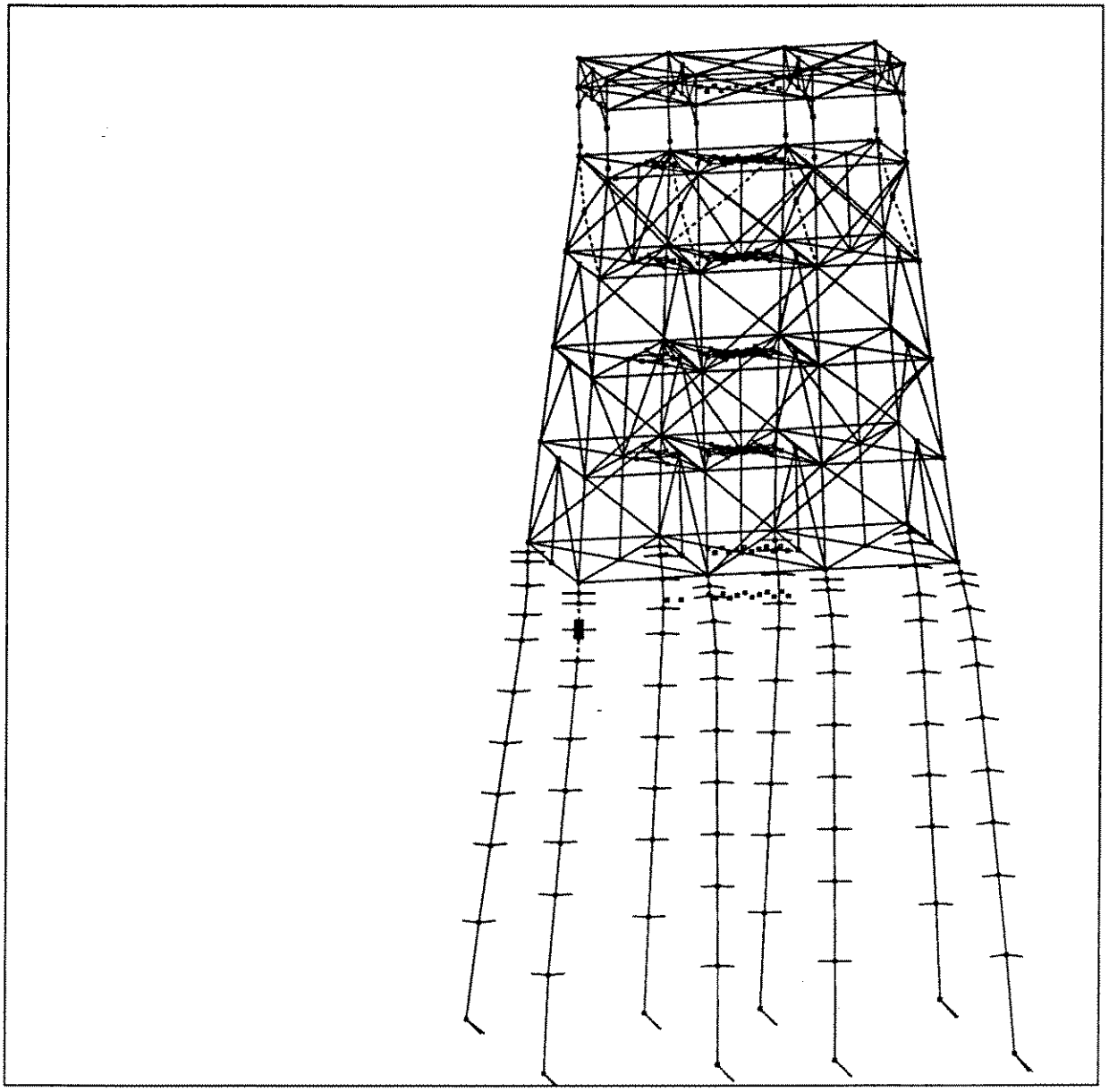

Figure 3-5 Basic Model - Intermediate Load Step

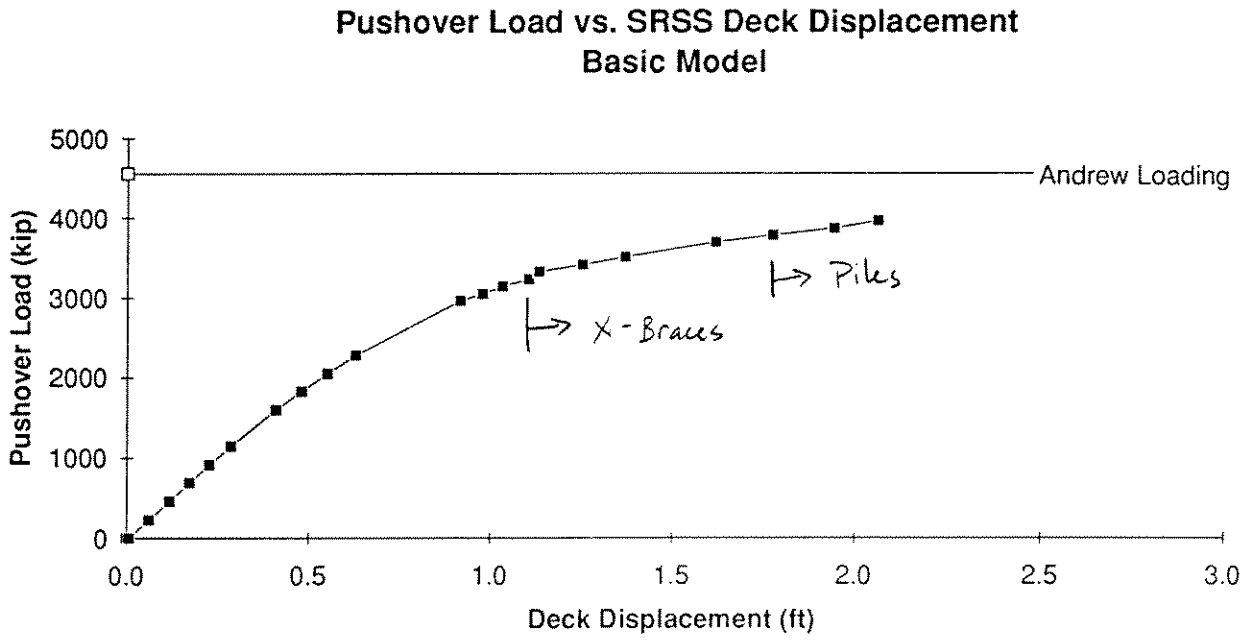

Figure 3-6 Basic Model - Analysis Results

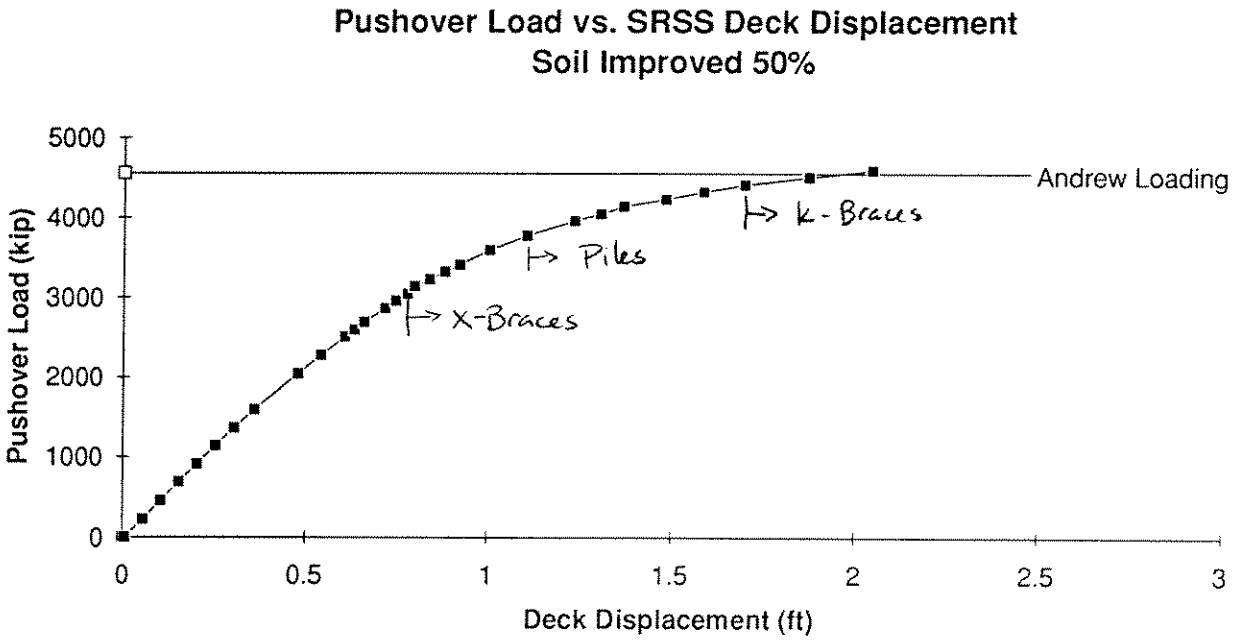

Figure 3-7 Soil Improved 50% - Analysis Results

Project: ChevST177B Model: push267 Version: 10 Wed Feb 2 18:15:17 1994 *

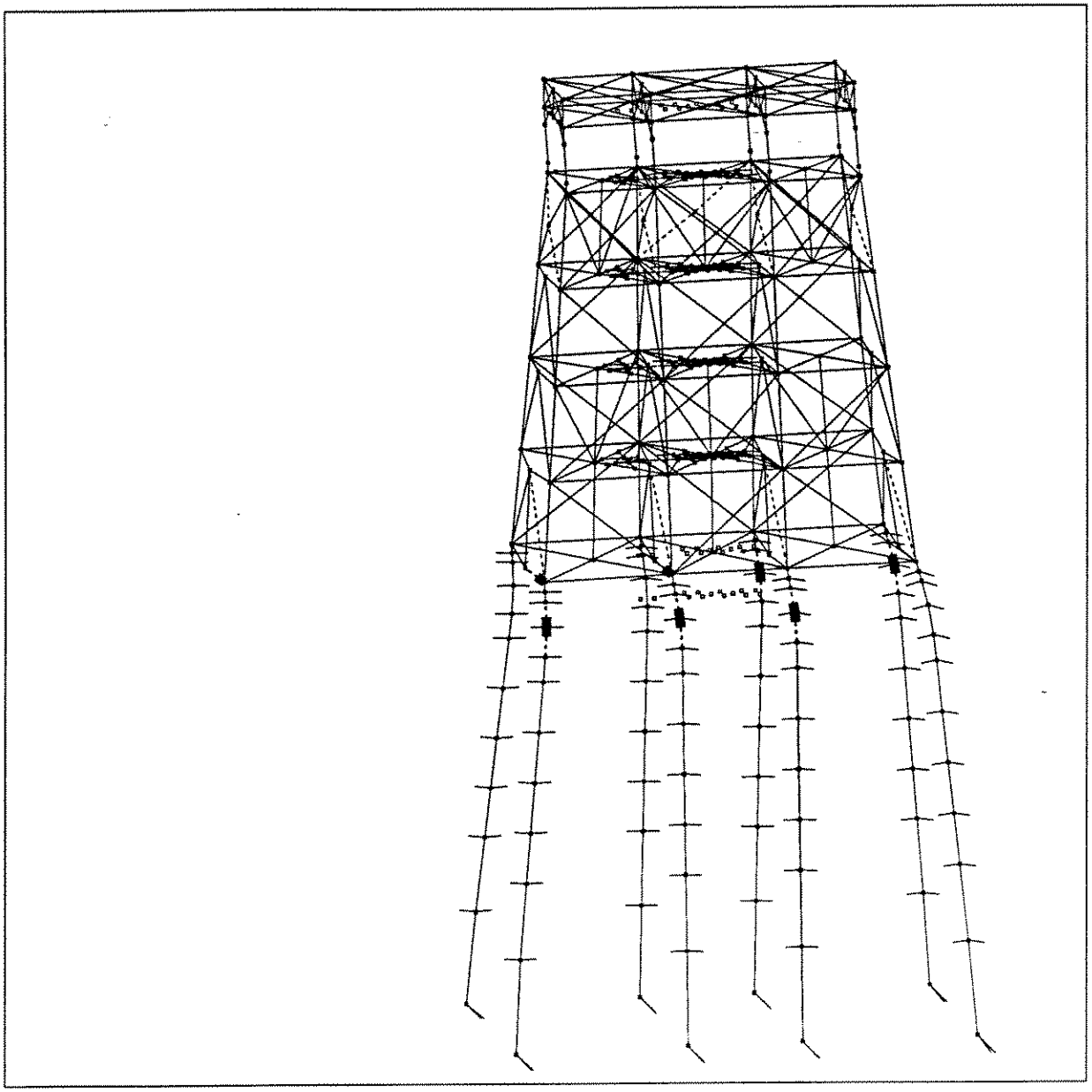

CAP Z X Soil Improved 100%, Jnt Cap. Iter., Snapshot 2

Inelastic Events Legend

Elastic	Strut Buckling
Strut Residual	Strut Reloading
Plastic Strut/NLTruss	Beam Clmn Initial Yield
Beam Clmn Fully Plastic	

Figure 3-8 Soil Improved 100% - Intermediate Load Step

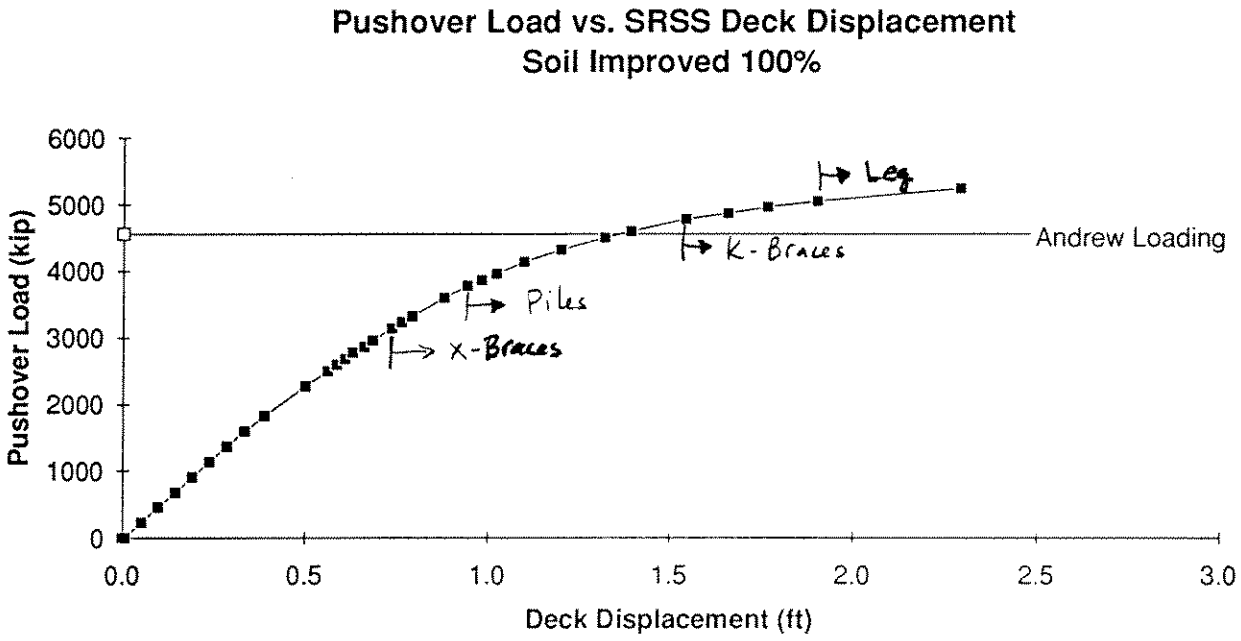

Figure 3-9 Soil Improved 100% - Analysis Results

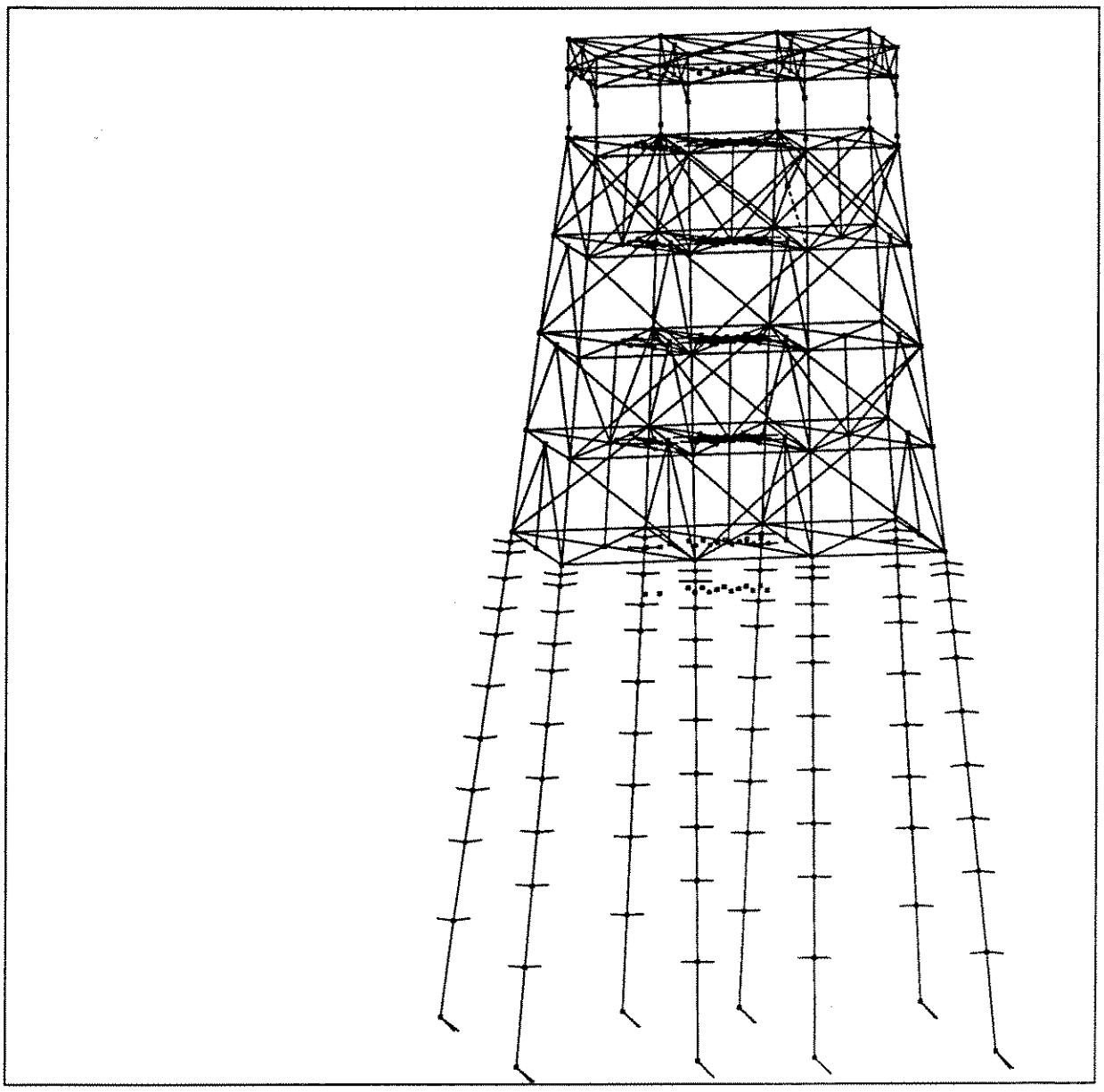

Figure 3-10 Fixed Base - Initial Member Failure

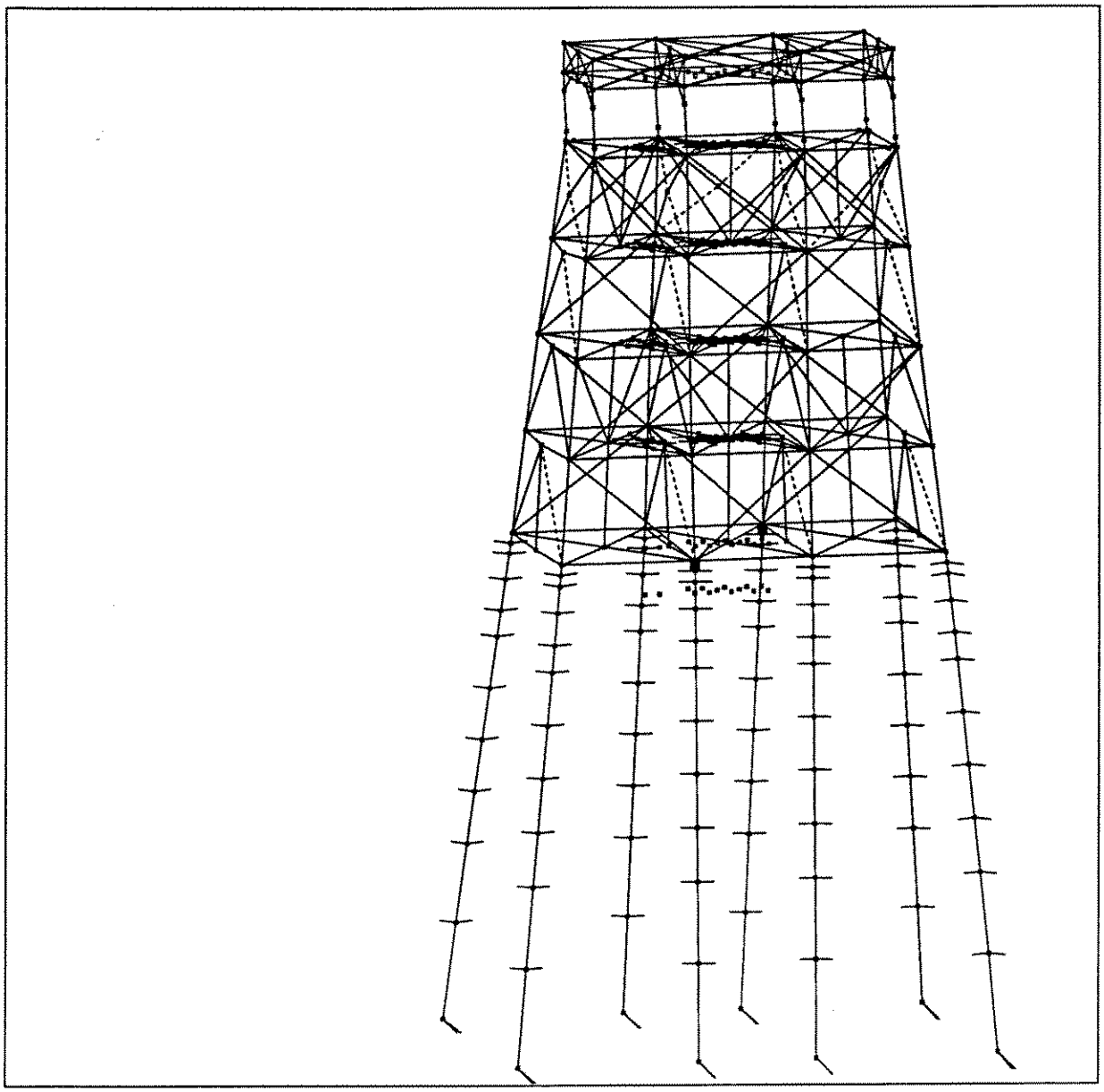

Figure 3-11 Fixed Base - Intermediate Load Step

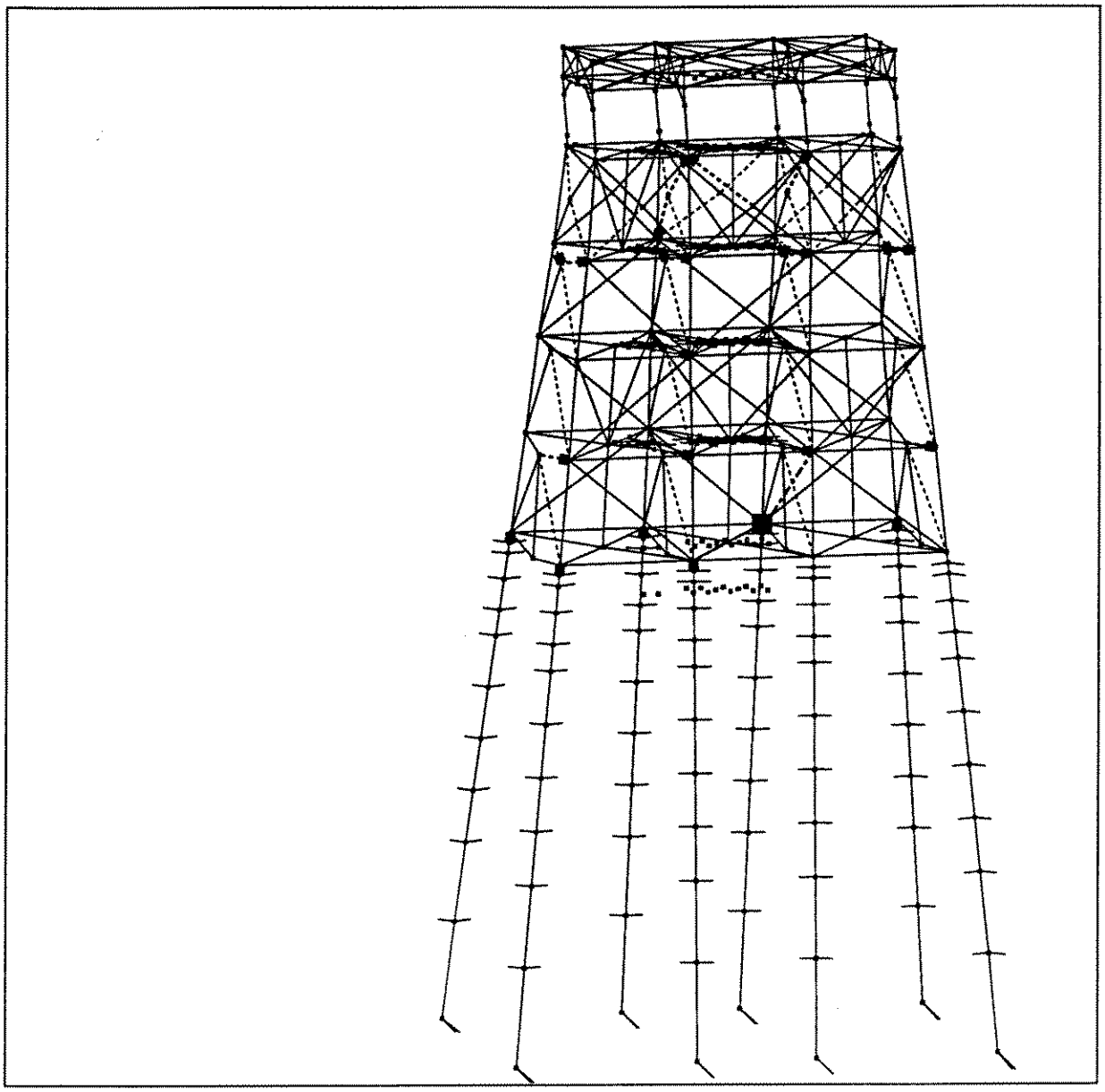

Figure 3-12 Fixed Base - Final Load Step

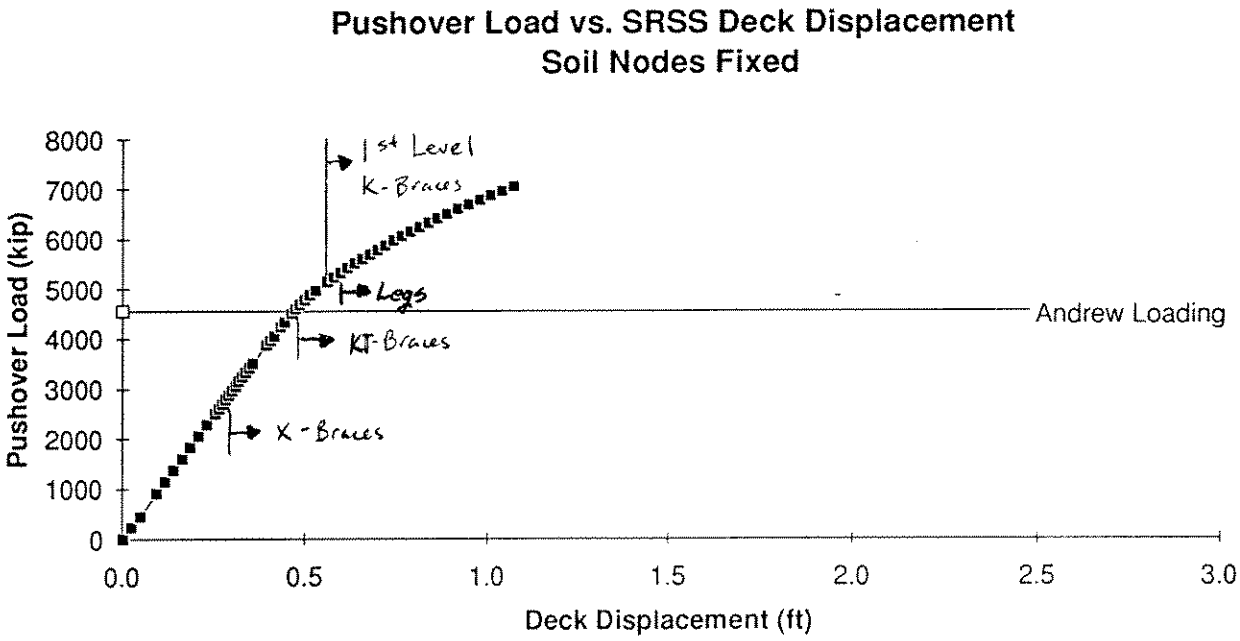

Figure 3-13 Fixed Base - Analysis Results

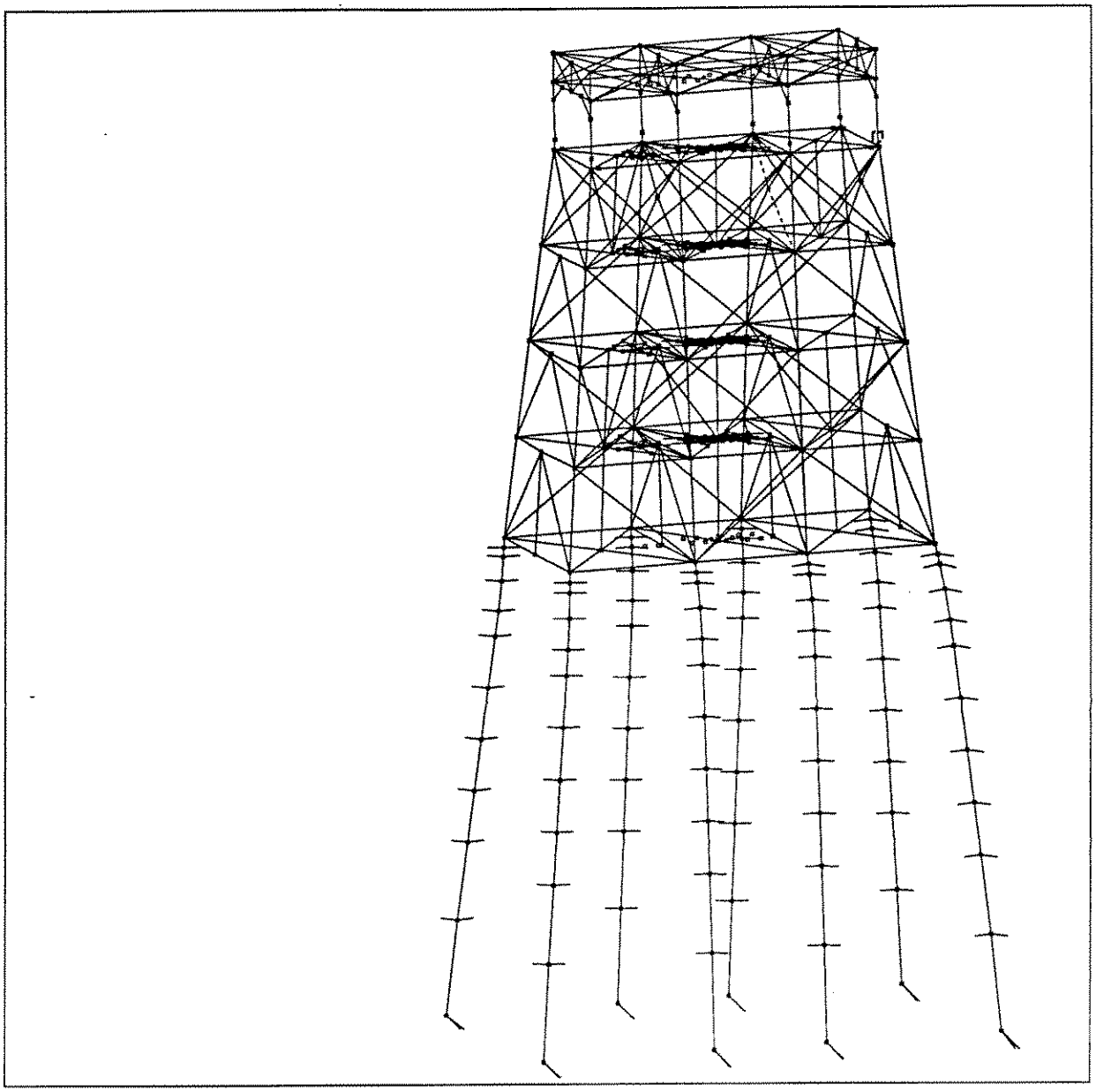

Figure 3-14 Brittle K Joints - Initial Failure

Project: ChevST177B Model: push267 Version: 11 Tue Feb 1 11:52:18 1994 *

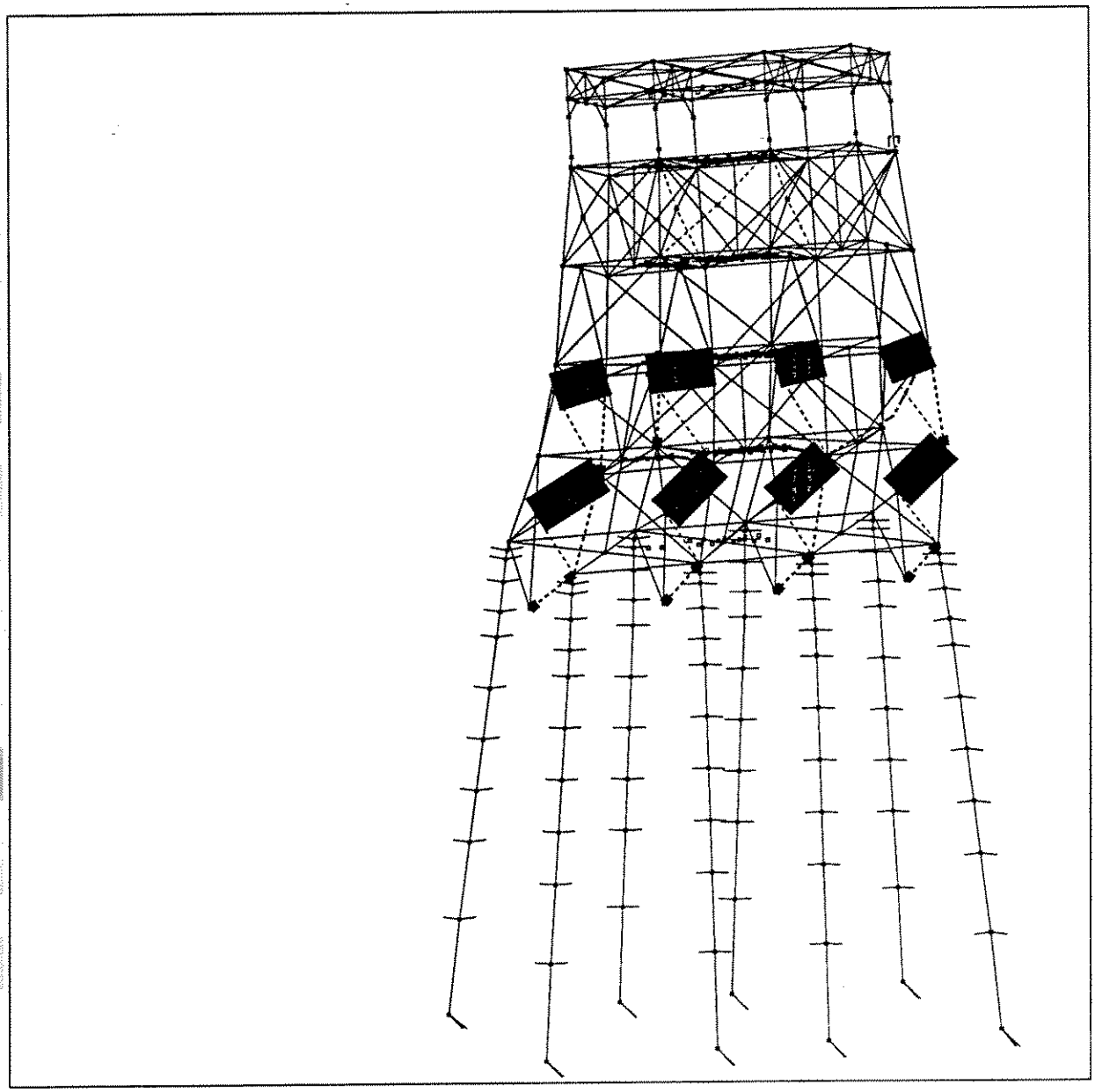

CAP Z X Brittle K-Joint, Soil Improved 100%, Snapshot 2

Inelastic Events Legend

Elastic	Strut Buckling
Strut Residual	Strut Reloading
Plastic Strut/NLTruss	Beam Clmn Initial Yield
Beam Clmn Fully Plastic	

Figure 3-15 Brittle K Joints - Intermediate Load Step

Project: ChevST177B Model: push267 Version: 11 Tue Feb 1 12:08:38 1994 *

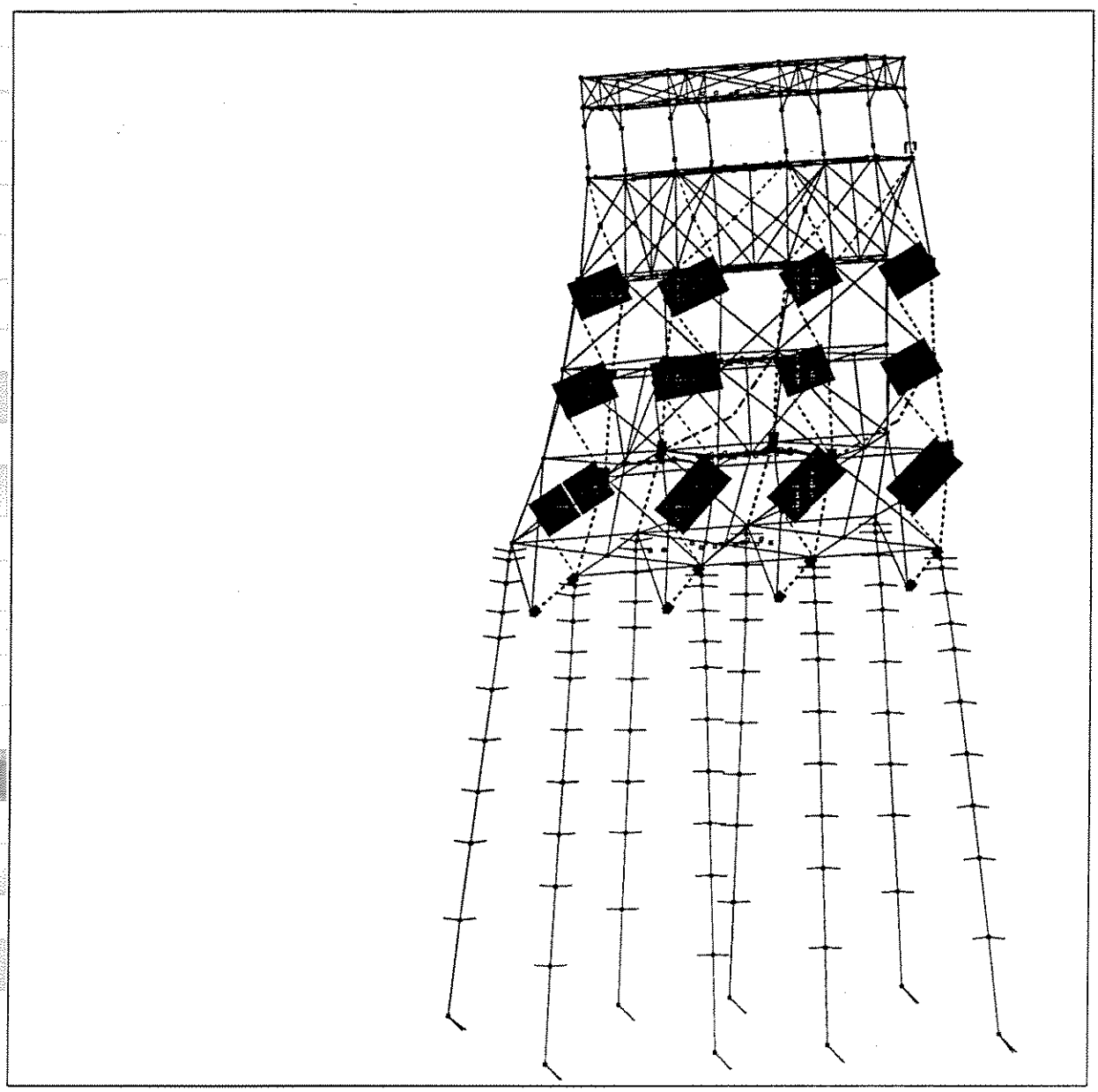

CAP Z X Brittle K-Joint, Soil Improved 100%, Snapshot 3

Inelastic Events Legend

Elastic	Strut Buckling
Strut Residual	Strut Reloading
Plastic Strut/NLTruss	Beam Clmn Initial Yield
Beam Clmn Fully Plastic	

Figure 3-16 Brittle Joints - Final Load Step

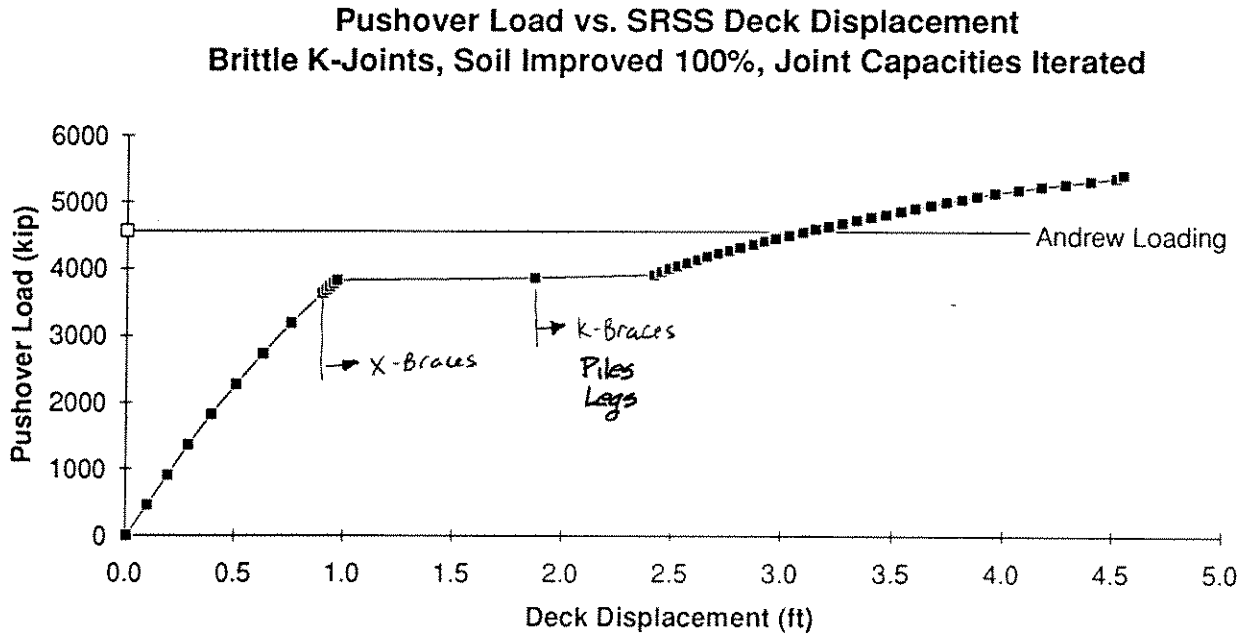

Figure 3-17 Brittle Joints - Analysis Results

SECTION 4 CONCLUSIONS AND RECOMMENDATIONS

4.1 PLATFORM INSPECTION

The ST 177B structures sustained serious damage to joints at the intersection of X, K and KT braces. The failures appear to be attributable to the lack of joint cans and the problem of chord and brace diameters of the same size. This is a problem that probably exists in a number of platform of this vintage and needs to be accounted for when evaluating the platform for fitness of purpose.

Note that there were no joint failures at the legs (which were grouted), helping to confirm the industry perception of increased joint strength due to the composite action of the leg, grout and pile.

The platform legs showed a slight curvature in the direction of the Andrew waves. This "damage" is attributable to large deformation of the legs once the K joints had sheared. This frame action resistance by the legs ultimately allowed the platform to remain standing after Andrew even though almost all of the joints had been damaged.

Overall, there were no other signs of damage of any kind to the platform, such as fatigue cracking, dented members or corrosion. Joints sand blasted clean during the inspection were in remarkably good condition for a 28 year old platform. It appeared that the platform operator's maintenance program provided an adequate job for this particular structure.

Several intact and damaged joint specimens were cut from the platform and placed in storage in one of Chevron's yards in the New Orleans area. It recommended that these joints be used for further testing of material properties as well as ultimate strength. These joints are unique since they provide the specific type of steel materials and fabrication techniques (rolling, welding, etc.) typical of the 1960's vintage of platforms.

One possibility is to propose the effort in the form of a Joint Industry Project (JIP) funded by industry and regulators such as the MMS and HSE. The testing could be performed at a university or other testing facility that can handle large specimens. The work would be similar to that previously performed at Texas A&M for damaged platform braces under a JIP managed by PMB (PMB, 1990).

4.2 PLATFORM ANALYSIS

The initial "Base Case" computer model predicted that the platform would have collapsed during Andrew. The failure mode predicted by the analysis was in the foundation, with little or no damage to the jacket. However, the post Andrew platform inspection indicated that the failure

mode was instead in the jacket, with serious damage to almost all of the joints in the jacket. There was no indication of foundation damage or failure.

The computer models were therefore adjusted in terms of the foundation and jacket joint modeling in order to try to adjust the analytical evaluation until it more closely matched the observed results.

The foundation adjustments indicate that an increase in soil shear strength on the order of 50 to 100 percent provides sufficient foundation resistance to allow joint failures in the jacket prior to failure of the platform. A similar pattern of analytically predicted foundation failures, yet none that were observed in the filed, was seen in the Andrew JIP.

The jacket joint strength adjustments indicate that elastic-brittle joint modeling of the K joints, which mimics the complete shear of the joint as seen in the platform inspection, provides a good match to the observed platform performance and damage that occurred in Andrew. The brittle joint model also included the adjusted foundation with increased soil shear strength. The model predicted that almost all of the jacket joints would have failed in Andrew but the platform would have survived due to bending resistance of the grouted leg-pile. There would also have been some initial yielding of the legs. This is essential the same type of damage as indicated by the platform inspection.

For this particular study, the computer model was modified until it predicted that the platform would perform as indicated by the onshore inspection. The analytical "recipe" that worked well for this case (i.e. increased foundation strength and brittle joints) needs to be tested using other platforms that were damaged or survived large storms. A parallel study being performed by PMB for the MMS (PMB, 1994d) that is evaluating three more platforms from Andrew, indicates that the "recipe" that worked well for this platform does not perform as well for two of the three platforms, where the recipe indicates that the platform should have collapsed, or at least seriously damaged, yet the platforms survived undamaged.

Based upon the above, it is obvious that further study is required before a well established recipe for evaluating platforms under extreme environmental conditions can be developed. The recipe first identified in the Andrew JIP and then further refined in this study appears promising, but several adjustments are still required. Foundation strength is currently being further studied by PMB in a study funded by the MMS and API (PMB, 1994a). Joint strength and modeling will be one of the key issues investigated in the proposed Andrew Phase II JIP, where the joint specialist firm of MSL Engineering will be assisting PMB on the further evaluation of platform performance in Andrew. Both of these projects will enable development and testing of a much improved recipe.

SECTION 5 REFERENCES

American Petroleum Institute, 1993. Recommended Practice for Planning, Designing, and Constructing Fixed Offshore Platforms, API RP 2A, Twentieth Edition, Washington, D.C.

American Petroleum Institute, 1994. API RP 2A Draft Section, April 30, Dallas, Texas.

Daniels, G. R., 1994. Hurricane Andrew's Impact on Natural Gas and Oil Facilities on the Outer Continental Shelf, Interim Report as of November, 1993, OCS Report MMS 94-0031.

Imm, G.R., et.al., 1994. South Timbalier 161 A: A Successful Application of Platform Requalification Technology, OTC Paper 7471, May 2-5, Houston, Texas.

Oceanweather, Inc., 1992. Hindcast Study of Hurricane Andrew, Offshore Gulf of Mexico, Prepared by V.J. Cardone and A.T. Cox, Oceanweather Inc., Cos Cob CT.

PMB Engineering Inc. and Texas A&M, 1990. Testing and Evaluation of Damaged Jacket Braces, Joint Industry Project, Houston, Texas, May.

PMB Engineering Inc., 1993. Hurricane Andrew - Effects on Offshore Platforms, Joint Industry Project, San Francisco, California, October.

PMB Engineering Inc., 1994 a. Further Evaluation of Offshore Structure Performance in Hurricane Andrew - Development of Bias Factors for Pile Foundation Capacity, Joint Industry Project for the API and MMS, Kickoff Meeting Handout, March 22, San Francisco, California.

PMB Engineering Inc., 1994 b. Hurricane Andrew - Effect on Offshore Platforms, Proposal for a Joint Industry Project, Phase II, April, San Francisco, California

PMB Engineering Inc., 1994 c. The Effect of API RP2A 20th Edition Criteria on the Design of Offshore Caisson-Type Structures, Report to the MMS, July, San Francisco, California.

PMB Engineering Inc., 1994 d. Platform Inspection and Analysis, Final Report for the MMS, A&E Contract No. 14-35-0001-30700 (Task Order 1), July, San Francisco, California.

APPENDIX A - Joints Selected for Further Testing

PMB ENGINEERING

By_____ Date _/_/_ Checked by_____ Sheet No._____

Project_____ Job No._____

Subject PLATFORM STITTR.

MAIN DECK ELEV. (+) 50'
CELLAR DECK ELEV. (+) 39'

PLATFORM MEMBER SIZES (TYP)

40'-0"

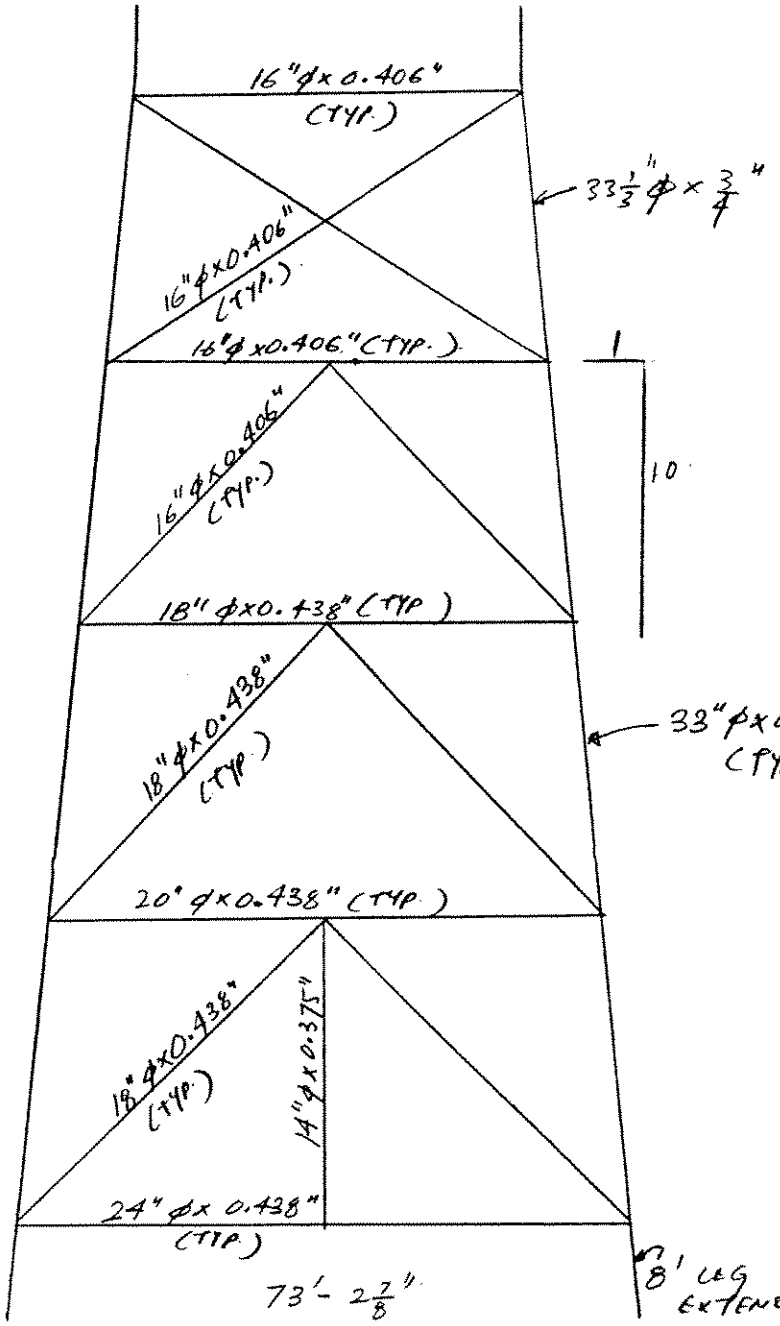

8-30"φ PILES WITH 187' PENETRAT.
12-30"φ CONDUCTORS

ROW 1-4

PMB ENGINEERING

By_____ Date __/__/__ Checked by_____ Sheet No._____

Project_____ Job No._____

Subject PLATFORM STI77B

PLATFORM MEMBER SIZES (TYP)

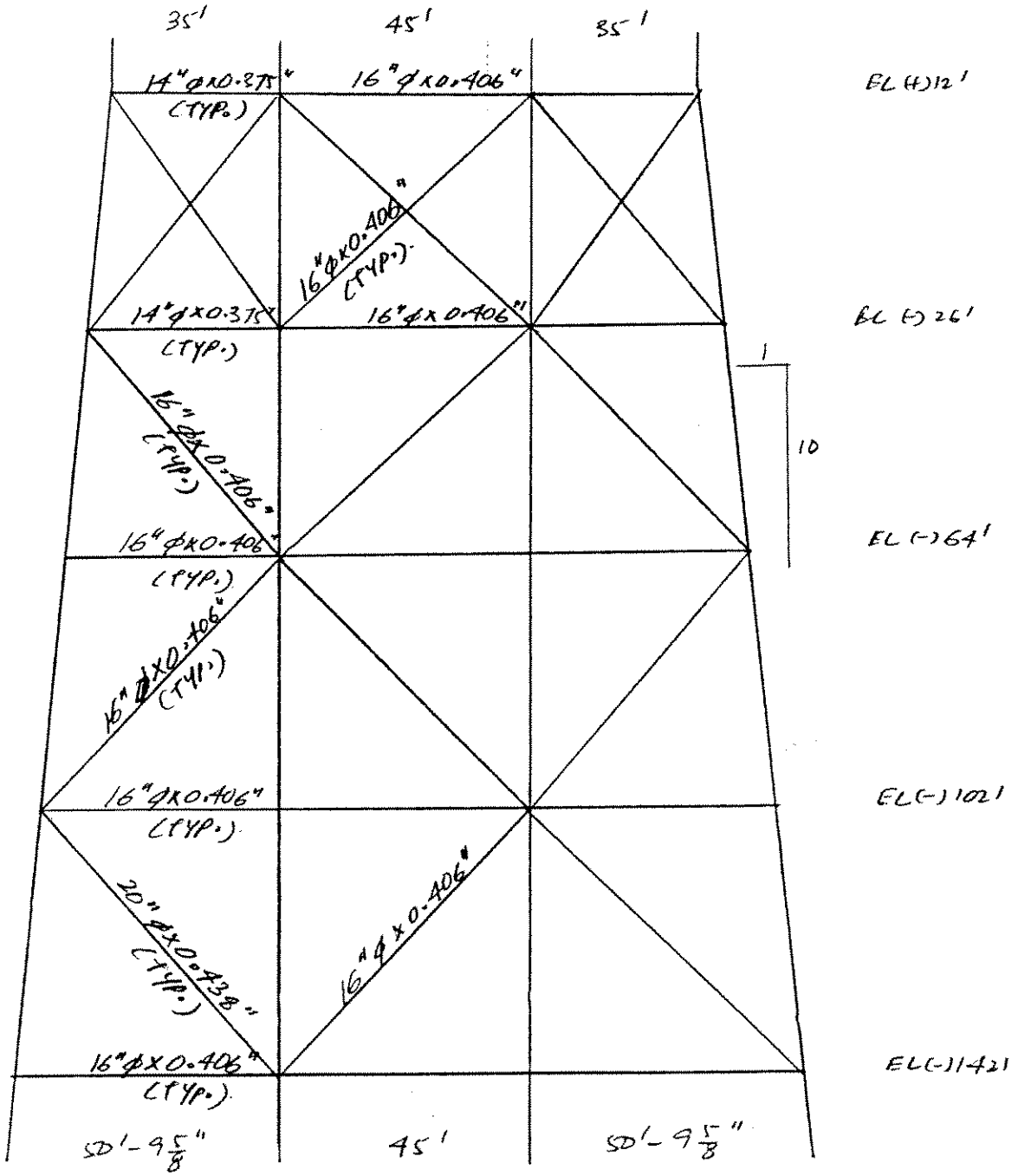

ROWS A & B

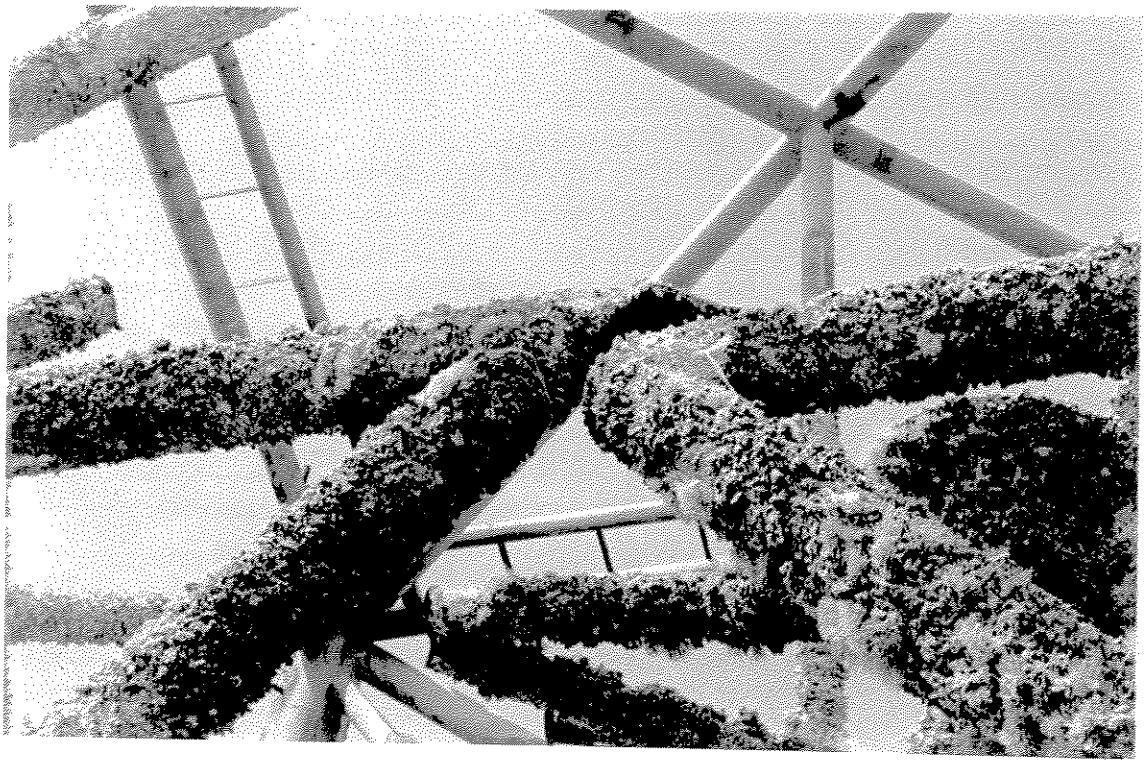

Specimen 1 - TN Row B K Joint (Damaged)

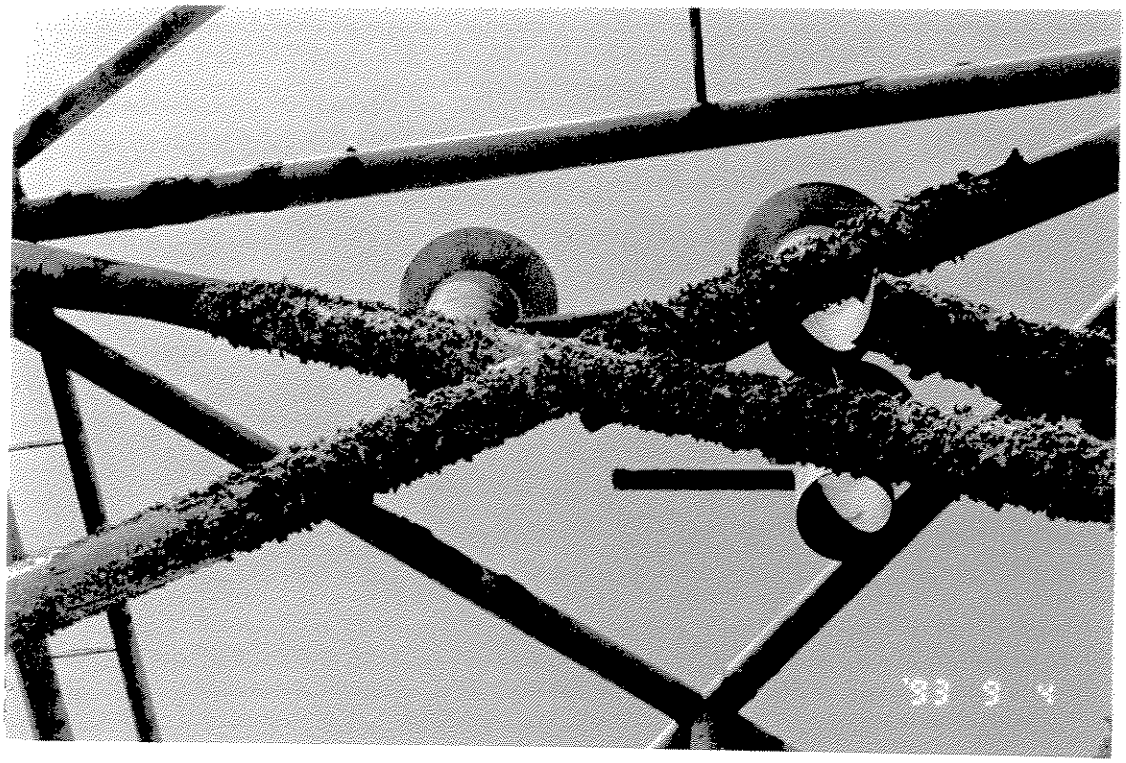

Specimen 2 - TN Row B X Joint (Damaged)

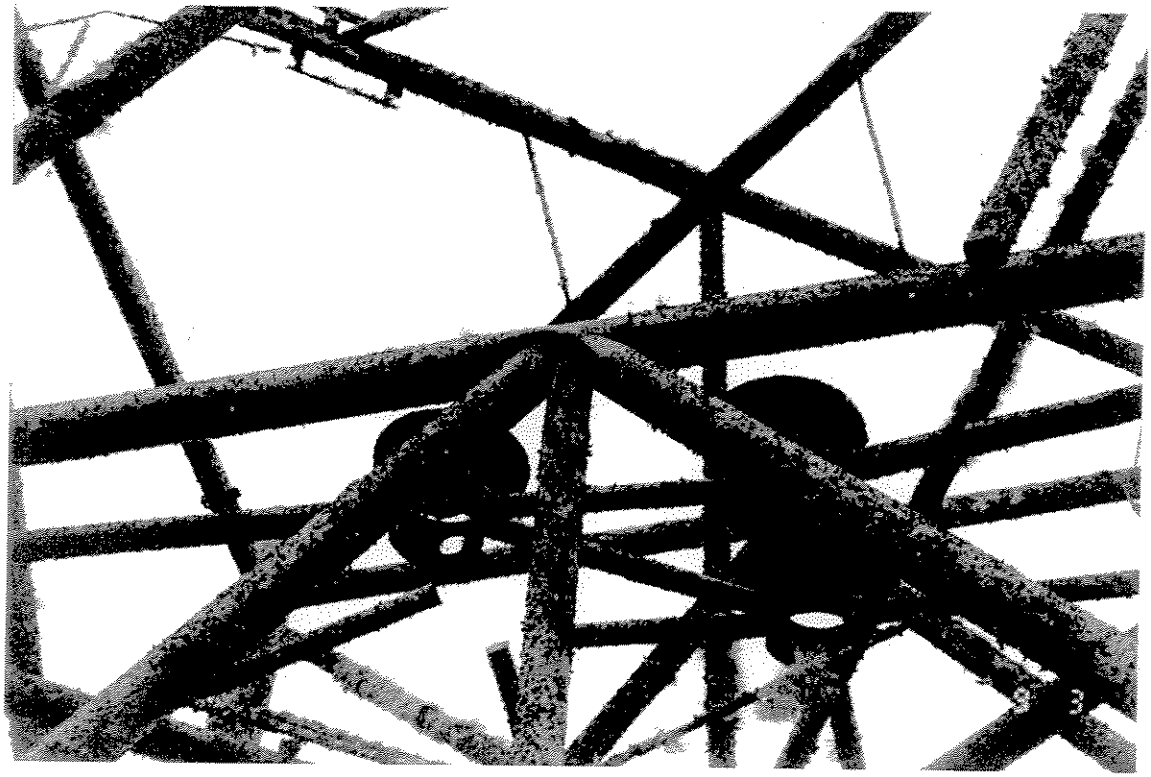

Specimen 3 - BN Row B KT Joint (Damaged)

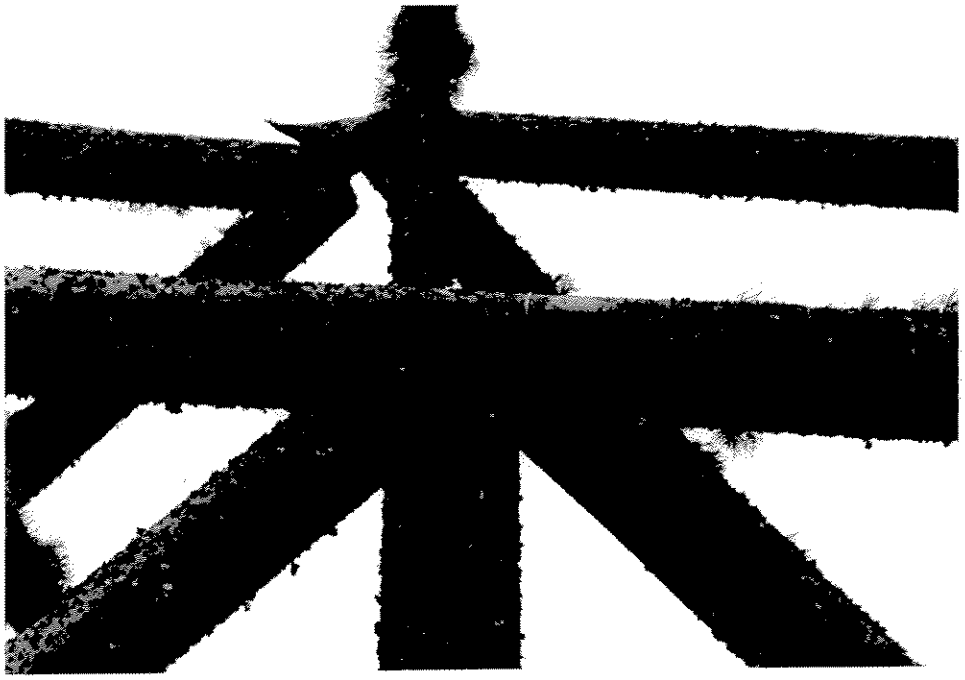

Specimen 4 - BS Row C KT Joint (Damaged)

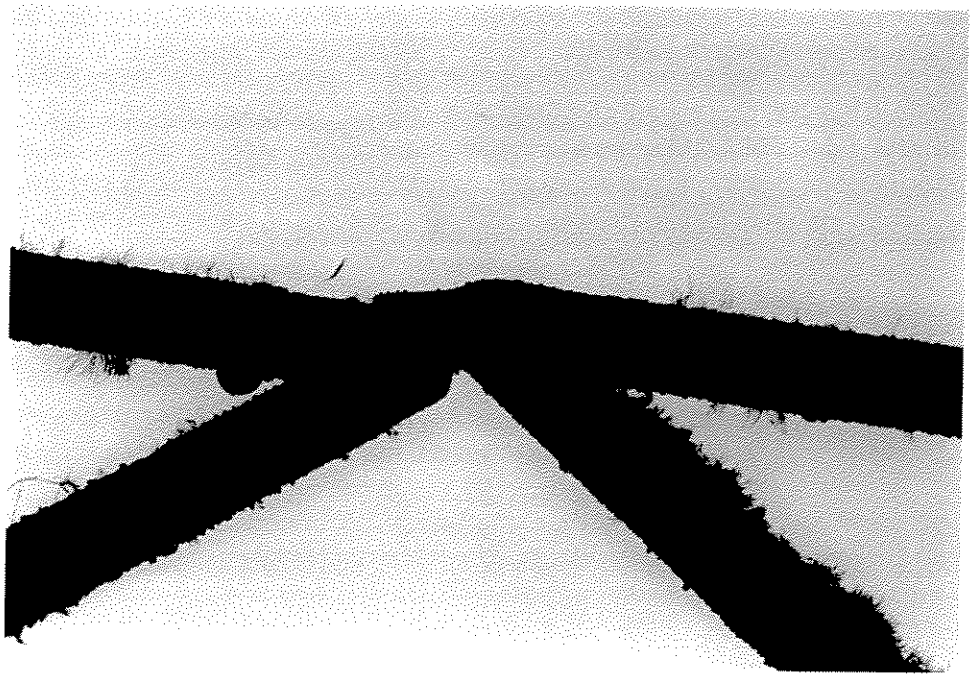

Specimen 5 - BS Row C K Joint (Damaged)

Specimen 6 - TN Row 1 X Joint (Intact)

Specimen 7 - TN Row 2 X Joint (Intact)

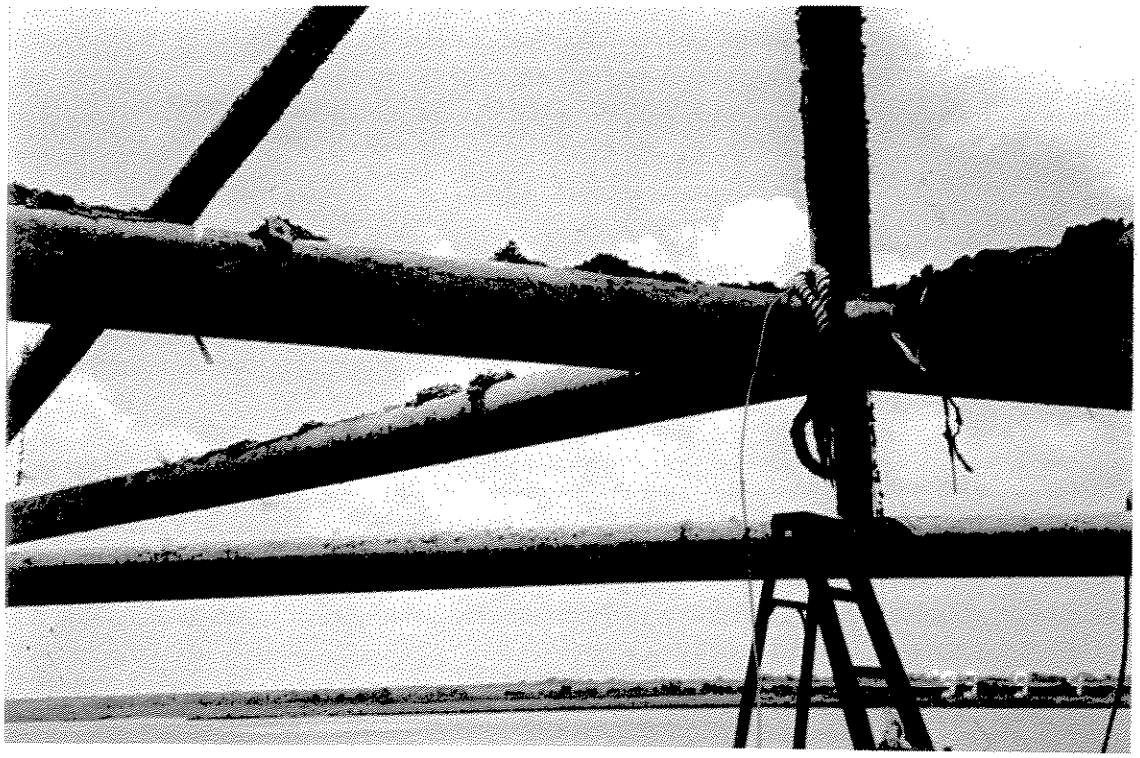

Specimen 8 - BS Lower Horiz X Joint (Intact)

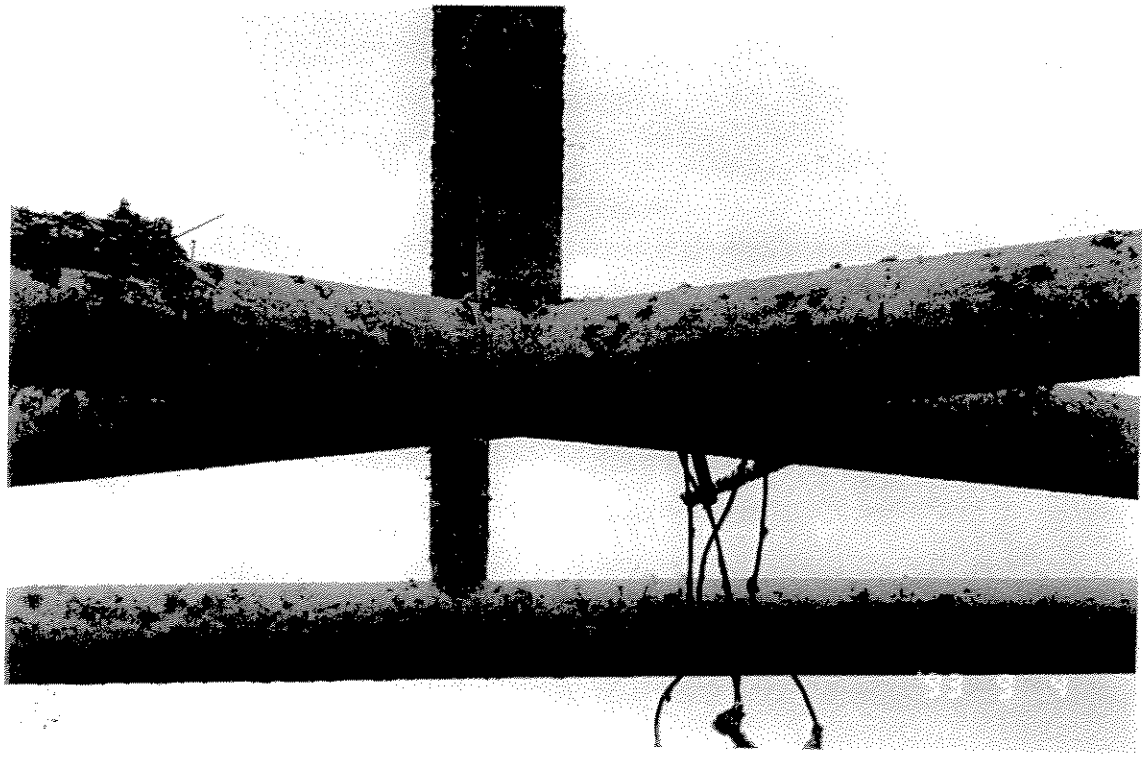

Specimen 9 - BN Lower Horiz X Joint (Intact)

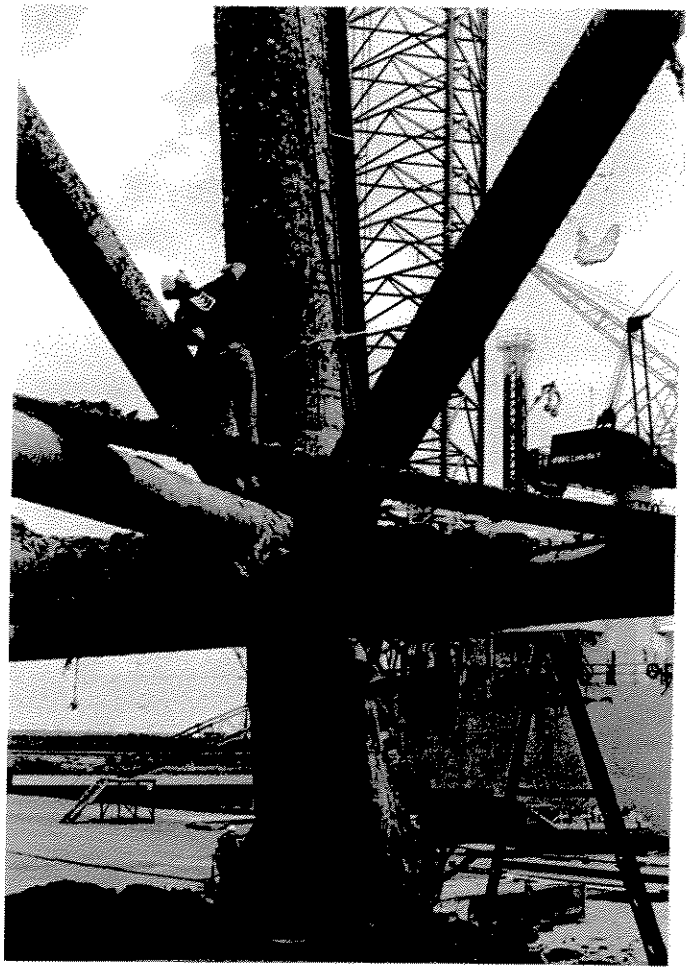

Specimen 10 - BN B2 Leg/Pile Joint (Intact)

Coupon - B AUX Brace

Coupon - B AUX Leg

APPENDIX B - Joint Capacity Methodology

JOINT CAPACITY CALCULATION METHODOLOGY

1. Introduction

The joint capacity equations in API RP 2A-WSD (20th edition, 1993) give lower bound capacities with additional safety factors. While these are appropriate for design, they grossly underestimate the average expected joint strength. Thus, ways of calculating the mean joint capacities were investigated.

The API equations contain the following conservatisms:

- There is a 1.7 safety factor in the basic equations, and an equivalent safety factor (1/0.6) in the term representing chord stress effects.
- The joint strength terms, Q_u, are adjusted to fit the lower bound of the experimental data, not the mean.
- The API equations are based on data from OTC paper 3690 (Yura, Zettlemoyer and Edwards), which was published in 1980. Additional joint capacity test data have become available since then from various sources, data which more often than not predicts a slightly higher mean capacity than the 1980 equations.

2. Recommended Joint Capacity Equations

A review of various sources of data (see References) was performed, and a set of recommended joint capacity equations was formulated for X, K and overlapping KT joints, which apply to the ST-177B structure. A description of these equations follows.

2.1 X Joint Axial Compression Capacity

(see notes)

2.2 K Joint Axial Capacity

(see notes)

2.3 In-Plane Bending Capacity

(see notes)

2.4 Out-of-Plane Bending Capacity

(see notes)

2.5 Overlapping KT Joint Axial Capacity

(see notes)

2.6 Overlapping KT Joint In-Plane Bending Capacity

(see notes)

2.7 Overlapping KT Joint Out-of-Plane Bending Capacity

(see notes)

3. Joint Capacity Equation Comparison

For one X brace in compression and one K brace in the ST-177B structure, the following capacities were calculation for comparison:

- API RP 2A-WSD (20th) with all safety factors

  These are the lower bound capacities, with safety factors, that are typically used for design.

- API RA 2A-WSD with safety factors removed

  These represent lower bound capacities, without the additional safety factors.

- OTC 3690 equations, adjusted to represent mean capacity

  The API equations (above) are based on the equations presented in this paper. These equations, with an additional factor to convert from lower bound capacity to mean capacity (also presented in this paper) were used to calculate the mean capacities.

- Recommended Equations

  These are equivalent in intent to the OTC 3690 mean equations, but are based on the study of more recent data.

The results of this comparison are presented in Table 1. For simplicity, this comparison assumes negligible chord stress (i.e. the Q_f term is unity). Removing the safety factor (compare the first case and second case) results in a capacity increase of about two. Adjusting the equations for mean rather than lower bound capacity (compare the second case and third case) results in an additional increase of approximately 20% for the moment capacities, 7% for the X-joint axial compression capacity (there was little scatter in the experimental results), and about 50% for the K-joint axial capacity (because OTC 3690 and API adopted different formulations for the gap effect factor, the only place in which they are substantially different).

The recommended equations, based on more recent data, represent an increase in capacity over the OTC 3690 equations. The increase in mean capacity over the OTC 3690 equations (compare the third and fourth cases) ranges between 5% and 30%.

Thus, the recommended mean capacities are between two and four

times greater than the API capacities for design.

4. Use of Joint Capacities in Analysis

For model elements which do not model moments, but only axial forces, the effective axial joint capacity must be adjusted to account for the presence of moments. This is done as follows:

(1) Estimate the maximum water particle velocity (maximum wave-induced plus current with blockage) at the brace's average water depth.

(2) Using the element length (face to face), estimate the brace-end moments due to the drag force on the element. Assume partially fixed ends (i.e. moment is 1/10 of the distributed load times the length squared). Assume a drag coefficient of 1.05 for members with marine growth and 0.65 for members without marine growth. For X braces, take the full length of each brace, not the half-length, because the crossing brace does not provide much restraint against out-of-plane bending.

(3) Use the API RP 2A-WSD (20th edition, 1993) axial/bending interaction equation. For simplicity, assume the moment calculated in the previous step is out-of-plane (which is close enough to correct). Find the axial force at combined axial/bending failure with this moment. Take this to be the effective axial capacity for the element.

COMPARISON OF JOINT CAPACITY FORMULAS
FOR END X BRACES AND END UPPER K BRACES

Brace	Load Case	API 20th ed. with safety factors	API 20th ed. w/o safety factors	Yura et al 1980 (OTC 3690), adjusted for mean	Recommended Equations
X	Axial	105	208	222	233
	IP Bending	85	168	207	236
	OP Bending	71	141	165	190
K	Axial	126	250	378	482
	IP Bending	103	204	251	326
	OP Bending	86	170	200	230

Note: There is assumed to be no stress in the chord (hence a Qf factor of 1).

TABLE 1

PMB ENGINEERING

By LAN Date 9/17/93 Checked by _____ Sheet No. 1

Project _____ Job No _____

Subject _____

RECOMMENDED MEAN X JOINT CAPACITIES

AXIAL COMPRESSION

USE THE FORMULA PRESENTED IN OTC 4189 (BILLINGTON, LALANI + TEBBETT, 1982) AND BOSS '88 MA + TEBBETT, WITH API'S Q_f TERM (WITH A MINOR MODIFICATION) ADDED:

$$P = \frac{F_{yc} T^2}{\sin\theta} (3 + 15.2\beta) Q'_\beta K_a Q_f$$

WHERE $Q_f = \frac{1 - 0.030\gamma A^2}{}$

$A = \sqrt{f_{cAx}^2 + f_{cIP}^2 + f_{cOP}^2} / F_{yc}$ (API'S SAFETY FACTOR REMOVED)

f_{c*} = NOMINAL COMPONENT STRESSES IN CHORD

NOTE THAT, UNLIKE IN API 20TH, Q_f IS NOT TO BE TAKEN EQUAL TO 1 IF ALL CHORD EXTREMA ARE IN TENSION; VAN DER VALK (1991 OMAE) DEMONSTRATED THAT CHORD TENSION DOES INDEED DECREASE THE JOINT CAPACITY, MORE SO THAN CHORD COMPRESSION.

THE API EQUATION DOES NOT INCLUDE THE K_a TERM. MA + TEBBETT (BOSS '88) DEMONSTRATED THAT IT SHOULD BE INCLUDED. THE LINEAR β TERM ABOVE IS THAT GIVEN BY MA + TEBBETT, FOR CONSISTENCY; THE EQUIVALENT API TERM IS ONLY SLIGHTLY DIFFERENT.

THERE IS SOME QUESTION AS TO WHETHER CHORD STRESS EFFECTS ARE SIGNIFICANT WHEN $\beta = 1$ (SEE VAN DER VALK, 1991 OMAE, AND SANDERS + YURA, OTC 5437). FOR NOW, ASSUME THAT NON-UNITY Q_f'S ARE POSSIBLE WHEN $\beta = 1$.

PMB ENGINEERING

By LAN Date 9/20/93 Checked by _____ Sheet No. 2

Project _____ Job No _____

Subject _____

AXIAL TENSION

USE THE ULTIMATE CAPACITY FORMULA PRESENTED IN OTC 5437 (SANDERS & YURA, 1987), WITH THE STANDARD SIN θ AND K_a TERMS ADDED TO MAKE THIS DT EQUATION APPLICABLE TO ALL X JOINTS:

$$P = \frac{F_{yc} T^2}{\sin\theta} 36 \beta Q_{\beta\gamma} K_a Q_f$$

WHERE $Q_{\beta\gamma} = \gamma/8.6$ FOR $\beta > 0.9$
$= 1.0$ FOR $\beta \leq 0.9$

THIS REFERENCE WAS USED BECAUSE ITS EXPERIMENT DATABASE IS LARGER THAN THOSE OF EARLIER REFERENCES, AND IT ACCOUNTS FOR THE BETA-THINNESS FACTOR, $Q_{\beta\gamma}$, UNLIKE THE EARLIER ONES. IT IS BASED ON ULTIMATE CAPACITY, NOT FIRST CRACK LIKE API; THE REFERENCE RECOMMENDS THAT ULTIMATE, NOT FIRST CRACK, IS MORE APPROPRIATE. THE REFERENCE ALSO NOTES THAT COMPRESSION CHORD LOAD HAS NO EFFECT ON TENSION CAPACITY, SO NO Q_f FACTOR NEED BE USED, AS LONG AS β IS AT OR NEAR 1.

THUS, USE Q_f AS DEFINED FOR AXIAL COMPRESSION FOR $\beta \leq 0.9$. FOR $\beta > 0.9$, USE $Q_f = 1$.

PMB ENGINEERING

By HAN Date 9/17/93 Checked by _____ Sheet No. 3

Project _____ Job No. _____

Subject _____

IN-PLANE BENDING

IT IS GENERALLY ACCEPTED (AND THERE IS NO EVIDENCE TO THE CONTRARY) THAT X JOINTS BEHAVE LIKE T/Y JOINTS IN IN-PLANE BENDING. THUS THE GENERAL EQUATION WILL BE USED.

THE MOST UP-TO-DATE EQUATION IS PRESENTED IN BOSS '88, MA & TEBBETT (WITH Q_f ADDED):

$$M = F_y T^2 d\, 6.1 \beta \gamma^{0.5} K_{bi} Q_f$$

THIS IS IDENTICAL TO THE EQUATION FROM OTC 4189 (BILLINGTON, LALANI & TEBBETT, 1982) BUT WITH THE K_{bi} FACTOR ADDED TO ACCOUNT FOR ANGLES OTHER THAN 90°. THIS EQUATION INCLUDES A γ TERM NOT PRESENT IN API 20TH.

Q_f HAS BEEN ADDED PER API 20TH, AS THE OTHER REFERENCES DO NOT STUDY THE EFFECT OF CHORD STRESSES:

$$Q_f = 1 - 0.045 \gamma A^2$$

WHERE A IS DEFINED AS FOR AXIAL COMPRESSION

NOTE THAT THIS EQUATION, UNLIKE API 20TH (THOUGH LIKE MOST OTHER FORMULATIONS) DOES NOT CONTAIN $\sin\theta$ IN THE DENOMINATOR. THIS IS REPLACED BY THE MORE RIGOROUS K_{bi} TERM, WHICH IS FAIRLY SIMILAR OVER MOST VALUES OF θ (AND THE SAME AT $\theta = 90°$).

FOR BENDING (UNLIKE AXIAL LOAD), TAKE $Q_f = 1$ IF ALL CHORD EXTREMA ARE IN TENSION, AS RECOMMENDED BY API (VAN DER VALK, OMAE 1991, PRESENTS NO EVIDENCE RELATING TO BENDING CAPACITY)

PMB ENGINEERING

By LAN Date 9/20/93 Checked by _____ Sheet No. 4

Project _____ Job No. _____

Subject _____

OUT-OF-PLANE BENDING

IT IS GENERALLY ACCEPTED (AND THERE IS NO EVIDENCE TO THE CONTRARY) THAT X JOINTS BEHAVE LIKE T/Y JOINTS IN OUT-OF-PLANE BENDING. THUS THE GENERAL EQUATION WILL BE USED.

THE MOST UP-TO-DATE EQUATION IS PRESENTED IN BOSS '88, MA + TEBBETT (WITH Q_f ADDED):

$$M = \frac{F_{yc} T^2 d}{\sin\theta} (1.4 + 9.8\beta) Q'_\beta Q_f$$

THIS IS THE SAME EQUATION PRESENTED IN OTC 4189 (BILLINGTON, LALANI + TEBBETT, 1982).

Q_f HAS BEEN ADDED PER API 20TH, AS THE OTHER REFERENCES DO NOT STUDY THE EFFECT OF CHORD STRESSES:

$$Q_f = 1 - 0.021 \gamma A^2$$

WHERE A IS DEFINED AS FOR AXIAL COMPRESSION

FOR BENDING (UNLIKE AXIAL LOAD), TAKE $Q_f = 1$ IF ALL CHORD EXTREMA ARE IN TENSION, AS RECOMMENDED BY API (VAN DER VALK, OMAE 1991, PRESENTS NO EVIDENCE RELATING TO BENDING CAPACITY).

PMB ENGINEERING

By LAN Date 9/17/93 Checked by _____ Sheet No. 5

Project _____ Job No. _____

Subject _____

NOTE ON FRAME ACTION

RESULTS FROM IIW CONFERENCE 1989, CONNELLY & ZETTLEMOYER, INDICATE THAT FOR AXIAL CAPACITY OF K BRACES, THE FRAME ACTION (AS OPPOSED TO AN ISOLATED JOINT) INCREASES THE CAPACITY BY 11-26%. PERHAPS AN INCREASE OF ABOUT 20% SHOULD BE APPLIED TO ALL JOINT CAPACITIES TO ACCOUNT FOR FRAME ACTION. BECAUSE RESULTS HAVE NOT BEEN OBTAINED FOR OTHER LOADINGS AND OTHER JOINT TYPES, HOWEVER, IT IS SUGGESTED THAT THIS INCREASE NOT BE CONSIDERED UNTIL FURTHER RESULTS HAVE BEEN OBTAINED.

FACTORS USED IN THE EQUATIONS

$$Q'_\beta = \frac{0.3}{\beta(1 - \frac{5}{6}\beta)} \quad \text{FOR } \beta > 0.6$$

$$= 1 \quad \text{FOR } \beta \leq 0.6$$

APPROXIMATE EQUATIONS FOR INTERSECTION LENGTH FACTORS:

$$K_a = \frac{1}{2}\left(1 + \frac{1}{\sin\theta}\right)$$

$$K_{bi} = \frac{3 + 1/\sin\theta}{4 \sin\theta}$$

X-JOINT MEAN CAPACITY COMPARISON

d=D=16", t=T=0.406", theta=39 deg, Fy = 42 ksi
Qf=0, Ka calculated by approximate formula

Equation	Type	Axial Compression (lb)	Axial Tension (lb)	In Plane Bending (ft-lb)	Out of Plane Bending (ft-lb)
API 20th	min	325	246	263	220
UEG 1985	min	267	200	141	168
AWS	min	180	(API)	(API)	(API)
UT/Lloyd 1993	min	542	542	---	---
w/ Ka term	min	701	701	---	---
Yura 1980 (mean API)	mean	347	348	322	257
Billington et al 1982	mean	467 *	1009	250	296 *
w/o Ka term	mean	360	779	---	---
Sanders/Yura 1987	mean	---	1174 *	---	---
w/o Ka term	mean	---	907	---	---
Ma/Tebbett 1988	mean	467 *	---	456 *	296 *
w/o Ka & Kbi term	mean	360	---	250	---

* use these values

PMB ENGINEERING

By HAN Date 9/20/93 Checked by _____ Sheet No. 1

Project _____ Job No. _____

Subject _____

RECOMMENDED MEAN K JOINT CAPACITIES
(NONOVERLAPPING ONLY)

AXIAL

USE THE FORMULA PRESENTED IN OTC 4189 (BILLINGTON, LALANI + TEBBETT, 1982), WITH API's Q_f TERM ADDED:

$$P = \frac{F_{yc} T^2}{\sin\theta}(4.1 + 20.3\beta) Q_\beta' Q_g' K_a Q_f$$

WHERE $Q_g' = 1.9 - 6\zeta$ FOR $\zeta < 0.15$

$= 1.0$ FOR $\zeta \geq 0.15$

$\zeta = g/D$

FOR Q_f, USE API 20TH RECOMMENDATIONS:

$$Q_f = \frac{1 - 0.030\gamma A^2}{}$$

$$A = \sqrt{f_{cAx}^2 + f_{cIP}^2 + f_{coP}^2} / F_{yc}$$ (API's SAFETY FACTOR REMOVED)

f_{cx} = NOMINAL COMPONENT STRESSES IN CHORD

Q_f MAY BE TAKEN AS 1 IF ALL CHORD EXTREMA ARE IN TENSION. (VAN DER VALK, 1991 OMAE, DEMONSTRATED THAT THIS IS UNCONSERVATIVE FOR X JOINTS, BUT THERE ARE NO EQUIVALENT DATA FOR ANY OTHER JOINT TYPES, SO CONTINUE TO USE API RECOMMENDATIONS.)

THE API EQUATION DOES NOT INCLUDE THE K_a TERM. OTC 4189 SHOWS THAT USE OF K_a IS APPROPRIATE.

PMB ENGINEERING

By LAN Date 9/17/93 Checked by _____ Sheet No. 2

Project _____ Job No. _____

Subject _____

IN-PLANE BENDING

IT IS GENERALLY ACCEPTED (AND THERE IS NO EVIDENCE TO THE CONTRARY) THAT K JOINTS BEHAVE LIKE T/Y JOINTS IN IN-PLANE BENDING. THUS THE GENERAL EQUATION WILL BE USED.

THE MOST UP-TO-DATE EQUATION IS PRESENTED IN BOSS '88, MA & TEBBETT (WITH Q_f ADDED):

$$M = F_y T^2 d \; 6.1 \beta \gamma^{0.5} K_{bi} Q_f$$

THIS IS IDENTICAL TO THE EQUATION FROM OTC 4189 (BILLINGTON, LALANI & TEBBETT, 1982) BUT WITH THE K_{bi} FACTOR ADDED TO ACCOUNT FOR ANGLES OTHER THAN 90°. THIS EQUATION INCLUDES A γ TERM NOT PRESENT W API 20TH.

Q_f HAS BEEN ADDED PER API 20TH, AS THE OTHER REFERENCES DO NOT STUDY THE EFFECT OF CHORD STRESSES:

$$Q_f = 1 - 0.045 \gamma A^2$$

WHERE A IS DEFINED AS FOR AXIAL LOAD

NOTE THAT THIS EQUATION, UNLIKE API 20TH (THOUGH LIKE MOST OTHER FORMULATIONS) DOES NOT CONTAIN $\sin\theta$ IN THE DENOMINATOR. THIS IS REPLACED BY THE MORE RIGOROUS K_{bi} TERM, WHICH IS FAIRLY SIMILAR OVER MOST VALUES OF θ (AND THE SAME AT $\theta = 90°$).

PMB ENGINEERING

By LAN Date 9/20/93 Checked by _____ Sheet No. 3

Project _____ Job No. _____

Subject _____

OUT-OF-PLANE BENDING

IT IS GENERALLY ACCEPTED (AND THERE IS NO EVIDENCE TO THE CONTRARY) THAT K JOINTS BEHAVE LIKE T/Y JOINTS IN OUT-OF-PLANE BENDING. THUS THE GENERAL EQUATION WILL BE USED.

THE MOST UP-TO-DATE EQUATION IS PRESENTED IN BOSS '88, MA & TEBBETT (WITH Q_f ADDED):

$$M = \frac{F_{yc} T^2 d}{\sin\theta} (1.4 + 9.8\beta) Q'_\beta Q_f$$

THIS IS THE SAME EQUATION PRESENTED IN OTC 4189 (BILLINGTON, LALANI & TEBBETT, 1982).

Q_f HAS BEEN ADDED PER API 20TH, AS THE OTHER REFERENCES DO NOT STUDY THE EFFECT OF CHORD STRESSES:

$$Q_f = 1 - 0.021 \gamma A^2$$

WHERE A IS DEFINED AS FOR AXIAL LOADS

PMB ENGINEERING

By LAN Date 9/17/93 Checked by _____ Sheet No. 4

Project _____ Job No _____

Subject _____

NOTE ON FRAME ACTION

RESULTS FROM IIW CONFERENCE 1989, CONNELLY & ZETTLEMOYER, INDICATE THAT FOR AXIAL CAPACITY OF K BRACES, THE FRAME ACTION (AS OPPOSED TO AN ISOLATED JOINT) INCREASES THE CAPACITY BY 11-26%. PERHAPS AN INCREASE OF ABOUT 20% SHOULD BE APPLIED TO ALL JOINT CAPACITIES TO ACCOUNT FOR FRAME ACTION. BECAUSE RESULTS HAVE NOT BEEN OBTAINED FOR OTHER LOADINGS AND OTHER JOINT TYPES, HOWEVER, IT IS SUGGESTED THAT THIS INCREASE NOT BE CONSIDERED UNTIL FURTHER RESULTS HAVE BEEN OBTAINED.

FACTORS USED IN THE EQUATIONS

$$Q'_\beta = \frac{0.3}{\beta(1 - \frac{5}{6}\beta)} \quad \text{FOR } \beta > 0.6$$

$$= 1 \quad \text{FOR } \beta \leq 0.6$$

APPROXIMATE EQUATIONS FOR INTERSECTION LENGTH FACTORS:

$$K_a = \frac{1}{2}\left(1 + \frac{1}{\sin\theta}\right)$$

$$K_{bi} = \frac{3 + 1/\sin\theta}{4 \sin\theta}$$

K-JOINT MEAN CAPACITY COMPARISON

d=18", D=20", t=T=0.4375", g=2", theta=48.5 deg, Fy = 42 ksi
Qf=0, Ka calculated by approximate formula

Equation	Type	Axial Compression (lb)	Axial Tension (lb)	In Plane Bending (ft-lb)	Out of Plane Bending (ft-lb)
API 20th	min	308	---	264	167
UEG 1985	min	266	425	239	166
Yura et al 1980	mean	437	---	324	195
Billington et al 1982	mean	486 *	---	317	219 *
w/o Ka term	mean	416	---	---	---
Ma/Tebbett 1988	mean	---	---	458 *	219 *
w/o Ka & Kbi term	mean	---	---	317	---

* use these values

PMB ENGINEERING

By LAW Date 9/10/93 Checked by _____ Sheet No. 1

Project _____ Job No. _____

Subject _____

OVERLAPPING KT JOINT CAPACITY CALCULATION METHOD

THIS METHOD CALCULATES THE EFFECTIVE CAPACITY OF THE K BRACES ONTO THE CHORD, ACCOUNTING FOR SOME LOAD TRANSFER DIRECTLY THROUGH THE T BRACE TO THE OTHER K BRACE.

AXIAL

USE API RP2A-WSD (20TH) RECOMMENDATIONS (SECTION 4.3.2), NEGLECTING THE "HIDDEN" PART OF THE K THROUGH-BRACE. (IN REALITY, THE "HIDDEN" PART WILL CARRY A REDUCED LOAD. HOWEVER, BECAUSE THE LOAD TRANSFER IS THROUGH THE T BRACE TO THE OTHER K BRACE INSTEAD OF DIRECTLY INTO THE T BRACE AS ASSUMED BY API, RESULTING IN A SLIGHTLY MORE FLEXIBLE BRACE-TO-BRACE LOAD PATH, THE LOAD INTO THE T BRACE WILL BE SLIGHTLY LOWER THAN PREDICTED BY API. ASSUME THAT THESE TWO EFFECTS COUNTERBALANCE EACH OTHER.)

SEE API RP2A-WSD 4.3.2 FOR DEFINITION OF TERMS.

API EQN. 4.3.2-2:

$$P_I = \left(P_a \sin\theta \frac{l_1}{l}\right) + (2 V_{wa} t_w l_2) \Rightarrow$$

JOINT CAPACITY OF K-BRACE ON CHORD =

$$P_K = \left(P_a \frac{l_1}{l}\right) + \left(\frac{2 V_{wa} t_w l_2}{\sin\theta_K}\right)$$

WHERE P_a = SIMPLE JOINT CAPACITY OF K-BRACE ON CHORD, ASSUMING K-TYPE JOINT WITH GAP EQUAL TO THE TRUE GAP BETWEEN THE K-BRACES

V_{wa} = SHEAR STRESS IN WELD AT FAILURE
= $0.4 \times F_y$ FOR MINIMUM ALLOWABLE VALUE (AISC)
= $F_y/\sqrt{3}$ FOR MEAN VALUE (VON MISES YIELD CRITERION)

PMB ENGINEERING

By LAN Date 9/10/93 Checked by _____ Sheet No. 2

Project _____ Job No. _____

Subject _____

t_w = MINIMUM OF WELD THROAT THICKNESS OR MINIMUM BRACE THICKNESS (IF WELD NOT KNOWN, ASSUME BRACE THICKNESS)

θ_K = ANGLE BETWEEN K-BRACE AND CHORD

l_2 = l_2 OF WELD BETWEEN K AND T (SEE API FIGURE 4.3.2-1)

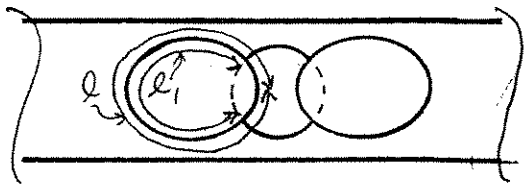

← "FOOTPRINT" OF BRACES ON CHORD

APPROXIMATE FORMULA FOR l: $\frac{\sqrt{2}}{2}\pi\sqrt{d^2+d_2^2}$

BETTER: $l = \pi d \frac{1}{2}(1 + 1/\sin\theta_K)$

WHERE d = DIAMETER OF K-BRACE

$d_2 = d/\sin\theta_K$

l_1 IS BEST DETERMINED GRAPHICALLY OR USING GEOMETRY.

NOTE: THIS APPROACH ASSUMES THAT THE STRENGTH OF THE K-BRACE TO T-BRACE JOINT IS EITHER SUFFICIENTLY LARGE TO AVOID FAILURE OR IS NOT OF INTEREST.

IN-PLANE BENDING

USE UEG "DESIGN OF TUBULAR JOINTS FOR OFFSHORE STRUCTURES" (1985) RECOMMENDATIONS, AS API DOES NOT ADDRESS MOMENTS:

JOINT CAPACITY OF K-BRACE ON CHORD = M_{IP} = SIMPLE JOINT IPB CAPACITY OF K-BRACE ON CHORD, ASSUMING K-TYPE JOINT WITH GAP EQUAL TO THE TRUE GAP BETWEEN THE K-BRACES